Human organ-specific vascular heterogeneity and the endothelial role in fetal liver hematopoiesis

Yoon Jung Choi

A dissertation submitted in partial fulfillment of the requirements for the degree of

Doctor of Philosophy

University of Washington

2018

Reading Committee:

Ying Zheng, Chair

Brandon K. Hadland

Marta Scatena

Program Authorized to Offer Degree:

Department of Bioengineering

University of Washington

Abstract

Human organ-specific vascular heterogeneity and the endothelial role in fetal liver hematopoiesis

Yoon Jung Choi

Chair of the Supervisory Committee:

Associate Professor Ying Zheng

Department of Bioengineering

For a long time, the endothelium was considered to be a homogenous passive surface that existed primarily to support blood flow. In recent decades, however, both the heterogeneity of the endothelium and its importance in supporting organ-specific function have been increasingly recognized. Endothelial cells from different vascular beds have been shown to differ markedly, both across the arterial, venous, and lymphatic systems of the large vasculature, as well as between the microvascular beds of different organs. Endothelial cells themselves are now known to communicate with surrounding parenchymal tissue, and thereby to play an important role in non-vascular organ development and function. In vivo studies have provided extensive knowledge of organ-specific vascular heterogeneity; however, these studies have predominantly been performed in murine models and may not be directly applicable to human biology or the development of human therapeutics. To date, very few works have studied organ-specific endothelial functions and their underlying molecular mechanisms. The following

dissertation reports on the properties of endothelial cells isolated from four major human organs—the heart, lung, liver, and kidneys—in individual fetal tissues at three months' gestation, at structural, gene expression, and cellular functional levels. After characterizing differences across organ vascular beds, this research next explores liver endothelial specific contributions to fetal liver hematopoiesis. We replicated the human fetal vascular niche in vitro and investigated the role of *WNT5A* in supporting hematopoiesis. Overall, these studies provide a "library" of information about the different characteristics of organ-specific endothelial cells, and report on the creation of organotypic endothelial cell lines with in vitro stability. These findings, and the cell lines described, can be directly applied to future mechanistic studies within the fields of tissue engineering and regenerative medicine.

TABLE OF CONTENTS

LIST OF FIGURES

LIST OF TABLE

Acknowledgements

The work presented here would have only been made possible through the love, devotion, support, and guidance of my mentors, friends, and family.

First and foremost, I would like to thank my Ph.D. advisor Dr. Ying Zheng for providing the opportunity to work on very interesting research and giving unparalleled support and advice throughout my time in the lab. I am grateful for Ying's positivity and enthusiasm for science keeping me motivated and inspired. I am incredibly fortunate to have been a part of Zheng Lab.

Thank you to my collaborator and committee member Dr. Brandon K. Hadland for his incomparable dedication and thorough instruction. I am also appreciative of my other supervisory committee members, Dr. Marta Scatena, Dr. Buddy D. Ratner, and Dr. Edward J. Kelly for their time, support and invaluable insights.

To my lab mates, graduate school classmates and friends made in Seattle, you are the best. Without you, I would not make it through my Ph.D. From coffee breaks, lab happy hour, Korean barbeque night, Chi-mac times, weekend brunch and dim sum, K-pop concerts and conferences have made these past five years very entertaining. I will miss all of you a lot and look forward to seeing you again in the near future!

Most importantly, thank you to my parents and to my entire family for your unconditional love and support. To my boyfriend, I am immensely thankful for you.

Chapter 1

Introduction

1.1 Background

During embryonic development, endothelial cells (ECs) form a highly branched and interconnected network of vasculature which permits the transport of blood, nutrients, gases and hormones to a growing embryo. In addition to supporting blood flow, mounting evidence suggests that ECs provide an instructive signal to non-vascular tissue cells and contribute to further organogenesis. Recent attention has been given to the organ-specific role of microvascular endothelial beds in organ development. Understanding how endothelial cells instruct organogenesis over the course of embryonic development will provide important insights for tissue engineering and regenerative medicine, and may help guide the ex vivo development of replacement organs supported by a functional microvasculature.

This chapter reviews the basics of vascular development and the role of the microvascular endothelium in organogenesis, with a focus on the developing heart, lung, liver, blood and kidney

1.2 Vasculogenesis

During embryonic development, the blood vessel is formed by two successive processes: vasculogenesis and angiogenesis (Figure 1.1). Vasculogenesis involves the *in situ* differentiation of ECs from angioblasts, and the assembly of ECs into tubules that fuse to form a nascent vascular network. Murine vasculogenesis begins in the extraembryonic yolk sac mesoderm at embryonic day 7 (E7) with the formation of blood islands. Blood islands are mesodermal cell aggregates composed of a loose inner mass of embryonic erythroid progenitors and an outer luminal layer of angioblasts. Angioblasts differentiate into endothelial cells and form a rather homogenous primitive capillary plexus. Within the embryo itself, however, the major blood vessels of the trunk, dorsal aorta and cardinal vein, as well as endocardium of the heart are directly formed from the

aggregation of angioblasts.

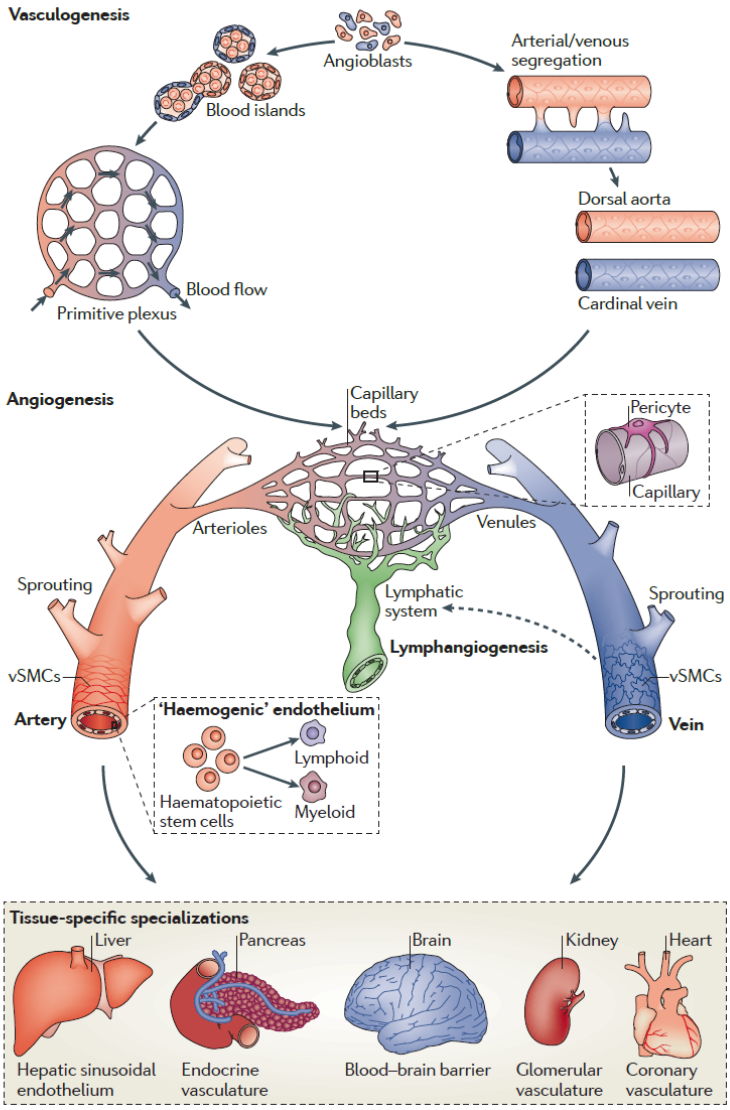

Figure 1.1 Schematic overview of vascular development. The basic processes of vascular development are demonstrated here, including vasculogenesis and angiogenesis [1]

1.3 Angiogenesis

Angiogenesis refers to the formation of new vessels from existing vessels through sprouting and anastomosis [2]. Angiogenesis in the embryo leads to the sprouting of

vessels into developing organs such as the retina, heart and central nervous system [3-7] as well as remodeling of the primary vascular branch to establish a hierarchical network of arteries, arterioles, capillary beds, venules and veins. Angiogenesis is induced by several signaling molecules that are secreted from local tissue during early embryogenesis, including vascular endothelial growth factor (VEGF). The VEGF family plays an important role in regulating angiogenesis, endothelial cell chemotaxis, vessel barrier integrity and permeability [2, 8]. A subset of endothelial cells reached by the proangiogenic VEGF signal takes on the role of endothelial tip cells. Tip cells are characterized by their distal position on a close-ended outgrowing vessel, presence of filopodia, and low proliferation rate. Tip cells direct the outgrowth of blood vessel sprouts along a gradient of VEGF, by loosening endothelial junctional contacts and proteolytically degrading the surrounding basement membrane [1]. Upregulated expression of delta-like ligand 4 (DLL4) in the tip cells activates Notch signaling in the adjacent stalk cells. Stalk cells trail tip cells by maintaining connectivity with the parent vessels and support sprout elongation by proliferation. Upon contact with other vessels, tip cells lose their motile phenotype and generate tight EC to EC junctions, and the vessels fuse to neighboring vessels by the process of anastomosis [1].

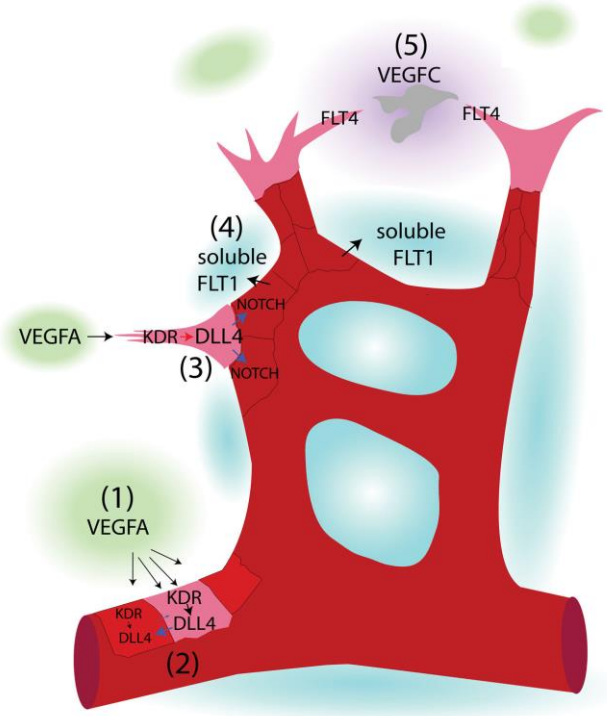

Figure 1.2 Schematic model of sprout angiogenesis. (1) Angiogenesis is initiated in response to VEGF secreted from local tissue. (2) & (3) Activated ECs are specified into tip cell as well as stalk cells. Tip cells have upregulated expression of delta-like ligand 4 (DLL4) and activate Notch signaling in the adjacent stalk cells (4) Tip cells lead the outgrowth of blood vessel and stalk cells proliferate to support sprout elongation. (5) Anastomosis occurs when the tip cells on a sprouting vessel encounters a neighboring vessel [2].

1.4 Blood vessel maturation: vascular mural cell recruitment

The nascent hierarchical vessel tree matures into a largely quiescent structure through recruitment of mural cells such as pericytes and vascular smooth muscle cells (vSMCs). Pericytes primarily associate with the smallest blood vessels, including venules and capillaries, whereas vSMCs line the wall of larger-diameter vessels, such as arteries and veins. During maturation, the endothelium secretes platelet-derived growth factor B (PDGFB) which acts as a chemoattractant for migrating vascular mural cells which express PDGF receptor β (PDGFRβ) [9]. The physical contact between ECs and mural cells activates multiple signaling pathways that suppress endothelial proliferation and sprouting and also stabilize the existing vascular tubes. EC-derived transforming growth factor- β (TGF- β) signaling induces mural cell differentiation from undifferentiated

mesenchymal cells [10] and reinforces TGF- β synthesis in ECs in an autoregulatory manner [11]. Angiopoietin-TIE2 signaling is also involved in vessel maturation. Angiopoietin-1 released from vascular mural cells binds to TIE2, a tyrosine kinase receptor expressed on ECs, and induces subsequent mural cell attachment and endothelial stabilization [12-14].

1.5 Organ-specific blood vessel patterning

ECs are a heterogeneous population. These cells make up arterial, venous, and lymphatic vascular systems which are specified during the early development, as well as the microvascular endothelial beds of different organs which are characterized by organ-specific structure and function. The nascent endothelial plexus enters developing organs and forms a barrier between blood and the organ microenvironment. Through specific junctional proteins and receptors, ECs communicate regionally with underlying organ tissues. Through these interactions, endothelial cells modulate their phenotype to support the local organ parenchyma. Molecularly, the crosstalk between ECs and the organ microenvironment leads to a series of nonlinear signaling pathways. Differences in these pathways within each organ are thought to contribute to organ-specific endothelial heterogeneity [16, 17] (Figure 1.3). Epigenetic regulation, such as DNA methylation and histone methylation, is also thought to contribute to a large, and potentially heritable, portion of EC heterogeneity. The microenvironment regulates non-heritable spatial and temporal changes in EC phenotype through receptor-mediated posttranslational protein modifications, leading to distinct structure and function of endothelial cells in various organs.

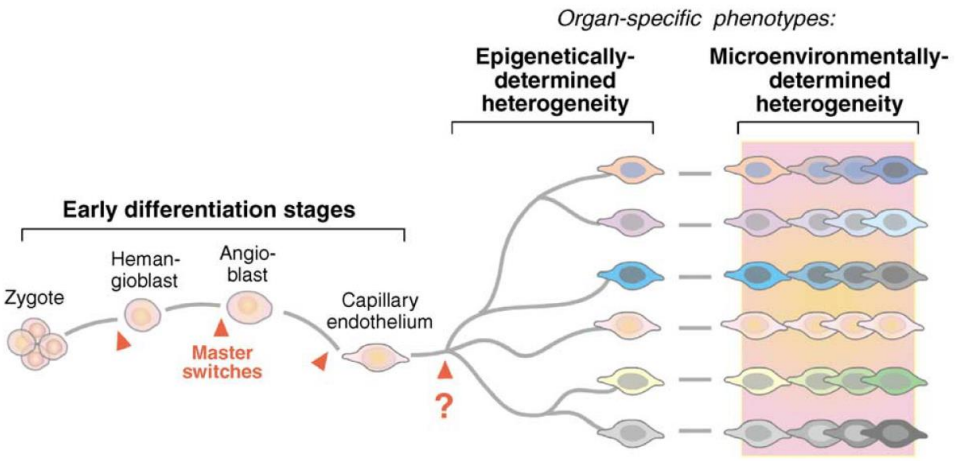

Figure 1.3 Organ-specific endothelial cell phenotypes are established via two mechanisms. EC properties are shaped under epigenetic control and organ-specific microenvironmental stimuli including cytokines, angiocrine factors, metabolites, and biophysical signals [15].

1.6 Heart vasculature

1.6.1 Cardiac capillary ECs have multiple developmental origins

There are multiple developmental sources of cardiac capillary ECs, including the proepicardium, sinus venosus and endocardium [16, 17]. For two decades, the proepicardium was proposed as the major source of the cardiac capillary ECs as demonstrated by lineage tracing of chick embryo cardiac vascular endothelial cells [18]. A subset of proepicardial cells delaminating from the epicardium undergoes an epithelial-mesenchymal transition (EMT). The newly formed mesenchymal cells progressively invade into the myocardium and differentiate into coronary vascular endothelial cells, smooth muscle cells, and fibroblast [18-20]. Coronary vascular endothelial cells assemble into the myocardial capillary plexus as well as coronary arteries [21]. However, lineage tracing studies in the murine system using epicardial markers *Wt1* [22, 23], *Tbx18* [24], *Tcf21* [25], or *Scx [26]* revealed that only a small fraction of coronary vascular ECs arise from proepicardium, in conflict with previous avian studies. Recent seminal works in the murine context have shown that the sinus venosus serves as a major source for cardiac capillaries. Endothelial sprouts from the sinus venosus invade the myocardium and

establish an extensive vessel network of coronary arteries, cardiac capillaries and veins [7, 27]. In addition, a subsequent study demonstrated that endothelial cells arise from the ventricular endocardium and form a cardiac capillary bed [28].

1.6.2 Cardiac EC contribution to heart development

In the heart, at least one capillary is located next to nearly every cardiomyocyte to provide sufficient oxygen and nutrients [29]. The crosstalk between cardiac capillaries and cardiomyocytes has known to play a significant role in cardiac development, cardiomyocyte survival, and function. During early heart development, endocardial endothelial cells secrete neuregulin-1 which binds to the receptor ErB2/4 expressed in cardiomyocytes. Neuregulin-1/ErbB signaling is necessary for multiple aspects of cardiac development. Mice lacking neuregulin-1, ErB2 or ErB4 exhibit cardiac developmental defects in trabeculae and cardiac cushion formation, and die around E10.5 [30, 31]. PDGFB secreted from the endothelium is also important for heart development. Endothelium-restricted PDGF-B deletion has been shown to lead to myocardium abnormalities [32].

1.7 Lung vasculature

The pulmonary circulation system is composed of an expansive capillary endothelial plexus in close contact with an intricate alveolar epithelium. During embryonic development, pulmonary ECs are important for lung morphogenesis. Indeed, tight coupling of pulmonary ECs and epithelial cells is associated with differentiation of the lung tubules into canaliculi, saccculi, and alveoli, which is required for efficient gas exchange and fluid clearance at birth [33]. Blocking VEGF, which is essential for blood vessel development, causes a defect in primary septae formation [34] and altered alveolar patterning [35]. In parallel, overexpression of VEGF within the respiratory epithelium leads to abnormal lung morphogenesis with disruption of the epithelial-capillary interface, tubular dilation, and absence of Type I alveolar cells. [36]. Collectively, these findings support the notion that proper vascularization in the developing lung is important for proper lung morphogenesis.

1.8 Liver vasculature

The liver has a complex vascular architecture. The liver receives a dual supply from the hepatic artery and the portal vein. The oxygenated blood from the hepatic artery and the nutrient-rich blood from the portal vein mix in the sinusoids, where filtration occurs. The sinusoids are lined by capillary ECs, also known as liver sinusoidal endothelial cells (LSECs). LSECs are characterized by their abundant fenestrae, lack of a basement membrane and absence of diaphragms (Fig. 1.4). Fenestrae are pores in the endothelial cell body which can have a thin membrane, called the diaphragm, stretched across the opening. These structures facilitate the transport of water, small solutes, albumin, and other macromolecules across the endothelial wall [37]. These unique structural features of LSECs allow them to supply the parenchymal tissue with oxygen and nutrients, serve as a gate keeper for leukocyte entrance in hepatic inflammation, and function in the rapid clearance of toxicants and foreign bodies [38]. The structural phenotype of liver sinusoidal endothelial cells is critical to their function. Further understanding of the developmental processes involved in the development of vasculature and other liver cell populations, such as hepatocytes in the human context is needed.

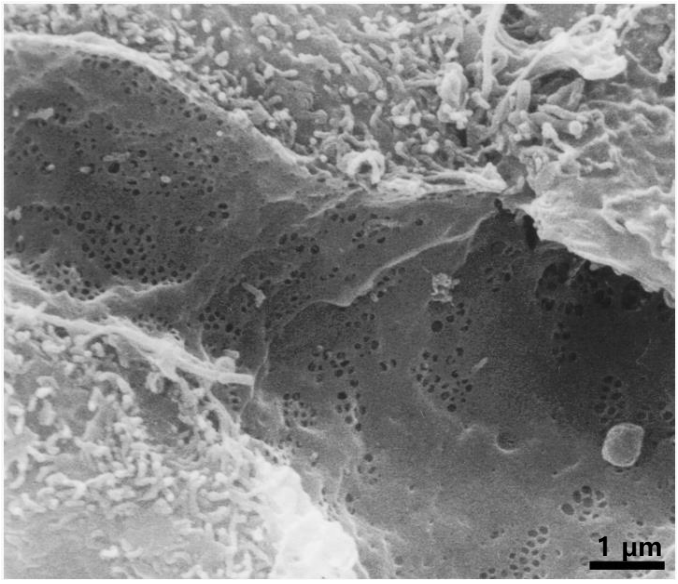

Figure 1.4. Scanning electron microscopy of rat liver sinusoidal endothelial cells shows fenestrated structure. Liver-specific structure of the sinusoidal endothelial cells are seen through the presence of fenestrae and pores in the cell body, facilitating transport

and filtration [39].

1.8.1 Hepatic EC contribution to liver development

The liver vasculature is known to be important for proper liver development during embryogenesis. The septum transversum mesenchyme, a mesoderm-derived tissue that is partially comprised of endothelial cells is closely apposed the foregut hepatic endoderm and actively induces the nascent liver bud formation [40]. In *VEGFR2 (flk-1)* mutant embryos, the migration of hepatic epithelial cells to the septum transversum was shown to be inhibited [41]. Embryonic liver explants treated with an angiogenic inhibitor showed impaired hepatic differentiation, highlighting the necessity of continued vascular support for proper hepatic morphogenesis [41].

1.8.2 The hematopoietic stem cells (HSC) niche in the fetal liver

The fetal liver serves as a hematopoietic organ during mid-late gestational development, where HSCs undergo an extensive proliferation, maturation, and differentiation before ultimately migrating to the fetal bone marrow just prior to birth. HSCs are known to express several cell adhesion molecules, including a receptor for vascular cell adhesion molecule-1 (VCAM-1) which mediates HSC homing to hematopoietic organ. Previous findings show that the fetal liver sinusoidal endothelium and bone marrow endothelium, the eventual tissue of HSC residence express VCAM-1 during development, suggesting a possible role of LSECs in modulating the homing of HSPCs, their retention in the niche, and release into the blood stream [42, 43]. LSECs have also been shown to modulate the survival and differentiation of HSCs in development. Murine endothelial protein C receptor (EPCR) explicitly marks HSCs with high hematopoietic reconstitution activity and high levels of engraftment in vivo [44]. In the fetal liver, EPCR-positive HSCs were located adjacent to the liver sinusoidal vascular networks where a cell survival factor, activated protein C (APC) is abundant [45]. Protease-activated receptor 1 (Par1) expression in $EPCR^{+}$ HSCs suggests the involvement of an anti-apoptosis APC/EPCR/Par-1 pathway in HSC self-renewal and maintenance [45]. In vitro, fetal liver hematopoietic cells cultured with murine endothelial cell lines exhibited higher proliferation and differentiation potential [46]. These observations

suggest a possible role for LSEC in hematopoiesis; however, no mechanistic studies exist to describe these observations and the endothelial-specific factors that promote HSC survival, self-renewal and differentiation.

1.8.3 Wnt signaling pathways in hematopoiesis

Many pathways are involved in the regulation of cellular fate within the HSC niche. One set of signaling pathways are those activated by the Wnt family of ligands. Wnt ligands are a family of secreted glycoproteins essential for normal development. Nineteen different WNT proteins have been identified in the mouse and human genome. The best characterized Wnt signaling pathways are the canonical Wnt pathway and noncanonical pathway (Figure 1.5). In the canonical pathway, the Wnt ligand binds to the Frizzled receptor and the lipoprotein receptor-related protein 5/6 (LRP) corecptor [47]. The absence of Wnt ligand leads cytoplasmic β catenin sequestration in a multifactor complex that ultimately degrades β catenin by the ubiquitin pathway [48]. Wnt binding to Frizzled recruits Dishevelled (Dvl) to the plasma membrane, leading to Axin-GSK- 3α/ β complex recruitment and LRP5/6 phosphorylation [49]. This, in turn, recruits additional Axin-GSK-3α/ β which phosphorylates other residues on LRP 5/6 and disrupts the multifactor complex formation. β catenin is subsequently translocated to the nucleus and interacts with T-cell factor (TCF)/lymphoid enhancer factor (LEF) transcription factors [50]. One of the most characterized non-canonical pathways is the Frizzled-dependent Wnt-cGMP/Ca^{2+} pathway. Upon activation by Wnt5a, a non-canonical Wnt ligand, the Frizzled receptor activates phospholipase C (PLC), releases diacylglycerol (DAG) and inositol-phosphate (IP3) and increases intracellular calcium [51]. The Wnt-Frizzled-G protein complex also activates p38 kinase and stimulates phosphodiesterase 6 (PDE6). PDE6 hydrolyzes cyclic GMP (cGMP), inactivates protein kinase G (PKG), and increases intracellular concentrations of calcium [52]. Increased Ca^{2+} activates calcineurin and the protein calcium/calmodulin-sensitive protein kinase II (CamKII) [52, 53], which in turn induces the nuclear localization of NFAT transcription complexes as well as TAK1-NLK kinases [52]. TAK1-NLK kinase has been proposed to inhibit canonical Wnt signaling by inducing β catenin degradation [54]. It was reported that Wnt5a protein competes with Wnt3a for LRP5/6 co-receptor binding sites [55].

During embryonic development, dynamic regulation of the canonical Wnt signaling pathway is required for HSC development. In murine embryos, Wnt/β catenin activity is transiently required for the emergence of HSCs from the AGM hemogenic ECs [56] but must be downregulated for subsequent rapid maturation and development of the HSC [57]. The role of non-canonical pathways in hematopoiesis during early development is not as defined. Louise et al. showed that Wnt4 maintains the pool size of bone marrow $Lin^{-}Sca1^{+}Kit^{hi}$ cells (LSKs) and normal thymic cellularity in a non-canonical fashion [58].

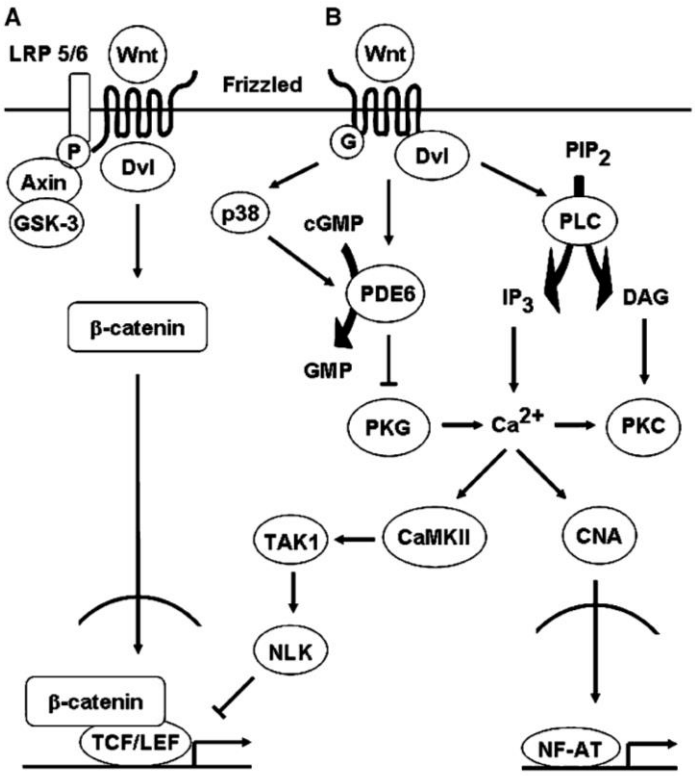

Figure 1.5 Canonical and non-canonical Wnt signaling. A simplified schematic of canonical (A) and non-canonical (B) Wnt signaling pathways is displayed [52]

1.9 Kidney vasculature

The kidney glomerulus contains four cell types: fenestrated glomerular capillary ECs, podocytes, perivascular mesangial cells, and parietal epithelial cells. The glomerulus branches out from the afferent arteriole and is surrounded by Bowman's capsule, a part of the nephron. As a first step in urine formation, constant ultrafiltration of

blood across the glomeruli capillaries into Bowman's space occurs. The glomerular capillary tube is made up of fenestrated ECs that have relatively large pores (50-100 nm in diameter) where fluid and solutes pass through, to the exclusion of circulating blood cells and large proteins. The efferent arterioles, which develop within the center of the glomerular tuft, transport blood to peritubular capillary beds. Peritubular capillaries surround the proximal tubule, distal tubules and the loop of Henle where extensive reabsorption and secretion occur.

Endothelial signaling to other kidney cell populations is significant to the proper development of organ. Specifically, renal endothelial cells play an important role in glomerular morphogenesis by supporting podocyte and mesangial cell maturation. Gao et al. showed that VEGFR2 signaling is required to maintain expression of Pax2 in the mesenchyme of the early kidney [59]. Pax2 stimulates expression of Gdnf, which in turn stimulates branching of the ureteric bud [59]. Podocyte-specific VEGF-null mice were shown to have an impaired recruitment and maturation of ECs in the glomerulus, which in turn, resulted in abnormal podocyte and mesangial cell maturation [60]. Genetic ablation of *Pdgfb* in endothelial cells led to mesangial cell defects and glomerular abnormalities [32]. Further characterization of human developmental cell-cell interactions can reveal further signaling pathways necessary for organ patterning and formation.

1.10 Dissertation overview and significance

The research presented in this dissertation investigated the properties of endothelial cells isolated from the microvascular beds of four human major organs: heart, lung, liver, and kidneys. Cells were obtained from individual fetal tissues at three months gestation, and the properties of ECs from different vascular beds explored at the levels of structure, gene expression, and cellular function. Building on the characterization of fetal liver endothelium formed during this first part of the project, this research next explores fetal liver hematopoiesis with an emphasis on the contribution of the organ-specific endothelium. Chapter 2 through 3 describes the rationale, scientific methods and results of the following aims:

Aim 1: Isolate human organ-specific fetal endothelial cells and characterize inter-organ endothelial cell heterogeneity

Aim 2: Identify vascular niche function and underlying molecular mechanisms in human fetal liver hematopoiesis

The work contained in the following chapters has many implications for the fields of tissue engineering and regenerative medicine. The results from aim 1 provide a comprehensive human vascular heterogeneity reference library at structural, molecular and functional levels. To the best of our knowledge, this study provides the first known description of stable and passageable organ-specific human EC lines from four major organs of single donors. We describe the organ-specific transcription profiles which shape the unique features of organotypic ECs and support the development and function of their respective associated organs. In addition, global gene expression in cultured endothelial cells and their freshly isolated counterparts were compared to validate phenotypic differences among the endothelial cell types and to determine changes conferred by passaging them in vitro. Using a representative source of organ-specific endothelial cells cultured in perfusable engineered vascular constructs, we engineered the organ-specific vasculature in vitro. The inter-organ endothelial heterogeneity that we demonstrated here may have significant importance for future therapeutic strategies targeting the endothelium. The in vitro engineered organ-specific vasculature model that we describe in this aim will be useful for the future study of how basic processes such as angiogenesis, biotransport, endothelial-parenchymal signaling, and endothelial response to toxins/pharmaceuticals vary by vascular bed. The results found in aim 2 precisely define the cellular populations involved in fetal liver hematopoiesis, as well as the fetal liver vascular niche's contribution to hematopoietic cell expansion and differentiation. This study provides insight into the progression of hematopoiesis within human fetal liver. Liver endothelial-specific paracrine signals that we identified herein will provide a strong foundation for understanding how the liver niche supports HSC self-renewal and proliferative expansion. These findings will have potential impact for the future development of in vitro systems for hematopoietic stem/progenitor cell expansion and differentiation for therapeutic purposes.

Chapter 2

Isolate human organ-specific endothelial cells and characterize inter-organ endothelial cell heterogeneity

This chapter has been published in *iScience*:

Raluca Marcu*, **Yoon Jung Choi***, et al. "Human Organ-specific Endothelial Cell Heterogeneity" iSicence, 2018. **4**: p. 20-35, * equal contribution.

2.1 Abstract

The endothelium first forms in the blood islands in the extra-embryonic yolk sac and then throughout the embryo to establish circulatory networks that further acquire organ-specific properties during development to support diverse organ functions. Here, we investigated the properties of endothelial cells (ECs), isolated from four human major organs—the heart, lung, liver, and kidneys—in individual fetal tissues at three months' gestation, at gene expression, and at cellular function levels. We showed that organ-specific ECs have distinct expression patterns of gene clusters, which support their specific organ development and functions. These ECs displayed distinct barrier properties, angiogenic potential, and metabolic rate and support specific organ functions. Our findings showed the link between human EC heterogeneity and organ development and can be exploited therapeutically to contribute in organ regeneration, disease modeling, as well as guiding differentiation of tissue-specific ECs from human pluripotent stem cells.

2.2 Introduction

Vascular development begins with the differentiation of endothelial cells (ECs) and *de novo* formation of a primitive vascular network derived from angioblasts that first appear in the blood islands of the yolk sac and then migrate to the fetus where vascular networks are formed [61-63]. As development proceeds, this primitive network remodels, presumably triggered by changes in hemodynamics, surrounding cell types and environment, to establish a hierarchical vessel tree with tissue-specific functionality

important for the function of each organ [64-67]. This development requires that ECs therefore deviate from an initial largely homogeneous embryonic population to acquire specific identities necessary to support the diverse needs of flow, transport, hormonal interactions, and cell trafficking across the endothelium of each organ [68, 69]. Recent studies also showed that ECs may be derived from local progenitors in different organs or tissues, which further enhances the complexity and diversity in the response of ECs to injury and regenerative capacity [70-74].

Although little is known about how each organ determines the functional properties of its endothelium, EC differences have been shown between arteries and. veins, large and small vessels, and different microvascular beds in various organs [75-78]. Some of these properties depend on the tissue environment. Site-specific microenvironmental cues (i.e. cytokines, metabolites, biophysical signals, and direct cell-cell contact from parenchyma cells) communicate with ECs and induce posttranscriptional modification. In transplantation studies, ECs can be induced to gain other tissue-specific structural and morphologic phenotypes, and gene expression patterns [79].

EC properties are also under epigenetic control. Epigenetic footprints that control basal expression of endothelial-specific genes in different organs are specified early during embryonic development and preserved during sequential mitotic cycles [80]. When cells are removed from their *in vivo* microenvironment and grown in culture, most, but not all gene expression patterns are lost upon passaging [81, 82]. Nevertheless, a previous analysis of messenger RNA (mRNA) from several human EC lines revealed heterogeneous signatures even in passaged cells, providing evidence that epigenetic modification mediates differential gene expression profiles of ECs [78].

A possible problem in the existing studies is that the ECs were isolated from different donors with various isolation methods for different tissues. Although this concern has been addressed in mouse species [77, 83], mouse ECs have different properties compared with human ECs and there are differences between human and mouse development [84]. These studies also failed to examine the cells as they formed vascular networks, a critical issue for organ-specific EC heterogeneity, or to show that

gene expression data correlated with differences in cell functions. The in vitro stability is particularly important, in that the preservation of expression with passaging is needed for the study of mechanisms in human ECs and vascular development in the future.

In the present study, we address these challenges and investigate human EC heterogeneity via the following different categories: (1) basal protein expression in *ex vivo* microvascular tissue beds; (2) organ-specific EC population in tissue; (3) morphology, structure, protein expression, transcriptional profiling, and vascular function of ECs after isolation, culture and passaging, and 4) transcriptional signature validation in freshly isolated ECs, for four major developing organs – the heart, kidney, liver, and lung – obtained from individual human fetal donors. Together, our findings provide a comprehensive heterogeneity reference library after multiple passages in stabilized culture for human organ-specific ECs at cellular, molecular, and transcriptional levels. This study will also contribute to understanding organ specific vascular development, injuries and potential development of targeted therapeutic interventions.

2.3 Experimental methods

Isolation and culture of organ specific endothelial cells

All experiments were approved by the Institutional Review Board of the University of Washington (IRB447773EA). Normal human fetal organs were obtained upon informed consent from abortion material (age 16-20 weeks) and the same donor tissues (kidney, lung, liver, and heart) were used to isolate organ specific endothelial cells. Tissues were minced finely in serum-free EBM-2 endothelial growth medium (Lonza) supplemented with 0.2 mg/ml Liberase and 100 U/ml DNase (Roche) and incubated for 30 min at 37 ^{0}C in a water bath with shaking. The resulting tissue homogenate was filtered twice through a 40 μm cell strainer to remove tissue debris and large vessels. For the isolation of fresh endothelial cells, EpCAM-positive cells were depleted first from the cell suspension using EpCAM microbeads (Miltenyi Biotec), followed by the depletion of CD45-positive cells using CD45 MicroBeads (Miltenyi Biotec). Then the CD144 positive cells were magnetically separated using CD144 MicroBeads (Miltenyi Biotec) on 2 different columns. For cultured endothelial cells, the cell suspension was plated on

gelatin coated T-75 flasks in EBM-2 medium supplemented with antibiotic/antimycotic (Invitrogen), 10% FBS (Invitrogen), 100 μg/ml ECGS (Millipore), 50 μg/ml Heparin (Invitrogen), and 40 ng/ml VEGF (R&D Systems). For kidney and lung samples, epithelial cells were removed from the cell suspension before plating using EpCAM microbeads (Miltenyi Biotec) to prevent epithelial cell overgrowth. Cells were cultured at 5% O_2 until confluent and then endothelial cells as the CD144 positive and CD45 negative population were sorted on BD FACSAria II at the UW SLU Flow Cytometry Facility. After sorting, organ specific endothelial cells were cultured in EBM-2 supplemented with antibiotic/antimycotic, 10% FBS, 100 μg/ml ECGS, 50 μg/ml Heparin, and 20 ng/mL VEGF, on gelatin-coated plates and used for further experiments between passages 1-3.

Histology

Human fetal organs (kidney, lung, liver and heart) were embedded in Tissue-Tek O.C.T. compound (Sakura) and kept as frozen blocks at -80 ^{0}C. Frozen organ sections were cut to a thickness of 9 μm using a cryostat (Leica CM 1850) and placed on HistoBond adhesive glass slides (Marienfeld). The glass slides were air-dried for 30 min and fixed in 4% formaldehyde. Fixed tissues were stained with hematoxylin and eosin (H&E).

Immunofluorescence

Tissue cryosections and organ specific endothelial cells plated on gelatin-coated glass slides were fixed with 3.7% formaldehyde, permeabilized with 2% BSA and 0.5% Triton x-100 in PBS, blocked with Background Buster (Innovexbio), and incubated overnight at 4 ^{0}C with primary antibodies against CD31 (Life Technologeis), CD144 (Abcam), PLVAP (Abcam), Caveolin-1 (Abcam), vWF (Abcam), ART4 (Bioss Inc), TBX5 (Santa Cruz Biotechnology), HNF1B (Abnova), and KCNJ16 (LSBio), followed by Alexa-488, -568, or -647 secondary antibodies (Invitrogen) and Hoechst (Life Technologies) staining. Cells were imaged with a Nikon Confocal microscope or Nikon wide filed microscope using 20X and 40X objectives. Image analysis was performed using the Image J software (U.S. National Institute of Health, Bethesda, Maryland).

Flow cytometry analysis

To characterize single endothelial cell populations within each fetal organ, multiparameter FACS analysis of stained organ suspensions was performed on a BD FACSCanto II and quantitated with FlowJo software (Tree Star). The following antibodies were used: APC-anti-CD144 (eBioscience), FITC-anti-CD31 (BD Biosciences), Pacific Blue-anti-CD45 (BioLegend), FITC-CD34 (BD Biosciences), PE-EphB4 (R&D systems), FITC-anti-gp38 (R&D systems), FITC-anti-Robo1 (R&D system), PE-anti-CD144 (BioLegend), APC-anti-PDGFRβ (BioLegend), PE-anti-EpCAM(Miltenyi Biotec), PE-anti-α-SMA (R&D systems) and FITC-anti-NG2 (R&Dsystems). Unstained controls, single stained cellular controls, and single stained BD™ CompBead particles were used for compensation and voltage adjustment. Isotype control antibodies were used to distinguish non-specific background signals from specific signals.

RNA isolation, RNA sequencing and RT-PCR

Total RNA from cultured and freshly isolated organ specific endothelial cells was purified using the RNAeasy Mini Kit (Qiagen) and residual DNA was removed by on-column DNase digestion. RNA quality was assessed with the Agilent RNA 6000 Nano Kit using the Agilent 2100 Bioanalyzer (Agilent Technologies). Only samples with RNA integrity number higher than 8 were kept for further analysis. RNA sequencing was performed on poly-A-enriched samples using Illumina TruSeq. RT-PCR was performed using the Real-time PCR System (Applied Biosystems) with Fast SYBR Green Master Mix (Applied Biosystems). The abundance of each gene was determined relative to an internal control using GAPDH RNA.

RNA-seq data analysis

RNA-seq samples were aligned to hg19 using Tophat [85]. Gene-level read counts were quantified using htseq-count [86] using Ensembl GRCh37 gene annotations. Genes with total expression above 10 normalized read counts summed across RNA-seq samples were kept for further analysis. princomp function from R was used to for Principal Component Analysis. DESeq [87] was used for differential gene expression

analysis. Genes with fold change >1.5 and FDR<0.05 were considered differentially expressed. topGO R package [88] was used for Gene Ontology enrichment analysis. The gene expression data set has been submitted to the public database in Gene Expression Omnibus.

Western blot analysis

Cells and tissues were lysed in RIPA buffer (Sigma) supplemented with protease inhibitor cocktail (Thermo Scientific). 3 μg proteins were electrophoresed on NuPAGE 4-12% Bis-Tris Acrilamide gels (Invitrogen), transferred on PVDF membrane and probed overnight at 4°C with primary antibodies against Von Willebrand Factor (Abcam), caveolin (Abcam), PV1 (Abcam) and GAPDH (Cell Signaling). HRP-conjugated secondary antibodies (Thermo Scientific) were used for detection.

Endothelial barrier function measurements

The EC barrier function was evaluated by real-time measurements of electrical impedance with the xCELLigence RTCA SP instrumentation (ACEA Bioscience, Inc.). Organ specific endothelial cells were plated in a 96-well electronic microtiter plates (E-Plate 96, ACEA Bioscience, Inc.), 10,000 cells/well, and allowed to reach cellular confluence, as indicated by plateau values obtained for the electrical impedance (60-68 hours). At plateau, the electrical impedance readout expressed in arbitrary units as the Cell index parameter, reflects changes in barrier function and permeability of different endothelial cells.

Spheroid sprouting assay

Endothelial spheroids containing 1000 cells/spheroid were generated using the "hanging drop" technique in endothelial growth medium with 20% Methocel solution (2% Methyl cellulose (Sigma) in EBM2 growth medium). Spheroids were plated into 24 well plates, 40 spheroids/well, embedded in 2 mg/ml type I collagen and 30% Methocel matrix, overlaid with endothelial growth medium supplemented with 40 ng/ml VEGF. Spheroids were allowed to sprout for 24-48 hours and imaged using a 10x objective. Sprouts number and length were quantified using the Image J software (U.S. National Institute of Health, Bethesda, Maryland).

Fabrication of vascular networks

Three-dimensional, perfusable vascular networks were fabricated as described previously [89]. Briefly, microvessels were fabricated by seeding organ specific endothelial cells in microfluidic channels embedded in 6.5 mg/ml type I collagen matrix. The networks were cultured with gravity-driven flow of endothelial growth medium for 5 days, fixed and employed for either electron microscopy or confocal microscopy imaging.

Transmission electron microscopy

Microfluidic vascular networks were fixed by perfusion in 2.5% glutaraldehyde for 20 min followed by immersion in half-strength Karnovsky's solution (2% paraformaldehyde/2.5% glutaraldehyde in 0.2M cacodylate buffer) for 4 hr. These samples were rinsed in 0.1M cacodylate buffer then post-fixed using 2% OsO4 in 0.2M cacodylate buffer followed by another rinse with 0.1M cacodylate buffer. Sample dehydration was performed using immersions in graded solutions of ethanol, then propylene oxide (PO), before 1:1 PO/Epon 812 (vendor) immersion overnight. Fresh Epon 812 was then exchanged for 2 hr after which the blocks were cured for 48 hr at 60^{o}C. Ultrathin sections (70 nm) were cut from blocks using a diamond (vendor) blade on a Leica EMUC6 ultra-microtome and placed onto grids. Grids were stained with uranyl acetate for 2 hr and lead citrate for 5 min. Sections were imaged using a JEOL JEM-1400 Transmission Electron Microscope (JEOL Ltd., Japan) using a typical acceleration voltage around 100 kV. Images were acquired with a Gatan Ultrascan 1000XP camera (Gatan, Inc., Pleasanton, CA).

Metabolism

Oxygen consumption rate (OCR) and extracellular acidification rate (ECAR) were measured using the XF96 Seahorse Analyzer (Seahorse Bioscience). ECs were plated into 96-well Seahorse assay plates in complete growth medium, 7000 cells/well, 3 days before measurements. OCR and ECAR measurements were performed in XF Assay medium (Seahorse Bioscience), supplemented with 5 mM glucose, 1 mM sodium pyruvate and 10 mM glutamine, at 9 minutes intervals. Time course of OCR and ECAR was performed upon sequential addition of Oligomycin (1 μM), CCCP (1 μM), and

Rotentone/Antimycin (1 μM each). At the end of the measurements, the protein content for each well was quantified, and OCR and ECAR values were normalized per microgram of protein for each cell type.

Hepatocyte isolation, culture, and functional analysis

Hepatocytes were isolated from 100-140g adult female Lewis rats (Taconic), as described previously [90]. Briefly, the animals were anesthetized using isoflurane, the portal vein was cannulated with an 18G catheter, and the liver was perfused and digested with collagenase type IV (Sigma). Hepatocytes were purified via Percoll centrifugation and seeded at a density of 0.3e06 hepatocytes per well onto 24-well plates coated with 0.17 mg/ml rat tail Collagen-1 (BD Biosciences). The next day, normal human dermal fibroblasts (Lonza, ratio of 1:1) or fetal (isolated) liver, kidney, heart, lung, or human umbilical vein (Lonza) endothelial cells (ratio of 1:0.3) were seeded onto the hepatocytes. Cultures were maintained for eight days in a 1:1 mixture of "hepatocyte medium" [DMEM with high glucose (4.5g/L), 10% (v/v) fetal bovine serum (Biowest), 0.04 ug/ml dexamethasone, 7 ng/ml glucagon, 1% ITS+ culture supplement (Corning), 1.5% 1M HEPES, and 1% penicillin-streptomycin] and "endothelial medium" [EBM-2 supplemented with antibiotic/antimycotic, 10% FBS, 100 μg/ml ECGS, 50 μg/ml Heparin, and 20 ng/mL VEGF]. Culture media was collected daily from each well before replacement with fresh medium. Rat albumin in collected media was measured via enzyme-linked immunosorbent assay (Bethyl labs).

Statistical analysis

Single variable analysis between two samples was compared by Student's *t*-test and multivariable assays were analyzed by one-way ANOVA. Results are presented as mean ± SEM, and $p < 0.05$ was considered significant.

2.4 Results

Human fetal ECs show organ-specific heterogeneity *ex vivo*

We examined the human fetal organ sets from three donors, constituting three biological replicates at three months' gestation stage (100-125 days). At this stage, all

four major organs of interest – the heart, kidney, lung, and liver have an established microvascular supply, and exhibit organ-specific function. The heart beats at 120-160 bpm and is approximately 2 cm; the lungs have developed the entire air-conducting bronchial tree up to 20 generations with respiratory ducts and start to form barriers between alveoli and blood vessels; the liver is the major site of blood cell production and has also started to produce bile; and the kidneys have established nephrons and start to produce urine.

The vasculature of each organ displayed a heterogeneous organization, identified by the expression of EC markers, such as CD31, a transmembrane glycoprotein that constitutes endothelial intercellular junctions, CD144 (VE-cadherin), a major endothelial adhesion molecule, and von Willebrand factor (vWF), a glycoprotein that mediates platelet adhesion in the endothelium (Fig. 2.1A). In the heart, ECs formed an organized network and contained a large amount of Weibel-Palade bodies with high expression of vWF (Fig. 2.1A, ii-v). In the lungs, although the expression of vWF was overall high and comparable to the heart ECs (Fig. 2.1A and 1B), it varied in different regions. Lower VWF expression was associated with pulmonary capillary ECs located near small air sac-like structures, whereas a vWF mosaic pattern appeared in ECs neighboring the bronchioles and larger airways (Fig. 2.1A and 1C). In the liver, the ECs displayed low vWF expression in VECad+ cells (Figure 2.1A and 2.1B), whereas there are clustered non-ECs containing high granular vWF in the interstitium (Figure 2.1Av), indicating the presence of hematopoietic progenitors. In the kidneys, two distinct microvascular structures were identified, with higher VWF expression in glomerular ECs, and lower expression in peritubular microvascular ECs (Fig.2.1A, 2.1B, and 2.1D).

We then evaluated the structural differences of ECs in different fetal organs using the presence of caveolae, identified by the expression of caveolin-1 (Cav1), as well as stomatal and fenestral diaphragms, identified by the expression of plasmalemma vesicle-associated protein PLVAP (also called PV1) [91-93]. Our study showed that the heart and lung microvasculature has nearly complete Cav1 and PV1 colocalization, suggesting that the presence of PV1 was confined to stomatal diaphragms – a signature of continuous endothelium (Figures 2.1E and 2.1F). On the other hand, the kidney microvasculature, in

particular, presented higher levels of and more discrete PV1 outside of Cav1 colocalization, indicating the presence of fenestal diaphragms – a signature of fenestrated endothelium (Figures 2.1E and 2.1F).

Human fetal ECs present as diverse organ-specific populations

To characterize the EC population within different fetal organ microvascular beds and distinguish them from hematopoietic cells, we used the pan-hematopoietic marker CD45 in combination with CD144. ECs were identified as CD144 positive and CD45 negative ($CD144^{+}/CD45^{-}$) by flow cytometry. Single cell suspensions, obtained by enzymatic digestion of mechanically minced fresh tissue followed by the filtered removal of large vessels and tissue chunks, showed a well-demarcated $CD144^{+}/CD45^{-}$ populations in each of the four fetal organs (Fig. 2.1G, Appendix A, Supplementary Figure 1A). The highest percentage of ECs was from the heart (4.7 ± 0.7 %), whereas the lowest percentage of ECs was found in the liver (0.8 ± 0.3 %); the kidney and lung ECs represented 3.4 ± 1.6 % and 3.4 ± 0.7 %, respectively, of the entire cell suspension. The liver was the only tissue that showed a significant $CD144^{+}/CD45^{+}$ double-positive population, supporting the hematopoietic role of this organ during early stages of development. Kidney and lung ECs show distinct CD144+ population from the epithelial cell population (Epcam+) with no overlap (Appendix A, Supplementary Figure 1B). Among the $CD144^{+}/CD45^{-}$ cell population, the percentage for EphB4+ is 70 - 90 % for lung, liver and kidney with no statistical significance among three, whereas heart cell suspension has significantly lower percentage for EphB4+ (~25%). (Appendix A, Supplementary Figure 1C) The majority of these ECs are CD34+ (85%-90% for heart and kidney ECs) (Appendix A, Supplementary Figure 1C). Less than 2% ECs are GP38+ (podoplanin) for all four vascular beds, suggesting little lymphatic vascular development at this stage (Appendix A, Supplementary Figure 1C). There is no detection of Robo1+ cells in this population (data not shown), which also suggests sufficient removal of large vessel tissue and minimal EC contaminations from large vessels (Appendix A, Supplementary Figure 1D).

Human fetal ECs retain *ex vivo* heterogeneity upon *in vitro* expansion

To study the persistence of EC heterogeneity *in vitro* and the epigenetic

contribution to EC heterogeneity, we isolated and cultured the four human fetal organ derived-ECs through five passages (in each passage the cell number doubles). Important steps of the isolation procedure included the filtering and removal of large vessels and tissue chunks after enzymatic digestion, the removal of Epcam+ epithelial cell fraction from the whole tissue single cell suspension (particularly important for kidney and lung), the enrichment of the endothelial fraction through culture in low oxygen atmosphere with vascular endothelial growth factor (VEGF), the purification of the CD144+ endothelial fraction by flow cytometry, and the culture in VEGF-containing EC growth media for up to five passages (detailed in Methods). This isolation procedure also allows for the purification of other cell populations, important for further studies of regional organ heterogeneity and perivascular and parenchyma interactions (Figures 2.2A and Appendix A, Supplementary Figure 2A). The majority of cultured ECs are EphB4+ (> 90%), with little contamination of lymphatic (GP38+ % < 4%) or large vascular (Robo1+ % < 1%) ECs; the CD34+ population in these cultured ECs ranges between 25% (liver) to 85% (kidney) (Appendix A, Supplementary Figure 2B).

Isolated ECs displayed typical endothelial cobblestone appearance and maintained their morphologies through five passages in culture (Fig. 2.2B). ECs also expressed CD31 with a high purity greater than 99% for all four fetal organs (Fig. 2.2B). Similar to the *ex vivo* expression patterns, the isolated heart and lung ECs expressed higher vWF proteins, whereas the kidney and liver ECs have more PV1 protein expressions (Figs. 2.2B-D). PV1 distributed largely at the peripheral cell surface membrane of the kidney and to a lesser extent in the liver ECs, whereas only a small fraction colocalized with Cav1, indicating the presence and persistence of fenestral diaphragms in these two EC types after isolation and expansion. In contrast, the heart and lung ECs expressed much more Cav1 but less PV1 than the kidney and liver ECs, with PV1 located mostly in the perinuclear region in the heart and lung ECs.

We used these ECs at passage 2 to engineer three-dimensional endothelialized microvascular networks. These were embedded in collagen microfluidic channels and cultured under gravity-driven flow, as previously described [94]. Cells from four sources created similar networks of tubular endothelium (Figure 2.3A). Ultrastructural analysis

via transmission electron microscopy revealed the formation of junctional complexes at cell-cell contacts and distinctive structures along the cell periphery in four types of microvessels (Figures 2.3B and Appendix A, Supplementary Figure 3). Engineered heart and lung microvessels showed focal contacts between adjacent cells and contained caveolae with stomatal diaphragms. Engineered kidney and liver microvessels showed complex and intercalated junctions between adjacent cells and presented numerous fenestrae (black arrows) along the peripheral regions of the cell membrane. The fenestrae in kidney endothelium contained diaphragms and had uniform morphology and size, whereas liver endothelium had discontinuous openings and contained fenestrae in varying size and structure along peripheral membranes. Not all fenestrae in the liver endothelium had diaphragms. In addition, the liver endothelium showed multivesicular bodies, lysosomes, and other distinct structure inside cytoplasm (Figures 2.3B and Appendix A, Supplementary Figure 3). Although not directly compared with the microvascular ultrastructure in the four fetal tissues, these results establish the structural heterogeneity of organ-specific structural endothelium in vitro, which is consistent with known organotypic vasculature in vivo [17, 37].

Global RNA sequencing reveals heterogeneous gene expression profiles in cultured organ-specific ECs

We next sought to determine whether these cells have distinct molecular signatures after removal from the original microenvironment. We collected RNA for transcript profiling using RNAseq from single-donor derived heart, lung, liver and kidney ECs obtained in three different donors after two passages *in vitro*. A total 102 transcription factors and 93 co-factors were identified as highly expressed (top 20% transcript intensities) in all four types of cultured ECs (Appendix A, Supplementary Figure 4A). These factors include known key regulators of vascular development such as ETS factor family (i.e. *ETS1*, *FLI1*, *ELK3*, *ELF1* etc), *ID* proteins, *KLF* gene family (i.e. *KLF3, KLF6, KLF10* etc), and genes important for vascular remodeling and VEGF signaling (i.e. *SP1*, *HES1*, *SOX18*, *HIF1A, NFKB1, etc*).[95-97]

Principle component analysis showed distinct clustering of heart-derived ECs compared with the other three EC types (Fig. 2.4A) and Venn diagram defined the

characteristic gene clusters for heart specific ECs (Fig. 2.4B). Differential expression analysis and Gene Ontology terminology analysis (Fig. 2.4C, Appendix A, Supplementary Figure 4B and 4C) showed that cultured heart ECs have higher gene expression levels, when compared to the other three types of ECs, with respect to extracellular matrix and structure organization, blood vessel morphogenesis, angiogenesis, VEGF production, heart chamber and valve morphogenesis, coronary vascular development and morphogenesis, branching morphogenesis as well as regulation of vascular permeability. Compared with the heart ECs, lung ECs have higher expression for artery morphogenesis and development, developmental growth and regionalization; liver ECs have higher expression for pattern specification, embryonic skeletal system development, regulation of leukocyte and homotypic cell-cell adhesion, regulation and activation of immune response, bone marrow development; and kidney ECs in culture have higher expressions for regionalization, pattern specification process, embryonic organ morphogenesis/development/identity, hormone secretion and transport, and nephron development. These analyses are consistent with the corresponding stage of distinct organ development and function, and indicate the important roles of different ECs in their corresponding organ development.

Differential expression analysis further revealed differentially expressed genes in paired comparison (Figure 2.4D and Appendix A, Supplementary Figure 4D). For example, genes such as *GATA4*, *TBX5*, *TBX20*, *HAND2* are expressed more than 200-fold higher in heart ECs, with high counts in RNAseq, compared with kidney ECs. These genes, although not studied in ECs, are known to be critical heart development, heart valve formation, etc. [98, 99]. Kidney ECs, on the other hand, highly and uniquely express many HOX genes that are known to be critical for kidney development. We further identified clustered genes as bona-fide markers for organ-specific ECs by comparing one with the other three (fold change >1.5 and FDR<0.05). There are 74 heart-specific, 29 kidney-specific, 13 lung-specific highly expressed EC genes, whereas the numbers of liver-specific endothelial genes were not significant (Fig. 2.4B and Appendix A, Supplementary Figure 4E). These organ specific genes include transcription factors and regulation co-factors, angiocrine factors, extracellular matrix proteins, cell adhesion molecules, membrane transporters, signaling molecules and metabolism-related

genes (Fig. 2.4E).

Heart-derived ECs showed upregulated expression of zinc finger, T-box, and basic helix–loop–helix transcription factors involved in heart and embryonic vascular development [100-104] (*GATA6, HAND2, HEY2, TBX18*); transcription factors and co-factors involved in the heart valve and chamber development [105-107] (*FHL1*); as well as factors involved in signaling regulation [108-111] (*EBF3, NCOA7, PRRX1, RARB*, etc). Kidney-derived ECs displayed upregulated expression of the helix-loop-helix transcription factor *EBF1*, which is critical in glomeruli development and maturation [112, 113], and the transcription factor *PAX2*, important for the regulation of branching morphogenesis and kidney development [114]. In addition, kidney ECs also expressed a large number of homeobox transcription factors, known as master developmental regulators in the kidney [115, 116] (*HOXA9, HOXB7, HOXB8, HOXB9, HOXC8, HOXC9, HOXD3, HOXD4, HOXD9, HOXD11*, etc). Lung-derived ECs showed higher expression of the forkhead transcription factor *FOXF2*, known for the activation and regulation of pulmonary genes and embryonic development [117]; the T-box transcription factor *TBX4*, critical for lung branching,[118]; and the co-factor *KHDRBS2*, which regulates signal transduction during lung development[119]. These organ-specific genes have not been found and studied in ECs previously, which may be important for the study of specific EC contribution during organ development.

Beside transcriptional regulators, heart-derived ECs highly expressed clusters of genes encoding for angiocrine factors, including annotated cytokines and growth factors (*CCL2, IL6, IL33*), signaling molecules and extracellular matrix remodeling proteins (*BMPER, C1QTNF1, CTSK, HAPLN1, IL6ST, LTBP1, PCOLCE2, PLAC9, POSTN, RGS5, SFRP4, TNFAIP8L3).* Other identified heart-derived EC-specific gene clusters included glycoproteins and surface receptors that mediate host defense, cell-cell adhesion and cell-matrix interaction (*COLEC12, EFEMP1, ITGB3, LRRC4B, FBLN1, RADIL, PCDH10, PRRT2, SELL, SRPX*), cytoplasm and cytoskeleton associated proteins (*AMPH, CLMN, DRP2, FRMD3, MYRIP, GRB14*), transporters (*KCNH7, GRB14, ABCA8, ABCA9, EVA1C, GPR158, NIPAL1, RASSF10, SLC7A2*), and metabolic regulators (*ART4, ATP13A3, CAMK2B, GCNT1, GLT8D2, PDE3A, PLA2G5, PLPP1, PTGS1, ST6GAL1*,

etc) (Fig. 2.4E) .

We validated the expression of selected genes from the kidney-specific and heart-specific EC gene lists by real-time polymerase chain reaction (PCR) analysis on both the RNA subjected to RNA sequencing and the three new RNA sets collected from single-donor organ-specific ECs (Fig. 2.4F). The expression of EC genes identified as heart-specific (i.e. *HAND2, TBX18, IL33, ART4, ABCA8, BMPER, RGS5, TNFAIP8L3, HAPLN1, and SMAD7*) were significantly upregulated in heart-derived ECs compared with the kidney-derived ECs, and conversely kidney-specific genes (i.e. *PAX2, HOXC10, MMP7, and HNF1B*) were significantly upregulated in kidney-derived ECs. These organ-specific genes have minimal changes in the expression level through passage 5 (Appendix A, Supplementary Figure 4F). We further used quantitative PCR (qPCR) analysis to validate the low expression of perivascular cell genes (i.e., NG2 and PDGFRb), confirming the absence of contaminating perivascular cells (Appendix A, Supplementary Figure 4G).

Altogether, gene expression data shows that ECs from fetal organs maintain organ-specific transcription profiles; in particular, heart-derived ECs display distinct clusters of transcription factors, angiocrine factors, surface glycoproteins, and metabolism that significantly distinguish these ECs from the other three EC types.

In vitro-ex vivo correlation of EC heterogeneity

We then examined the EC heterogeneity via ex vivo RNAseq analysis and in situ immunofluorescence microscopy, to validate organ-specific gene clusters identified from cultured cells and further differentiate between the environmental and epigenetic contributions to EC heterogeneity. Freshly isolated ECs were collected via column purification with Epcam-CD144+/CD45-, and high-quality RNA were extracted for sequencing to assess gene expression in three single-donor organ sets. Column purification significantly enhanced cell survival during fresh isolation process. Fluorescence-activated cell soring analysis for the column-purified ECs showed 70 %-98 % CD144+ cells and with no detectable perivascular cell contaminations for all four organs (Appendix A, Supplementary Figure 5A). Principal component analysis revealed that ECs isolated from the four organs were distinct from each other, with organ replicates

clustering tightly together (Appendix A, Supplementary Figure 5B), suggesting higher degree of organ specificity when compared with the in vitro cultured ECs. Comparing heart and kidney ECs alone, there were more than 5000 genes differentially expressed with significance in freshly isolated ECs, whereas only 867 genes were identified in culture (fold change > 1.5 and FDR < 0.1). This suggests that majority of differentially expressed genes were likely dependent on the native microenvironment. However, a small portion of the expressed RNAs remained differentially expressed even in culture, suggesting that the differentiation has occurred at an epigenetic level. A potential epigenetic assay would help to confirm the epigenetic stability of ECs between in vivo and in vitro cultures.

Most top transcription factors and cofactors commonly expressed in culture were also highly expressed in freshly isolated ECs, whereas genes such as *KLF2*, *KLF4*, *SOX4*, *SOX7*, *ID2*, *SNAI1*, *NR4A1*, and *EGR3*, were significantly downregulated after *in vitro* expansion (Appendix A, Supplementary Figures 5C and 5D). Among these highly expressed genes in freshly isolated sets, 32 transcription factors and 17 cofactors were differentially expressed in at least one type of ECs, and five transcription factors (*ETS1*, *ELK3, SOX18, HMGA1, SOX7*) were highly expressed with significant variation among all the ECs (Appendix A, Supplementary Figure 5C), a difference not detected in cultured EC sets. Other top transcription factors such as *COUP-TFII (NR2F2)* and *ETS2*, were differentially expressed in kidney versus heart, whereas *ERF*, *ID1*, *E2F4*, *SOX4* in the liver are different from those in the kidney, heart and lung which appear similar. These transcription factors have been recognized as important regulators of EC development and specification, and their differential expression suggests that vascular development occurs at different pace in some of the four organs at the gestation time evaluated.

Next we validated the differentially expressed genes from cultured cells in freshly isolated cell sets, using heart and kidney paired comparison. Although the majority of differentially expressed genes in EC sets in vivo were lost after culture, over 100 highly upregulated genes (fold change > 10) in either heart or kidney ECs identified in culture remained elevated in freshly isolated ECs (Fig. 2.5A). These differentially expressed gene clusters represent the epigenetic contribution to the organ-specific EC signature,

which has the capacity to maintain in culture. Some of these identified genes were also verified in immunofluorescence staining in ex vivo tissues (Fig. 2.5B: human, and Fig. 2.5C: mouse). The loss of differential expression of the highly expressed genes, from freshly isolated ECs to the cultured ECs, suggested the significant microenvironmental specifications for the developing ECs.

Heart-derived ECs have the highest transendothelial electrical resistance, angiogenic potential and metabolic rates among all four ECs

We next evaluated whether the variations in the transcriptional profiles of the four different EC types in culture led to distinct functions with respect to their barrier properties, angiogenic potential, and metabolic rates *in vitro*. To match the cell condition (passage 2) in RNAseq analysis, we used four ECs from single donor sets at the same passage number and culture media conditions for all the functional studies. Using xCELLigence RTCA SP instrumentation (ACEA Bioscience), we measured the real-time electrical impedance of endothelial cell monolayers at a particular frequency ($f = 10\ kHz$). When EC monolayer reached confluency, the electrical impedance, recorded as the cell index (CI), reached plateau (Figure 2.6A), from which the transendothelial electrical resistance was measured. The monolayer of heart-derived ECs showed the highest electrical resistance (~ 35 ± 1 Ω at $f = 10kHz$) with statistical significance, whereas the electrical resistance of the kidney-derived ECs was the lowest among the four ECs (~ 21 ± 2 Ω) (Fig. 2.6A), supporting a better barrier function for the heart ECs when compared with cultured ECs from the fetal kidney.

We then evaluated the ability of the ECs derived from four organs to form new vessels in vitro using the spheroid sprouting assay [120]. Endospheroids were embedded in collagen and methylcellulose matrix and overlaid with endothelial growth medium, with or without 40 ng/ml VEGF, and grown for 24-48 hours to allow sprout formation (Fig. 2.6B,i). Without VEGF exposure, most endospheroids were quiescent and devoid of any sprouting, except for the heart endospheroids. In the presence of 40 ng/ml VEGF, all endospheroids showed enhanced angiogenic activity, which was evident from the extensive capillary-like sprout formations. However, under VEGF exposure, heart endospheroids displayed a significantly higher number of sprouts (Fig. 2.6B, ii).

Finally, we examined EC metabolism through the measurements of cellular oxygen consumption (respiration) and proton excretion (glycolysis) with a Seahorse Analyzer (Figures 2.6C and 2.6D). The oxygen consumption rate and extracellular acidification rate were measured at baseline, and in the presence of oligomycin, CCCP (carbonyl cyanide m-chlorophenylhydrazone), and rotenone/antimysin A, which were added sequentially (Fig. 2.6C), and allowed for the calculation of respiration rates due to mitochondrial activity, ATP synthase, and spare capacities, as well as the glycolysis rate. Heart ECs showed the highest oxygen consumption rate due to an increase in both non-mitochondrial and mitochondrial respiration, which relied on enhanced ATP synthase activity, but also a significant spare respiratory capacity. A significantly higher glycolysis rate in addition to the mitochondrial respiration (Fig. 2.6D) demonstrated that heart ECs possess the highest metabolic rate among the four types of ECs investigated, consistent with enhanced energetic support that can fuel a higher angiogenic potential.

Human fetal liver ECs support hepatocytes functions

We further examined whether organ-specific ECs can support specific parenchyma function. The four types of human fetal ECs at passage 2 were co-cultured with primary hepatocytes freshly isolated from rat liver. Each type of ECs was added on top of primary rat hepatocyte monolayers after their attachment for 24 hr following fresh isolation, at ratio of 1 endo: 3 hepatocytes. Rat albumin was measured via enzyme-linked immunosorbent assay (ELISA) in media collected every 24 hours, and compared after 7 days of culture. Co-culturing with ECs showed significant improvement in general compared with hepatocytes culture alone, in both albumin production and hepatocyte survival (Figure 2.6E and Appendix A, Supplementary Figure 6). Hepatocytes co-cultured with liver ECs showed significantly higher albumin production (~200 μg/million cells per day) than those co-cultured with heart, lung, and kidney ECs (Figure 2.6E). Liver ECs appeared to provide additional signaling that promotes hepatocytes function (Appendix A, Supplementary Figure 6C).

2.5 Discussion

Twenty years ago, studies in chick quail hybrids showed that the endothelium all

over the body arises from blood islands that first appear in the embryonic yolk sac [121, 122]. Cells that arise from these early structures migrate throughout the body forming branches, and with time, they organize themselves into the arborized network of the adult arteries, veins, and capillaries. The initial formation of blood islands and tubules is called "vasculogenesis". The lymphatic system develops in a similar fashion, originating from the venous branches. Blood vessel themselves can develop branches, primarily from the postcapillary venules. These branches form the vasculature of organs. More recently, it appears that endothelia can also arise locally within the mesenchyme of organs, including the heart and lungs. Thus diversity might arise both by interactions with parenchyma and by changes within the branched structure itself. Obviously, determining mechanisms that control local differentiation of ECs is difficult in whole tissue. We felt, therefore, that it would be desirable to develop cell lines. Because cells from fetuses usually have long replicative life spans, we chose to derive EC lines from our fetal tissues. We show that these human fetal ECs maintain stable organ-specific morphology and gene expression through five passages in culture. These fetal ECs express gens that are supportive to specific organ development and are different in metabolism, gene expression, and angiogenic responses to VEGF that may be relevant in vivo.

Among many possible organ specific endothelial properties, we focused on three major categories: (1) barrier function, (2) angiogenic potential, and (3) metabolic functions. From a structural point of view, we showed that heart and lung ECs are continuous endothelium with focal close-contact junctions and no fenestrae formation, whereas kidney and liver ECs contain abundant fenestrae along the peripheral cell membrane but have complex intercalated junctions. These transcellular fenestrae would allow for large molecules to transport directly across the kidney and liver endothelium with low resistance, coinciding therefore with lower barrier strength. In addition, heart ECs have higher expression levels for adherent junctions, which not only contribute to higher barrier but also play important roles in signaling [123]. Heart ECs also showed significantly higher transendothelial electrical resistance than kidney and liver ECs. Although not achieving physiological level of barrier in a monolayer culture [124], these data suggest that at least one route of transport (transcellular or paracellular) [125, 126] is higher in kidney and liver ECs compared with the heart ECs.

Our study specifically addressed ECs from the heart, liver, kidney, and lung, mainly owing to the tissue availability, and did not investigate ECs from other organs, such as the highly permeable high endothelial venules or the impermeable brain vasculature with unique distribution of tight junctions [127, 128]. Future studies of these ECs could provide more insight into the heterogeneous structure and molecular regulation and endothelial barrier.

The second organ specific property we demonstrated was the different angiogenic potential of ECs. Interestingly, heart ECs proved much more angiogenic than the other ECs derived from the other three organs under the same culture conditions and in the presence of identical stimuli. This higher angiogenic function in heart ECs is supported by a distinct cluster of genes categorized as angiocrine factors and signaling factors. These genes not only regulate angiogenesis but also provide important paracrine signaling for the maturation and function of developing cardiomyocytes. The different angiogenic potential may also be due to the specific origin of each EC type. Heart ECs are derived from at least three different sources, including the endocardium, sinus venous, and proepicardium [129]. Recent studies showed that ECs may even originate from different germ layers [130-134]. These varied origins could then lead to different capacities for angiogenesis via differential epigenetic control.

The endothelium has been shown critical to organ development and maturation, for example, in the pancreas, liver, and kidney [135-141], and can serve as progenitor for perviascualr cells [136]. It is possible that the endothelium is required to facilitate the differentiation of endoderm and mesoderm in the heart and to achieve mature function. Here, organ specific EC identities, defined from the developing organs, could provide instructional signals toward the construction of organ-specific vascular microenvironment, and further the maturation of the developing parenchyma. This regulatory feedback system involving the endothelium is likely critical for successful organ regeneration, and for engineering functional parenchyma in vitro using stem cells.

We also observed heterogeneity in organ specific EC metabolism. Remarkably, heart ECs showed the highest rates of oxygen consumption and glycolysis, supported by a distinct cluster of upregulated genes involved in metabolic regulation. ECs in mature

vessel beds, despite of their exposure to high oxygen levels, are known to be quiescent and to rely mostly on glycolysis [142]. During activation, ECs increase mitochondrial activity, [143] as well as glycolysis for energy production [144, 145]. However, little is known as to whether endothelial mitochondrial ATP generation is static or varies between vascular beds. Little is also known about the role of endothelial metabolism during development. Metabolism has been recently noted to be critical in regulating stem cell fate during early differentiation [146-148]. Our findings suggest that metabolism may also play an important role during the differentiation of endothelium towards organ specific vasculature.

We further demonstrated the supportive role of ECs in organ development and function by co-culturing with hepatocytes. Interestingly, fetal ECs support hepatocytes survival and function, and liver-specific ECs also showed significantly superior supportive function in terms of albumin production from the hepatocytes. Although the mechanisms remain elusive and require investigation in depth, this functional study showed proof-of-principle that organ-specific ECs would be beneficial to support organ development, and engineer organ-on-a-chip to better recapitulate structure and function *in vivo*.

In summary, we have examined transcription profiles from fetal ECs cultured and passaged from four major human organs – the heart, lung, liver, and kidneys. We showed the distinct structural and functional properties maintained over at least five passages in these four types of ECs. The results are still preliminary in several ways. First, we do not know how many more passages these cell line can go through while preserving these properties. Longer replicative life spans could provide us with cells that would be reproducible reagents for mechanistic studies. Second, we do not know how closely the cultured cells themselves have diverse expression patterns that could represent the diversity of different EC phenotypes in vivo. For example, the high incidence in EphB4-positive cells in cultured sets suggests that endothelium forms veins may be over-represented. Significant loss of differentially expressed genes from in vivo after culture suggest the importance of identifying environmental cues in vivo to understand and recapitulate the vascular and organ function. Third, although we did see some diversity in

the structures of the EC-cell junctions our measurement of electrical resistance suggests that none of these cell lines reproduce the functional impermeability of ECs with tight junctions. This is general issue with cultured EC with, as far as we know, only two reported exception. Aside from the cell junction, this may be important for other EC functions including control of endothelial differentiation by VE cadherin and shear-dependent transcription dependent on several cell junction proteins.

Nevertheless, our findings allowed us to identify for the first time the linkage between human EC heterogeneity and organ development, and differentiation between the epigenetic and microenvironment contribution to human EC heterogeneity. The availability of methods to culture organ specific ECs makes it feasible to understand several organ-specific processes, including the heart valve formation through the studies of endothelial-mesenchymal transition *in vitro*, the formation and functional maturation of the kidney filtration barrier and the gas exchange interface in the lungs. Our work also provides important insights towards identifying precise organ-specific vascular targets and developing appropriate therapeutic interventions towards the treatment of organ-related vascular injuries and diseases.

2.6 Figures

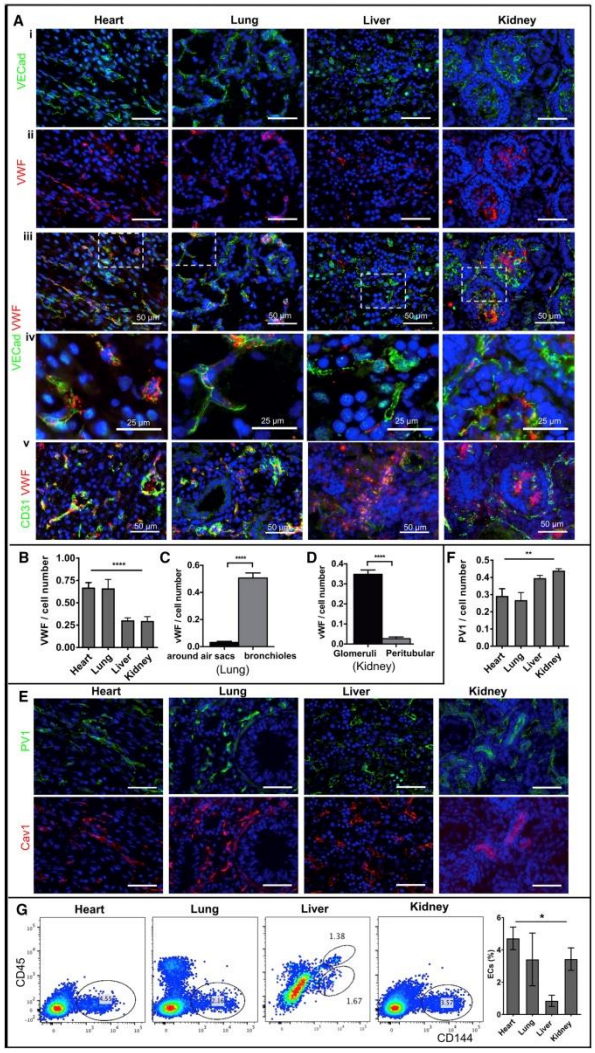

Figure 2.1 Human Fetal Endothelial Cells Show Organ-Specific Heterogeneity
Ex Vivo (A) Representative immunofluorescence images of frozen tissue sections from fetal human kidney, lung, liver, and heart stained with antibodies against VECad (i) and vWF (ii) with merged (iii) and zoomed (iv) views, and (v) CD31 and vWF. Scale bar: 50 µm (i–iii, v) and 25 µm (iv). (B–D) Quantification of vWF fluorescence area normalized to the number of CD31-positive cells for all four organs (B), within lungs (C), and kidneys (D). **** $p \leq 0.0001$.(E) Representative immunofluorescence images of frozen tissue sections stained with antibodies against PV1 and Cav1. Scale bar: 50 µm. (F) Quantification of PV1 fluorescence area normalized to the number of CD31-positive cells for all four organs. ** $p \leq 0.01$.(G) Representative flow cytometry profiles of fresh total cell tissue suspension from fetal human heart, lung, liver, and kidney stained with antibodies against CD45 and CD144. Endothelial population is gated as CD144-positive and CD45-negative cells (left panels). The percentage of endothelial cells is compared among tissues against the total cell number (right panel). Bar plots were made from n = 3

images per donor for two donors (B–D, F) or three donor sets (G). Data are presented as mean ± SEM *$p \leq 0.05$. SEM, standard error of the mean

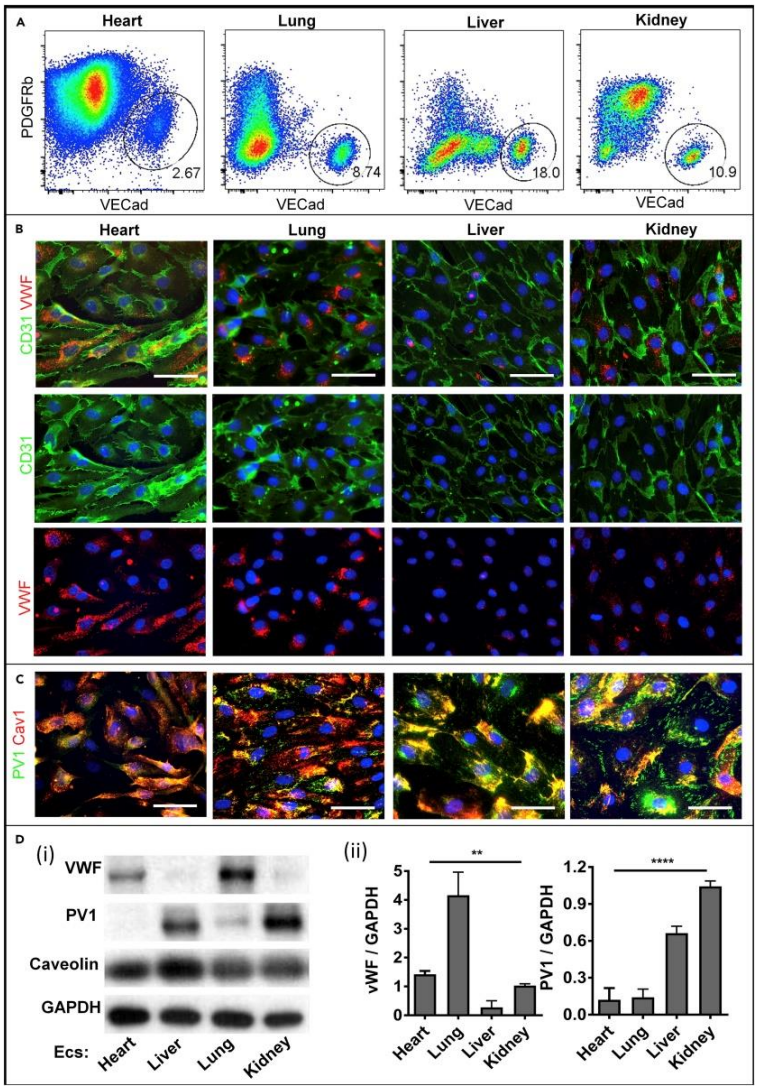

Figure 2.2 Human Fetal ECs Retain the *Ex Vivo* Heterogeneity upon *In Vitro* Expansion (A) Representative flow cytometry and sorting profiles of enriched cell suspension from fetal human heart, lung, liver, and kidney, stained with antibodies against VECad, PDGFRb. (B and C) Representative immunofluorescence images of CD31 and vWF (B) and PV1 and Cav1 (C) fluorescence in cultured heart, lung, liver, and kidney ECs (scale bars: 50 μm). (D) Representative western blot analysis (i) and densitometric quantification (ii) of vWF, PV1, and caveolin expression on cell lysates obtained from four ECs, using GAPDH as the loading control (n = 3 donors). Data are presented as mean ± SEM ** $p \leq 0.01$, **** $p \leq 0.0001$. SEM, standard error of the mean

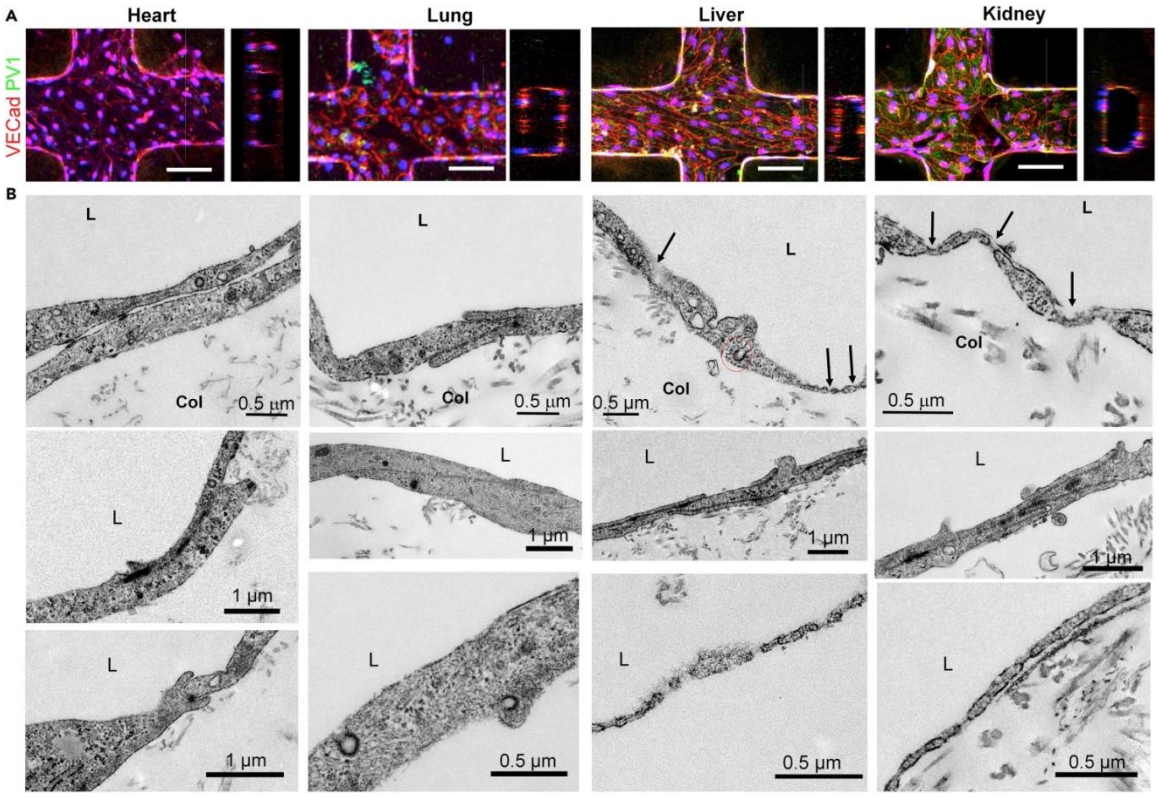

Figure 2.3 Ultrastructural Heterogeneity of Human Fetal ECs upon *In Vitro* Expansion (A) Projected immunofluorescence images and cross-sectional views of engineered perfusable, collagen-embedded, three-dimensional (3D) microvessel networks generated using the four types of organ-specific ECs (scale bar: 100 µm). (B) Transmission electron microscopy of 3D microvessel networks showing distinctive structural signatures. Black arrows indicate the presence of fenestrae, and red circles denote clathrin-coated alveolae.

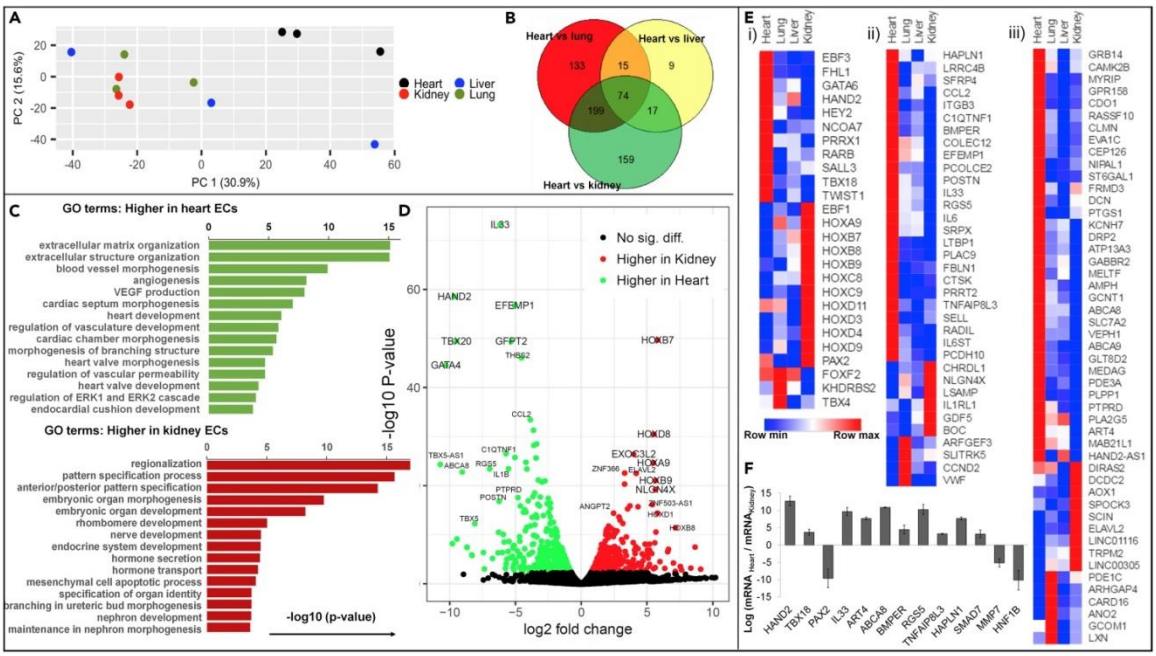

Figure 2.4 Global RNA Sequencing Reveals Heterogeneous Gene Expression Profiles among Four EC Types (n = 3 Donors) (A) 2D principle component analysis of RNA sequencing data for cultured organ-specific ECs showing clustered heart ECs compared with the kidney, lung, and liver ECs. (B) Venn diagram of differentially expressed heart-specific ECs genes with respect to kidney, lung, and liver ECs. (C and D) Gene Ontology terminology analysis (C) and volcano plot (D) showing different gene clusters for heart versus kidney ECs. (E) Heatmaps of bona fide markers for the heart-, kidney-, and lung-specific EC transcription factors and co-factors (i), angiocrine and signaling factors (ii), and metabolism-related and other genes (iii). (F) PCR validation of selected heart- and kidney-specific genes for additional three donor sets.

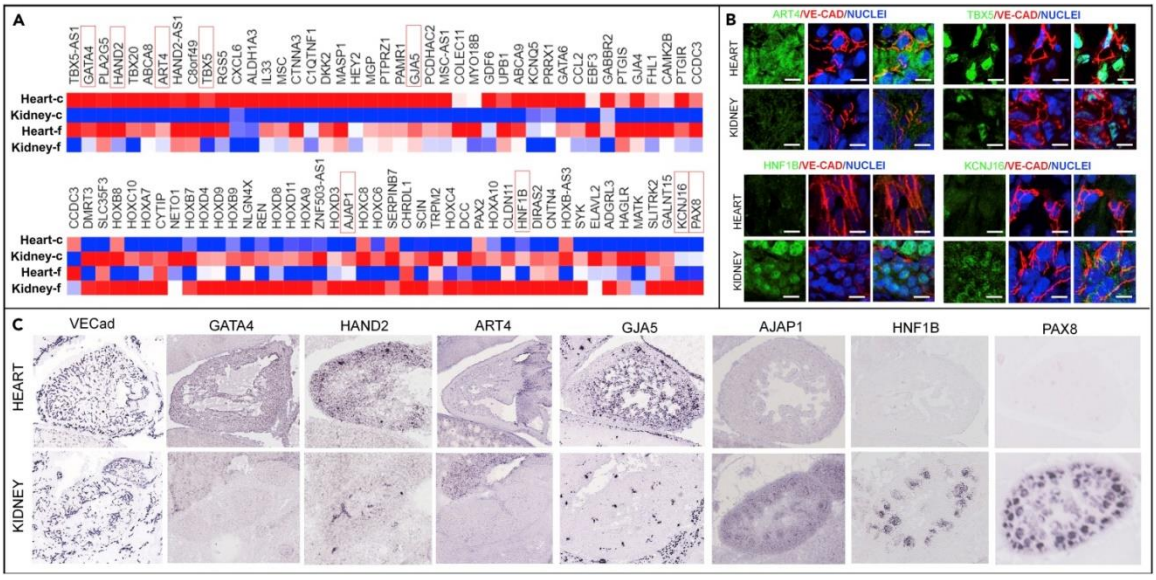

Figure 2.5 Validation of Heterogeneous Gene Expression Profiles in Freshly Isolated ECs and *Ex Vivo* Tissue Sections (n = 3 Donors) (A) Organ-specific genes identified from cultured sets (heart versus kidney) were validated in freshly isolated EC sets. (B) Immunostaining of selected genes for heart and kidney in human fetal tissues at 120 days. Scale bar: 100 μm. (C) Selected organ-specific gene expression in mouse embryo for heart and kidneys at E14.5 from Genepaint (genepaint.org).

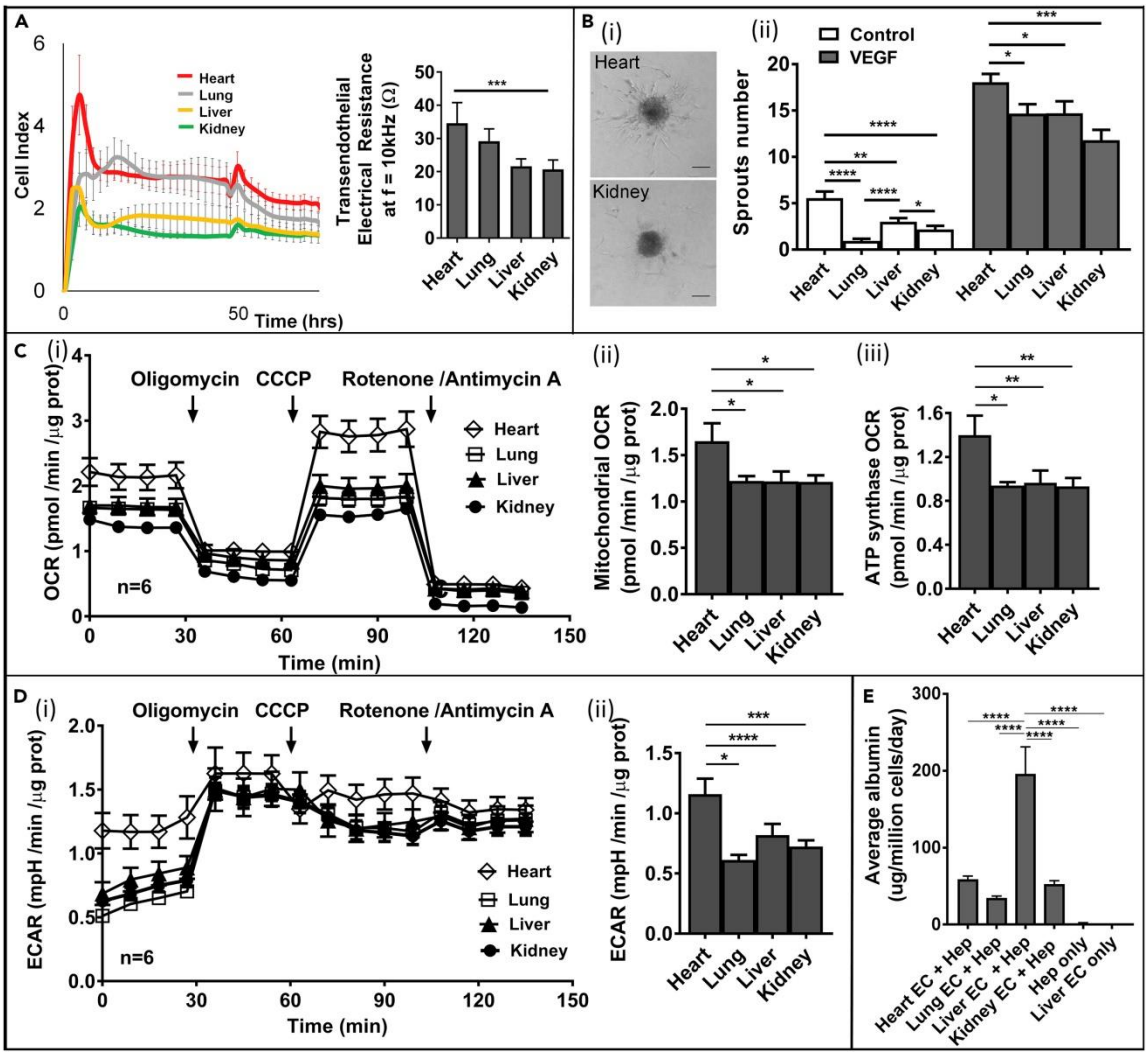

Figure 2.6 Cultured Organ-Specific Human Fetal ECs Display Distinct Vascular Functions and Bioenergetics and Support Specific Parenchyma Function (A) Left panel: Raw data of transendothelial electrical resistance measurement versus time for four types of ECs in monolayer culture. Cell index is calculated as $CI(t)=R(fn,t)-R(fn,t0)Zn$, where fn is the frequency at which the impedance measurement is carried out (*fn* = 10 kHz), *R(fn, t)* is the measured impedance at frequency *fn* at time point *t*, *t0* is the time when the background is measured, and *Zn* is the corresponding frequency factor of *fn* (*Zn* = 15 Ω). Right panel: Electrical impedance measurements (10 kHz frequency) for confluent monolayers of organ-specific ECs (n = 5 cultures). (B) Spheroid sprouting assay measurements of organ-specific EC angiogenic potential. (i) Representative bright-field images of heart and kidney EC sprouting spheroids, collagen-embedded, upon 24 hr of VEGF stimulation (40 ng/mL) (scale bar: 75 μm) and (ii) quantification of sprouts number at baseline and after VEGF stimulation (40 ng/mL) for organ-specific EC spheroids embedded in collagen matrix (24 hr) (n = 3 donors). (C) Seahorse measurements of total cellular oxygen consumption rate (OCR) in organ-specific ECs: (i) time course of cellular oxygen consumption upon sequential

addition of oligomycin (1 μM), CCCP (1 μM), and rotenone/antimycin A (1 μM each); (ii) quantification of mitochondrial OCR obtained upon electron transport chain inhibition with rotenone and antimycin A; and (iii) quantification of mitochondrial OCR due to ATP synthase activation obtained upon ATP synthase inhibition with oligomycin (n = 3 donors). (D) Seahorse measurements of total extracellular acidification rate (ECAR) in organ-specific ECs (n = 3 donors): (i) time course of extracellular acidification upon sequential addition of oligomycin (1 μM), CCCP (1 μM), and rotenone/antimycin A (1 μM each) and (ii) ECAR quantification. (E) ELISA measurement of albumin production from rat hepatocytes when cultured alone and when co-cultured with heart, lung, liver, and kidney ECs after 7 days (n = 4 replicates). Data information: data are presented as mean ± SEM *$p \leq 0.05$, **$p \leq 0.01$, ***$p \leq 0.001$, ****$p \leq 0.0001$. SEM, standard error of the mean

Chapter 3

Identify vascular niche function and underlying molecular mechanisms in human fetal liver hematopoiesis

This chapter is being prepared as a manuscript for submission to *Blood*:

Yoon Jung Choi, Brian J. Hayes, Daniel Lih, Samuel G. Rayner, Brandon K. Hadland, & Ying Zheng "Human fetal liver hematopoiesis is established by distinct populations of embryonic progenitors and supported by the fetal liver vascular niche." in preparation to Blood

3.1 Abstract

The human fetal liver is a critical site for prenatal hematopoiesis. However, the exact steps through which hematopoiesis is established in the fetal liver, and the progenitor cell populations involved in this process, remain poorly characterized. In this study, we identified multiple lineages of hematopoietic- and endothelial- progenitor cell populations present within human fetal liver, including phenotypic multilineage hematopoietic progenitor cells (HPCs, $CD45^{-}CD43^{+}CD235a^{-}$) and angiogenic hematopoietic progenitors (AHPs, $CD45^{-}CD43^{+}$ $CD144^{+}CD235a^{+}$). We showed that multilineage HPCs can develop into phenotypic hematopoietic stem cells (HSCs) and generate the entire spectrum of hematopoietic cells including T lymphocytes. In contrast, AHPs, which account for a small percentage of the hematopoietic population in the liver, have angiogenic and erythroid-myeloid-restricted hematopoietic potential. We demonstrated that these populations detected in the human fetal liver are phenotypically and functionally comparable to distinct hematopoietic progenitors identified by differentiation of human embryonic stem cells (hESCs) in vitro. Furthermore, we showed that human fetal liver endothelium, although lacking in hemogenic potential, contributes to hematopoiesis by secreting unique niche factors such as Wnt5a. Co-culture of bulk fetal liver HPCs ($CD45^{-}CD43^{+}CD144^{-}$) within an engineered liver vascular niche system led to a profound increase in phenotypic HSC numbers and multilineage colony-forming

progenitors. Knockdown of *WNT5A* in hepatic endothelial cells markedly reduced phenotypic HSC development and differentiation efficiency. Overexpression of *WNT5A* in non-liver endothelial cells improved their supportive role in hematopoiesis. Altogether, our findings show that fetal liver hematopoiesis is derived from distinct lineages of embryonic hematopoiesis including erythromyeloid-restricted AHP and multilineage HPCs, which are supported in part by the fetal liver endothelial-specific expression of Wnt5a. This study provides insight into the progression of hematopoiesis within human fetal liver, and will have import for the future development of in vitro systems for hematopoietic stem/progenitor cell expansion and differentiation.

3.2 Introduction

In the adult human, the bone marrow is the primary site of hematopoiesis – the process by which circulating blood cells are continuously formed and replaced throughout an organism's life. During development, however, the fetal liver is a major site of hematopoietic stem cell (HSC) differentiation, maturation, and proliferation [149]. Despite the importance of the fetal liver for establishing mature hematopoiesis, the exact process by which human fetal liver hematopoiesis occurs is not precisely understood and is largely extrapolated from studies of other mammals. In addition, the niche factors important for maintaining and guiding hematopoiesis in the fetal liver remain poorly characterized [45]. An improved understanding of human fetal liver hematopoiesis is necessary, both to increase knowledge of human hematologic and oncologic disorders, and because elucidating the pathways and niche factors involved in in vivo hematopoiesis will be valuable for in vitro regenerative medicine efforts [150].

Current understanding of mammalian hematopoiesis is derived largely from mouse studies. Murine hematopoiesis occurs in three distinct waves; primitive, erythro-myeloid progenitor (EMP), and multilineage hematopoiesis. Primitive hematopoiesis starts in the extraembryonic yolk sac mesoderm at embryonic day 7 (E7) with the formation of blood islands [151]. The first primitive erythroblasts – large, nucleated cells producing embryonic hemoglobin – emerge simultaneously with the development of the vasculature at E8. At E8.25, the yolk sac transiently gives rise to the second wave of hematopoiesis with the emergence of EMPs, which have broad erythroid and myeloid

potential, but rarely exhibit lymphoid potential [151, 152]. Erythroid progeny generated from EMPs are distinct from primitive erythroblasts as they develop into enucleated adult-like red blood cells and express fetal and adult hemoglobin. Definitive multilineage hematopoiesis commences in the aorto-gonad-mesonephros (AGM) at E10.5 [153, 154]. Definitive hematopoiesis is characterized by *de novo* generation of HSCs which give rise to the entire spectrum of hematopoietic cell types. HSCs differentiate from specialized vascular endothelial cells, hemogenic endothelial cells (HECs), which lose their vascular endothelial identity and acquire hematopoietic morphology and gene expression via an endothelial-to-hematopoietic transition (EHT) [155]. As development progresses, HSCs as well as their immature precursors migrate to the fetal liver, where they undergo further maturation, extensive expansion, and multilineage differentiation, before ultimately migrating to the fetal bone marrow just prior to birth. Previous studies have found that, in addition to being detected in the AGM, HECs capable of giving rise to HSC are found in the mouse head vasculature [156], vitelline and umbilical arteries [157], and placenta [158]. Whether the fetal liver contains HECs that contribute to HSC generation, or whether this organ merely serves as a site for the expansion and maturation of colonizing HSCs, is not fully determined [159]. Additionally, although HSC-derived hematopoiesis is known to contribute to cellular diversity in the fetal liver, recent studies in murine development suggest that HSC-independent waves of hematopoiesis, including yolk sac-derived EMP, also contribute to the initial progenitors colonizing the fetal liver hematopoietic niche [160].

Compared with the murine model, less is known specifically about human embryonic and fetal hematopoiesis. There is reason to believe the development of hematopoiesis proceeds differently in humans based simply on the size of the embryo, demand on the developing hematopoietic system, and different hematopoietic markers [161, 162]. Human pluripotent stem cells (hPSCs) can serve as a model of development, and recent advances in hematopoietic differentiation from hPSC have helped provide important insight of primitive and definitive hematopoiesis in humans [163]. One major focus in hPSC hematopoietic differentiation is to identify HECs that yield HSCs. Due to the overlap in endothelial and hematopoietic cell surface markers, however, distinguishing HECs from the vascular endothelium and the multipotent hematopoietic

precursor cells has been challenging [164]. CD43 is known to be expressed on all types of emerging clonogenic hematopoietic progenitors before the expression of pan-hematopoietic marker (CD45), and CD43 distinguishes the endothelial stage from the hematopoietic stage in hPSC differentiation [164, 165]. The markers for endothelial/mesenchymal stem cells (CD73) and arterial vascular endothelial cells (CD184) accurately distinguish HECs from non HECs amongst the global population of VE-cadherin^{+} (CD144) ECs in hPSC differentiation [164-166]. Gycophorin A (CD235a) is expressed on primitive and EMP progenitors whereas definitive HEC or HPCs are CD235a negative [167]. On the basis of these cell surface markers, three distinct CD144^{+} endothelial populations have been identified in the literature: 1) HECs (CD43-CD73-CD184-CD34+) [166, 168], 2) angiogenic hematopoietic progenitors (AHPs, CD43^{+}CD235a^{+}CD34^{+}) [165], and 3) non-HECs (CD43-CD73+) [165, 166, 168]. HECs undergo a stepwise progression to phenotypic multilineage HPCs (CD45^{-}CD43^{+}CD235a^{-}) and which subsequently express CD45 and are presumed to give rise to HSC with pan-hematopoietic activity including lymphocyte potential. AHPs are skewed toward hematopoietic differentiation, and can form hematopoietic colonies, but retain endothelial potential. Based on their capacity to give rise to progeny with erythroid and broad myeloid, but not lymphoid, potential, AHPs are thought to represent the hESC-derived equivalent of the transient wave of EMP hematopoiesis described in mouse yolk sac [164, 169]. Non-HECs have the features of endothelial cells, but do not retain hematopoietic differentiation potential. They have an inductive role in organ development and maintenance [69].

It is well established that the bone marrow vascular niche has an important role in maintaining adult HSC homeostasis [170-173]. Compared to bone marrow vascular niche, much less is known about the role of fetal liver endothelium in hematopoiesis. Fetal liver serves as the primary site where HSCs undergo extensive proliferation, maturation, and differentiation. Deciphering fetal liver endothelial specific molecular control in hematopoiesis could allow for the future *in vitro* expansion of HSCs with improved engraftment for therapeutic applications [150].

This study seeks to precisely define the cellular populations involved in fetal liver

hematopoiesis, as well as to explore the fetal liver vascular niche's contribution to hematopoietic cell expansion and differentiation. We exploited differences in cell-surface markers and T lymphoid differentiation potential to isolate and characterize endothelial and hematopoietic progenitors from human fetal liver (age 100-125 days). Consistent with previous studies in the murine embryo, we did not find HECs capable of giving rise to de novo hematopoiesis in human fetal liver, but rather identified distinct hematopoietic progenitor cell populations, namely AHPs and multilineage hematopoietic progenitor cells. We suspect that the presence of both AHPs and multilineage hematopoietic progenitor cells may reflect colonization of the fetal liver by distinct waves of EMP and HSC/multilineage progenitors, respectively, derived from initial embryonic hemogenic sites such as the yolk sac and AGM. To elucidate the role of the fetal liver endothelial niche in supporting hematopoiesis, we compared the effect of co-culture with either E4ORF1-transduced liver (E4LECs) or heart ECs (E4HECs) on hematopoiesis. We observed improved proliferation and differentiation of hematopoietic cells co-cultured with E4LECs. We further identified Wnt5a as a major liver vascular niche factor. Gain- and loss-of-function mutations of *WNT5A* in ECs confirmed the supportive role of *WNT5A* in hematopoiesis. Altogether, our study provides an enhanced understanding of human hematopoiesis, which will provide insight into human disease and may guide in vitro differentiation protocols for regenerative medicine.

3.3 Experimental methods

Flow cytometry analysis

All experiments were approved by the Institutional Review Board of the University of Washington (IRB447773EA). Human fetal tissues, including liver, kidney, heart, and lung were obtained upon informed consent from abortion material (age 16-20 weeks). Human fetal tissue was finely minced in serum-free EBM-2 endothelial growth medium (Lonza) supplemented with collagenase type IV (Sigma) and DNase (Roche) and incubated for 30 min at 37 ^{0}C in a water bath with shaking. The resulting tissue homogenate was filtered through a 40 μm cell strainer (BD Falcon) to remove tissue debris and large vessels. To investigate the hematopoietic and endothelial progenitor cells in the fetal liver, enzymatically digested liver populations were stained for the surface

markers of HSCs, MPPs, HECs, multilieage HPCs, AHPs, and non HECs. Multiparameter FACS analysis was performed on a BD FACSCanto II (Beckton Dickinson) and quantitated with FlowJo software (Tree Star). Unstained controls, single stained cellular controls, and CompBeads (BD Pharmingen) were used for voltage adjustments and compensation.

MACS sorting of fetal liver CD45-CD43-CD144+ endothelial cells

$CD45^{-}CD43^{-}CD144^{+}$ cells were isolated by MACS. CD45 negative cells were isolated by collecting the flow-through fraction after CD45 labeling. CD43-depleted cells were then obtained. This population was labeled with CD144, and the magnetically retained cells on the LS column were collected. Human anti-CD45 (Miltenyi Biotec), human anti-CD43 (Miltenyi Biotec), human anti-CD144 (Miltenyi Biotec), MicroBeads, LS+ column, and MidiMACS magnet were used.

Generation of hESC-derived HECs and AHPs

hESC differentiation was performed as previously described [174, 175]. In brief, hESC colonies were dissociated with Trypsin-Versene (Life Technologies) and resuspended in pluripotency medium containing CHIR99021(Cayman Chemical) for 24 h. Cells were then cultured with RPMI medium (Life Technologies) supplemented with 50 ng ml^{-1} activin A (R&D Systems) and 40 ng ml^{-1} BMP4 (R&D Systems) on days 0 and 1, respectively. On day 2, directed endothelial differentiation was performed by replacing the media with Stempro34 media (Life Technologies) containing 200 ng ml^{-1}VEGF (PeproTech), 10 ng ml^{-1} BMP4(R&D Systems), 5 ng ml^{-1} bFGF (PeproTech), 50 μg ml^{-1}ascorbic acid (Sigma-Aldrich), and 0.4 mM monothioglycerol (Sigma-Aldrich) for 5 days. From days 5-8, medium was changed to StemPro-34 with 10 ng ml^{-1} bFGF, 15 ng ml^{-1}VEGF, 10 ng ml^{-1} interleukin (IL)-6 (PeproTech), 25 ng ml^{-1} IGF-1 (PeproTech), 5 ng ml^{-1} IL-11 (PeproTech), and 50 ng ml^{-1} SCF (PeproTech). On day 8, freshly dissociated hESCs were stained and sorted using FACS. All FACS sorting was performed on a BD FACS Aria I or II cell sorter.

EHT assay and colony forming assays

Liver multilineage HPCs and AHPs and HECs and AHPs derived from both in

vitro hESC differentiation were co-cultured on E4EC in serum-free StemSpan SFEM (StemCell Technologies) supplemented with Pen-Strep (Invitrogen), 100 μM monothioglycerol (MTG; Sigma-Aldrich), 50 μg/ml ascorbic acid, 50 ng/ml rhSCF (Peprotech), 20 ng/ml rhTPO (Peprotech), 20 ng/ml rhIL6 (Peprotech), 20 ng/mlrh IL3 (Peprotech), and 20 ng/ml rhFLT3L (Peprotech) for 7 days. Half the media was replaced with fresh media on day 3. Following 7 days of co-culture, non-adherent cells were resuspended by vigorous pipetting and passed through a 40 μm cell strainer (BD Falcon). The harvested cells were either analyzed by flow cytometry or put through CD34-positive MACS selection. Positively selected populations were plated in complete methylcellulose medium containing human cytokines including SCF, GM-CSF, IL-3, G-CSF, EPO (Stem cell technologies). The complete methylcellulose media was additionally supplemented with 20 ng/mL rhFLT3L (Peprotech) and 50ng/mL IL-6 (Peprotech). Colonies were analyzed at day 14 for total colony number, and each colony classified based upon morphologic criteria as granulocyte, erythrocyte, monocyte, megakaryocyte (CFU-GEMM), granulocyte/monocyte/macrophage (CFU-GM), or burst-forming erythroid (BFU-E).

T cell differentiation

After EHT assay, non-adherent cells were resuspended by vigorous pipetting and passed through a 40 μm cell strainer (BD Falcon). The harvested cells were plated on OP9-Dll4 in α-MEM (Invitrogen) supplement with Pen-Strep (Invitrogen), 20% FBS (Hyclone), 100 μM monothioglycerol (MTG; Sigma-Aldrich), 50 μg/ml ascorbic acid, 50 ng/ml rhSCF (Peprotech), 20 ng/ml rhIL6 (Peprotech), 5 ng/mlrh IL3 (Peprotech), and 50 ng/ml rhFLT3L (Peprotech) for 14-21 days

RNA isolation and qRT-PCR

Total RNA from human fetal liver and heart endothelial cells was purified using the RNAeasy Mini Kit (Qiagen). Residual DNA was removed by on-column DNase digestion. RT-PCR was performed using the Real-time PCR System (Applied Biosystems) with Fast SYBR Green Master Mix (Applied Biosystems). The amount of target RNA gene was normalized to GAPDH RNA. Primer sequences were as follows: HBG1 F- 5'-AGA AGA TGG TGA CTG GAG TG -3' and R-5'- TTA TTT GAT TGC TTG CAG

AA -3', HBE1 F-5'- GTG CTG ACT TCC TTT GGA GA -3' and R-5'- ACA CCT GCA AAC TGG AAG AG -3', HBB F-5'- TCT GTC CAC TCC TGA TGC TG-3' and R-5'- CAC TGG TGG GGT GAA TTC TT -3', WNT5A F-5'- TAG CAG CAT CAG TCC ACA AA -3' and R-5'- CAA AAC ACG GCA TCT CTC TT -3', WNT5B F-5' - GCG AGG ACT CTC AGG ATG TA -3' and R-5'- AGA CAT CGA GGT TGA AGC TG -3', E4ORF1 F-5'- CCT GCG GGT ATG TAT TCC CC-3' and R-5'- GAC AGC TCC TCG GTC ATG TC-3'

Detection of Wnt5a protein by ELISA

The total protein concentrations of liver and heart EC lysates were quantified using Pierce™ BCA (Thermo Fisher Scientific). ELISA assay for Wnt5a quantification was performed using a commercially available ELISA kit (LS Bio) according to the manufacturer's instructions.

E4ORF1 transduction of hepatic and cardiac ECs

MSCV-N E4orf1 was a gift from Karl Munger (Addgene plasmid # 38063). For retroviral vector production, platinum GP retroviral packaging cells (Cell Biolabs) were cultured in 150 mm dishes (Corning Life Science) to 80-90 % confluency. The cells were transfected with VSV-G, gag, pol, E4orf1, and Lipofectamine 3000 (Invitrogen) in DMEM (Thermo Fisher Scientific) for 17 h. Cells were then cultured in complete medium for 48h and supernatant was collected, filtered, and concentrated via ultracentrifugation. The viral pellet was resuspended in serum-free DMEM and stored at -80 C. Isolation and cultivation of human fetal liver and cardiac ECs were performed as described previously [176]. 70 - 80% confluent hepatic and cardiac ECs were incubated twice with lentiviral particles at 12 hour intervals. After infection, cells were selected by 2.5 µg/ml Puromycin (Invitrogen) for 5-8 days. E4ORF1 transduction was verified by qPCR. The ability of transduced cell lines to survive without serum was verified. $CD43^+$ HPCs were plated on the transduced EC lines.

KO E4LEC and OE E4EC production

pGIPZ lentiviral shRNA against WNT5A plasmid (Dharmacon) was used for constitutive WNT5A knockdown. Lentiviral particles were generated in HEK293T cells

using a second-generation packaging system. E4LECs were transfected with lentiviral particles. After 7-10 days of transduction, Puromycin-resistant and GFP-positive KO E4LECs were sorted by flow cytometry and transgene expression levels were quantified by RT-qPCR. pLX304 lentiviral vector (Dharmacon) that encodes a blasticidin resistance genes and WNT5A ORF expression from a cytomegalovirus (CMV) promoter was used to generate WNT5A overexpressed HUVECs. WNT5A lentivirus was produced in HEK293T cells and used to infect HUVECs. After infection, cells were selected by 2.5 µg/ml blasticidin (Invitrogen) for 5-8 days. WNT5A transduction was verified by qPCR.

3.4 Results

Human fetal liver contains multiple lineages of hematopoietic and endothelial progenitor cells

To identify whether HECs are present in the fetal liver, we stained freshly digested human fetal liver at 3 month gestation with HEC surface markers ($CD144^+CD34^+CD73^-CD184^-$) [166]. In the population of human fetal liver studied here, no cells displaying a staining pattern consistent with HECs were identified (Fig. 3.1A). ITGB3 (CD61), which is a marker of HECs, was not expressed in liver-specific ECs ($CD144^+CD34^+CD45^-CD43^-$) either (Fig. 3.1Aii). To assess the functional properties of endothelial cells, $CD45^-CD43^-CD144^+$ liver ECs were cultured for 10 days on subconfluent E4ORF1-transduced primary human endothelial cells (E4ECs) in serum free media supplemented with hematopoietic cytokines for 10 days (Fig. 3.1Aiii). Under these conditions the cells failed to generate $CD43^+$ and $CD45^+$ cells and did not yield any hematopoietic colonies (Fig. 3.1A iv & v). These results are consistent with our inability to detect phenotypic HECs in the human fetal liver. This data suggests that human fetal liver hematopoiesis is established by migratory blood stem/progenitors generated elsewhere, rather than de novo generation from HEC in situ, although we cannot rule out the existence of transient HECs in the early fetal liver prior to the developmental stages analyzed here.

Given the strong evolutionary conservation of anatomical sites where hematopoiesis occurs in the mouse and human [177, 178], we hypothesized that yolk sac-

derived lineage-restricted erythroid myeloid progenitors and AGM-derived HSCs migrate to the human fetal liver and establish human embryonic hematopoiesis. Consistent with the established role of the fetal liver as a site of HSC expansion, flow cytometry analysis identified phenotypic HSCs (2.79 ± 1.19 %) amongst the fetal liver hematopoietic cells expressing the pan-hematopoietic marker CD45 (Fig.3.1B). In addition to a $CD45^+$ hematopoietic population, we detected a large number of $CD45^-CD43^+CD235a^{+/}$cells suggesting the presence of earlier hematopoietic progenitor populations that have not yet acquired CD45 expression (Fig.3.1C & Appendix B, Supplementary Figure 1C). A direct cytospin of the unsorted liver cells shows early hematopoietic progenitors constitute the most abundant cells in the human fetal liver (Appendix B, Supplementary Figure 1E). Importantly, the population of $CD45^-CD43^+$ hematopoietic progenitor cells in the liver is heterogeneous for CD144 expression and phenotypic AHPs were only detected in the liver. The presence of significant numbers of phenotypic multilineage HPCs in the liver, compared with other organs, suggests that this population uniquely colonizes the fetal liver, consistent with its role in supporting hematopoiesis during fetal development.

Multilineage HPCs and AHPs have different hematopoietic potential

We next sorted phenotypic multilineage HPCs and AHPs by FACS and cultured them separately on E4EC in pro-hematopoietic media to further explore their differentiation potential (Fig. 3.2). Phenotypic multilineage HPCs generated both phenotypic HSCs (7.26± 5.92 %) and multipotent progenitors (MPPs) (11.9± 3.82 %), whereas AHPs generated only cells with MPP phenotype (11.5± 6.27 %) (Fig. 3.2Bii &Cii). Both phenotypic multilineage HPCs and AHPs generated similar numbers of CFU-GEMM, CFU-GM, and BFU-E (Fig. 3.2B-Diii). To further assess the morphology of colonies, we examined Giemsa-stained cytospin smears (Fig. 3.2Biv & Civ). The presence of distinct phases of erythrocyte (polychromatic normoblast, orthochromic normoblast, polychromatic erythrocyte) and myeloid (promyelocyte, myelocyte, metamyelocyte) maturation, as well as multiple types of fully mature myeloid progeny (neutrophil, eosinophil, monocyte, basophil, and macrophage) was observed in both population pools, indicating their pan-erythroid-myeloid hematopoietic potential. We next examined the hemoglobin composition of CFC-derived colonies from phenotypic

multilineage HPCs and AHPs. qRT-PCR analyses showed that most colonies from multilineage HPCs and AHPs express γ-globin and show very low levels of ε-globin. (Fig. 3.2Div) Compared with cord blood, these two populations have significantly higher expression of γ-globin and less β-globin. Interestingly, in the presence of pro-angiogenic cytokines, AHPs formed a cobblestone like endothelial monolayer and expressed CD144, suggesting that this population contains cells that retain the potential for endothelial cell differentiation under different culture conditions. (Fig. 3.2Di) On the contrary, multilineage HPCs lack angiogenic potential (data not shown).

As T lymphoid potential is a key feature distinguishing HSCs from EMP [179], non-adherent hematopoietic cells generated from these two populations after E4EC coculture were harvested, seeded directly onto OP9-Dll4 stroma and cultured for 14-21 days to promote lymphoid development. Notably, lymphoid potential was restricted to the cells derived from multilineage HPCs (Fig. 3.3). Multilineage HPCs gave rise to CD5 and CD7 single and double positive. Our observations that AHPs have an erythroid/myeloid–biased fate potential and express endothelial markers correlate with prior research done on EMPs in the murine model [160, 180-182]. Together, these findings provide strong evidence that two types of hematopoiesis occur in the fetal liver: AHP-derived definitive erythromyeloid hematopoiesis and HSC-derived definitive hematopoiesis.

<u>In vitro hematopoietic differentiation of hESCs mirrors human fetal liver hematopoiesis</u>

To mimic human fetal liver hematopoiesis, we used a hESC system to map the generation of HECs and AHPs and define their lineage potential (Fig. 3.4A). The stepwise differentiation from hESC to phenotypic HECs and AHPs was achieved via posterior mesoderm formation (day 2) to endothelial fate specification (day 5) [183]. Phenotypic HECs and AHPs at day 8 were FACS sorted and cultured on E4ECs with pro-hematopoietic media. hESC-derived HECs gave rise to multilineage HPCs and further developed into phenotypic HSCs and MPPs (Fig. 3.4Bii). AHPs didn't developed into phenotypic HSCs, but did give rise to MPPs (Fig. 3.4Cii). Both HECs and AHPs gave rise to CD71 and CD235a single and double positive erythroid lineage cells and CD10

and CD13 single and double positive myeloid cells [184] (Fig. 3.4D). In contrast, CD4 T-lymphoid cell development occurred only from HECs (Fig. 3.4E)[185]. The fact that multilineage HPCs in the liver and hESC-derived HECs share common lineage fates suggests that HECs undergo a stepwise transition to form multilineage HPCs and subsequently HSCs. This correlates with the transient presence of HECs found in restricted anatomical sites. Our data suggests that multilineage HPCs migrate to the fetal liver and subsequently establish fetal hematopoiesis. We found that hPSC-derived AHPs exhibit a restricted lineage fate potential and phenotype that highly resembles that of the AHP population found *in situ* in the human fetal liver.

Fetal hepatic endothelium promotes development of phenotypic HSCs and multilineage colony forming progenitors

Endothelial cells within the bone marrow microenvironment are known to support HSC maintenance and hematopoiesis [186-188]. We therefore hypothesized that the fetal liver vascular niche populated by HSCs and $CD45^{-}CD43^{+}$ HPCs may represent a regulatory site for definitive hematopoiesis. To assess paracrine function we generated E4ORF1-transduced liver ECs (E4LECs) and heart ECs (E4HEC) which survive without serum, thereby minimizing serum-mediated HSC self-renewal inhibition when co-cultured (Fig. 3.5) [189]. To test whether the host endothelial cell transcriptome was significantly altered by viral infection, the transcripts of liver-specific (HOXB4, HOXB7) and heart-specific (i.e., HAND2, ART4, TBX5, RGS5) genes were quantified for both native ECs and E4ORF1-transduced ECs (Appendix B, Supplementary Figure 5). We observed that the engineered cell lines maintained their organ-specific gene expression profiles, validating the use of reprogrammed cells to study vascular niche function. We then compared in vitro generation of multilineage hematopoietic progenitors from bulk liver HPCs ($CD45^{-}CD43^{+}CD144^{-}$) co-cultured with E4LECs versus E4HECs. The HPCs co-cultured with E4LECs generated increased numbers of phenotypic HSCs and lineage-committed $CD34^{+}CD38^{+}$ cells compared with the cells co-cultured with E4HEC (Fig. 3.5Ci). The bulk HPCs co-cultured on E4LECs also generated increased numbers of colony forming progenitors (Fig. 3.5Cii), particularly CFU-GEMM and BFU-E. We next tested whether our engineered liver ECs support in vitro expansion of blood cells

developed from hESC-HECs. Interestingly, hESC-HECs cultured on E4LECs generated significantly higher numbers of phenotypic HSCs and $CD34^+CD38^+$ cells compared with other transduced endothelial cell lines (Figure 3.5D). Altogether, these findings demonstrate that the fetal liver EC niche plays a role in supporting multilineage hematopoiesis.

Wnt5a is a major liver-specific vascular niche factor that promotes hematopoiesis

We have previously shown that, compared with fetal heart ECs, fetal liver ECs are highly enriched for pathways involved in regulation of leukocyte and homotypic cell-cell adhesion, the immune response, and bone marrow development [176]. In this study, we sought to determine which factors were secreted by human fetal liver ECs that might explain their improved support of hematopoiesis, when compared with human fetal heart ECs. To this end, we performed qPCR on both fetal liver and heart ECs to quantify the expression of differentially expressed human fetal liver genes identified in our prior work that are known to regulate HSC maintenance and differentiation (Fig. 3.6A). Interestingly, Wnt family genes that are key regulators of definitive hematopoiesis (*WNT5A, WNT5B)* were much more highly expressed in the liver ECs, compared with heart ECs. Enzyme-linked immunosorbent assay (ELISA) for Wnt5a protein was performed on the lysates of liver ECs and heart ECs from the same donors, confirming that fetal liver ECs express higher levels of Wnt5A protein than heart ECs (Fig. 3.6B). Given the established role for non-canonical Wnt5a in the HSC-supportive niche [190-194], we hypothesize that differentially expressed *WNT5A* in the liver is a major niche factor governing embryonic HSC cell fate during development. To test the function of *WNT5A* in hematopoiesis, we generated E4LECs with endogenous *WNT5A* knocked down by small hairpin RNA (shRNA) (Fig. 3.6C). qPCR showed significant suppression of *WNT5A* in knockout E4LECs (KO E4LECs) compared with E4LECs (Appendix B, Supplementary Figure 6). We then compared *in vitro* hematopoietic differentiation from liver HPCs co-cultured with KO E4LECs versus E4LECs. The overall level of cells generated from $CD45^-CD43^+$ HPCs was reduced about 1.5 fold in KO E4LECs. The cells co-cultured with KO E4LECs showed a decreased percentage of phenotypic HSCs (1.58±0.22 fold reduction) and lineage committed $CD34^+CD38^+$cells (2.32±0.46 fold reduction) compared with

E4LECs (Fig 3.6C). The bulk HPCs co-cultured with KO E4LECs generated decreased numbers of colony forming progenitors, particularly CFU-GEMM (4.96±0.76 fold reduction) and BFU-E (2.76±1.07 fold reduction) (Fig. 3.6Cv). These findings indicate significant loss of hematopoiesis support in KO E4LECs. We then generated WNT5A overexpressed E4ECs (OE E4ECs) to confirm whether *WNT5A* overexpression could provide non-liver endothelial cells with an increased ability to support hematopoiesis (Fig. 3.6D). OE E4ECs had 5.75±1.77-fold higher *WNT5A* transcription compared with E4ECs. Co-culture with OE E4ECs led to a ~4-5 fold increase in hematopoietic cells, relative to co-culture with E4EC. The increase in clonogenic cells from bulk HPCs co-cultured with OE E4ECs was accompanied by an equivalent increase in phenotypic HSCs (2.25 ± 0.27 fold increase) and $CD34^{+}CD38^{+}$ cells (1.68 ±. 0.12 fold increase) compared with E4ECs. Similarly, hES-HECs cultured with KO E4LECs showed a 1.20± 0.01-fold reduction in HSC frequency compared with hES-HECs cocultured with E4LECs (Appendix B, Supplementary Figure 7). Collectively, these data suggest that Wnt5a expression in liver ECs plays a pivotal role in supporting fetal liver hematopoiesis.

3.5 Discussion

Studies in murine models have shown that fetal liver hematopoiesis is established by migratory hematopoietic cells, including EMPs and HSCs, rather than through de novo generation of HSCs from the liver endothelium [160, 195]. Until now, the contribution of embryonic waves of EMP and HSC to human fetal liver hematopoiesis has not been fully determined, due to factors including a scarcity of human tissue and a lack of appropriate techniques. In this study, we identified two distinct liver-specific differentiation programs: AHP- and HSC- hematopoiesis. Our work confirms that hematopoiesis proceeds without the presence of native liver-specific HECs, but rather through the influx of multilineage HPCs and AHPs generated early in human development. Our work characterizes the AHP cellular population, which we believe to be the progenitor of the human correlate to murine EMPs. We observed increased generation of phenotypic HSCs and differentiated hematopoietic progeny including cells with erythroid and multilineage CFU potential following co-culture with liver EC, highlighting the important role that the fetal liver vascular niche plays in supporting

hematopoiesis, and we identified Wnt5a as a key factor in this process.

AHP-hematopoiesis in the human fetal liver shares several features with murine EMPs, including a lack of lymphoid potential, and expression of the endothelial marker [160, 181, 182, 196]. Erythroid progeny generated from AHPs mature into enucleated erythrocytes and express fetal and adult hemoglobin genes, similar to the erythroid progeny generated from murine EMPs. Repressed ε-globin expression and γ-globin acquisition is reported to mark the onset of definitive erythroid hematopoiesis [197-199]. The switch from γ-globin to adult β-globin occurs shortly after birth [200]. Upregulated γ-globin and suppressed ε-globin expression of CFC-colonies from multilineage HPCs and AHPs suggest their definitive erythroid lineages. Significantly higher expression of γ-globin in these two populations, compared with cord blood, marks their fetal specific features. The overlap between erythroid progenies differentiated from AHPs or HSCs in morphology, hemoglobin composition, and spatiotemporal presence might represent their complementary contributions to human fetal erythropoiesis to meet the needs of the growing human fetus.

To trace the ontogeny of multilineage HPCs and AHPs, we used a hESC system to map early human hematopoietic programs. Based on our hESC differentiation model, we identified fundamental differences among HECs, AHPs, and non-HECs, consistent with previous findings [165, 201]. The different cell lineage capacity of these endothelial progenitors suggests that cells proceed through the hematopoietic hierarchy in a stepwise differentiation.

Recent attention has been given to EC progenitors in local tissues. EC progenitors develop into organ-specific ECs, aiding in the establishment of unique organ-specific vascular niches to support resident stem/progenitor cells. Our results support a model in which inductive signals from the fetal liver vascular niche support definitive fetal hematopoiesis, findings which could enhance directed hPSC differentiation models for the in vitro development of definitive hematopoietic cells for therapeutic use. We hope that the power of E4LECs to improve the differentiation efficiency of hESC-HECs during co-culture can be harnessed to enhance the in vitro generation of multilineage hematopoietic progenitors for human therapeutic purposes. Wnt family proteins, which

are highly expressed in the bone marrow, are known to be a major niche factor regulating HSC expansion and differentiation [202-204]. A recent study showed that hPSCs are triggered by canonical Wnt signaling to initiate definitive hematopoiesis [179]. Interestingly, canonical Wnt/β -catenin signaling is also required to establish HEC in the AGM [56], but must be downregulated for subsequent HSC induction [57]. Wnt5a is a non-canonical Wnt protein that can inhibit the canonical Wnt pathway. Here, using WNT5A KO E4LECs and OE E4ECs, we showed that non-canonical Wnt signaling plays a stage-specific role in the expansion and differentiation of ontogenetically divergent definitive hematopoietic cells in the fetal liver. Interestingly, the frequency of phenotypic HSC generated from liver HPCs or hESC-HECs was higher when co-cultured with E4LECs versus with OE E4ECs (Fig.6 and Fig. S7A), suggesting that there are likely other factors in addition to Wnt5A that are differentially produced by the fetal liver endothelium and support definitive HSCs generation in the fetal liver. Further studies will be required to identify other fetal liver-specific molecules and/or chemokines that shape the specialized functionality which supports fetal liver hematopoiesis.

In summary, we have characterized cellular populations important for human fetal liver hematopoiesis, outlined the different differentiation potential of multilineage HPCs and AHPs, replicated the human fetal vascular niche in vitro, and investigated the role of *WNT5A* in supporting hematopoiesis. Liver vascular-specific paracrine signals that we identified herein will provide a strong foundation for understanding how the liver niche supports HSC self-renewal and proliferative expansion. Our findings provide insight into native human hematopoietic programs that could be used for in vitro production of definitive hematopoietic cells for therapeutic applications

3.6 Figures

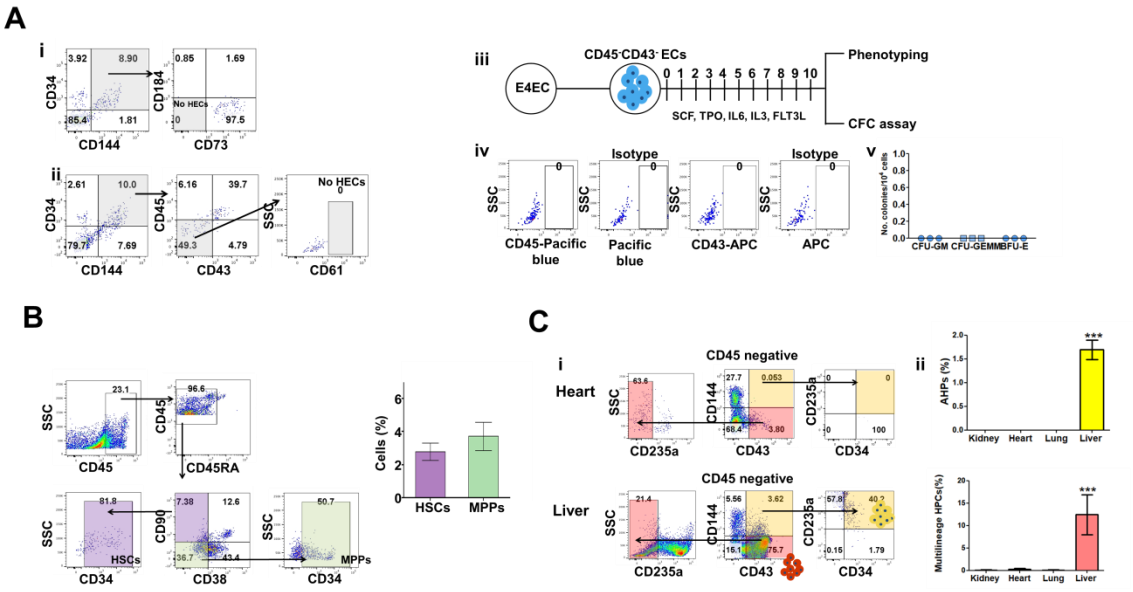

Figure 3.1 Human fetal liver contains multiple lineages of hematopoietic and endothelial progenitors A. FACS analysis was performed on freshly digested human fetal liver samples isolated from human fetal tissue at 3 month gestation. Analysis performed for two different combinatorial markers defining definitive hemogenic endothelial cells (HECs), i) CD144+CD34+CD73-CD184- and ii) CD144+CD34+CD43-CD45-CD61+ confirmed the absence of HECs in fetal liver, and corroborating this, iii) CD45 and CD43 depleted CD144+ populations were put through hematopoietic differentiation culture and didn't yield iv) hematologic cells or v) hematopoietic colonies (n=3 donors). B. Hematopoietic stem cells (HSCs, CD45+CD45RA-CD38-CD90+CD34+) and multipotent progenitors (MPPs, CD45+CD45RA-CD38-CD90-CD34+) were found in human fetal liver. The percentage of HSCs and MPPs versus the total number of liver cells was quantified (n=3 donors, mean ± SEM). C. i) Earlier hematopoietic progenitor populations, including angiogenic hematopoietic progenitors (AHPs, CD45-CD43+CD144+CD235a+CD34+) and multilineage hematopoietic progenitor cells (HPCs, CD45-CD43+CD144-CD235a-) take up residence in human fetal liver. ii) The percentage of AHPs and multlineage HPCs are compared among tissues from the same donors against the total cell numbers (n=3 donors, mean ± SEM).

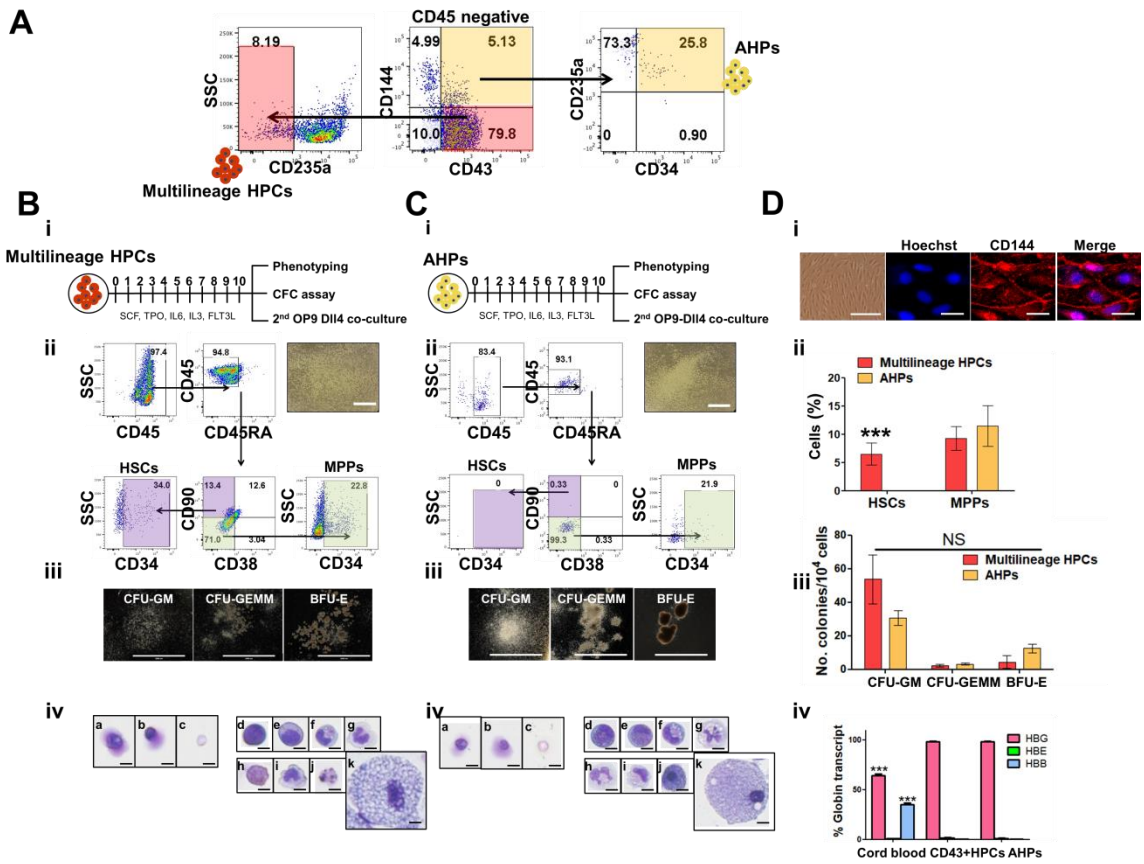

Figure 3.2 Multilineage HPCs and AHPs have different hematopoietic potential A. Multilineage HPCs and AHPs in the fetal liver were isolated by fluorescence-activated cell sorting (FACS) to further explore their differentiation potential. Bi) Multilineage HPCs and Ci) AHPs were FACS-sorted and cultured atop E4ECs in pro-hematopoietic media for 10 days (Bii) Multilineage HPCs have the features of both phenotypic HSCs and MPPs while (Cii) AHPs only have features of MPPs. Scale bar = 250 µm (right panel) Di) Representative bright-field images of AHPs cultured in endothelial media at passage 1 (Left, scale bar 200 µm) and stained with antibodies against CD144 and Hoechst (Right, scale bar 25 µm). Dii) Quantification of emerging hematopoietic cells (n=3 donors, mean ± SEM,***P<0.01) Biii) and Ciii) Both multlineage HPCs and AHPs have hematopoietic colony forming potential. (scale bar, 2,000 um). Diii) Quantification of CFC assay (n=3 donors). Cytospins of Giemsa stained (Biv) multilineage hematopoietic cells and (Civ) AHPs. (a) polychromatic normoblast, (b) orthochromic normoblast, (c) polychromatic erythrocyte, (d) promyelocyte, (e) myelocyte, (f) metamyelocyte, (g) polymorphonuclear neutrophil, (h) eosinophil, (i) monocyte, (j) basophil, and (k) macrophage. (Div) Hemoglobin composition of CFC-derived colonies from multilineage HPCs and AHPs were quantified by using qRT-PCR (n=3 donors, mean ± SEM,***P<0.01)

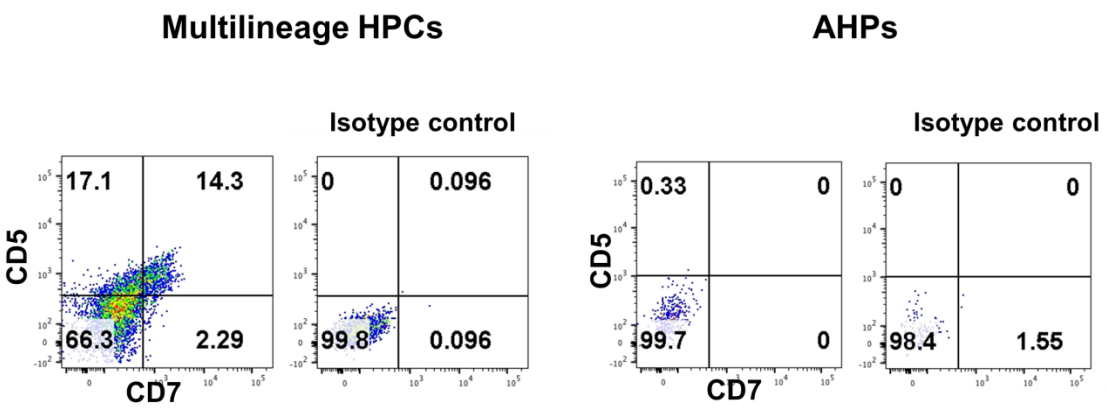

Figure 3.3 T lymphoid potential was restricted to the cells from multilineage HPCs
Representative flow cytometry profiles of cells arise from multilieage HPCs and AHPs after secondary OP9-Dll4 co-culture for 14-21 days. Cells were stained with T cell markers (CD5 and CD7).

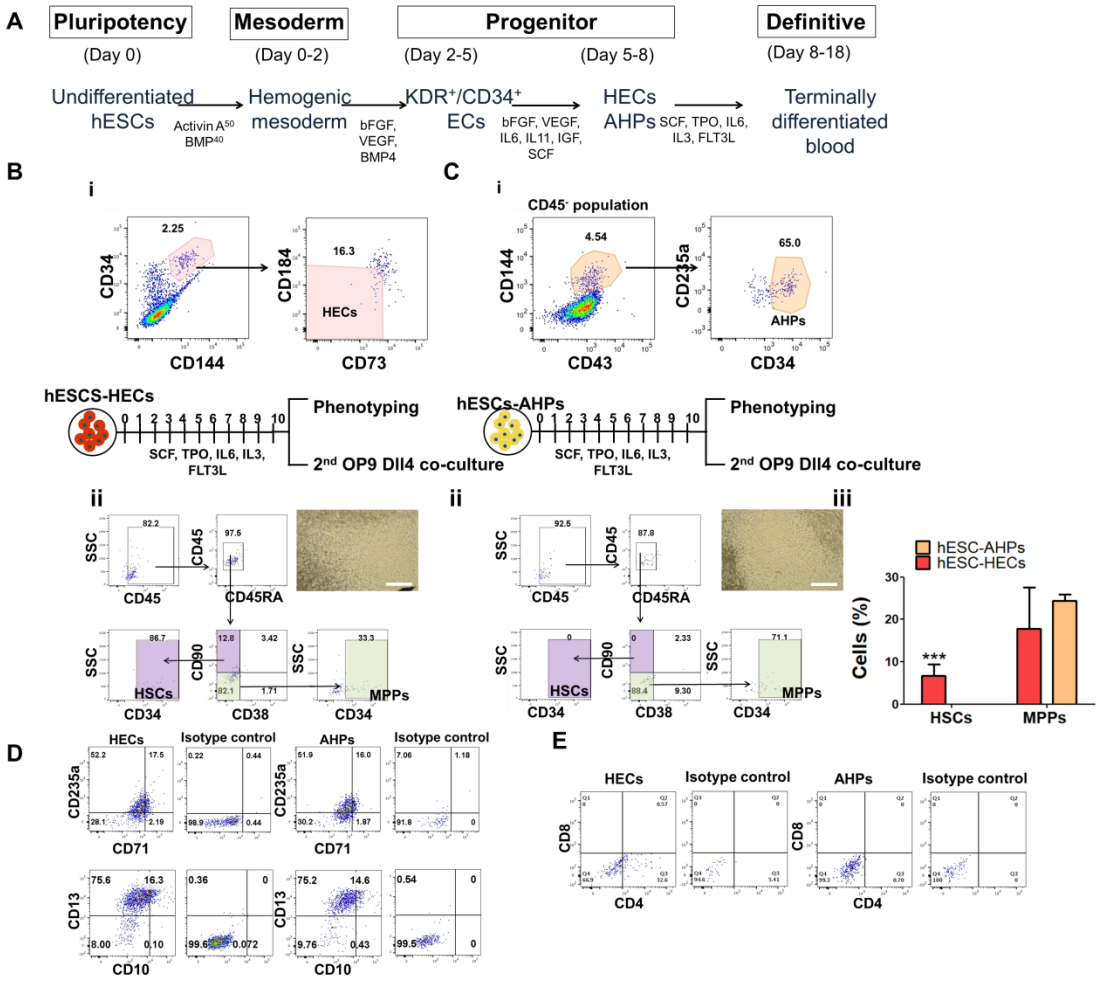

Figure 3.4 In vitro hematopoietic differentiation of hESCs mirrors human fetal liver hematopoiesis. A. Experimental scheme to generate HECs and AHPs and their transition to blood cells. hESCs cultured with low activin and high BMP on day 0 and 1, respectively were developed into posterior/hemogenic mesodermal population. This population was specified into endothelial lineage cells (day 5) which were then further cultured with VEGF, bFGF, IGF-1 and pro-hematopoietic cytokines for an additional 3 days. On day 8 iPSC-derived HECs and AHPs were FACS-sorted and cultured separately on E4EC in serum-free media supplemented with hematopoietic cytokines for 10 days. Detailed gating scheme of HECs (Bi) and AHPs (Ci). Lineage analysis of HECs (Bii) and AHPs (Cii) after EHTs. Scale bar = 250 um (right panel) (Ciii) Quantification of lineages generated from HECs and AHPs after EHT. (D) Representative flow cytometry data showing CD235a and CD73 single and double positive erytrhoid cells and CD13 and CD10 single and double positive myeloid cells. (E) CD4+ T-lymphoid cell development occurred only from HECs after secondary coculture with OP9-Dll4 cells.

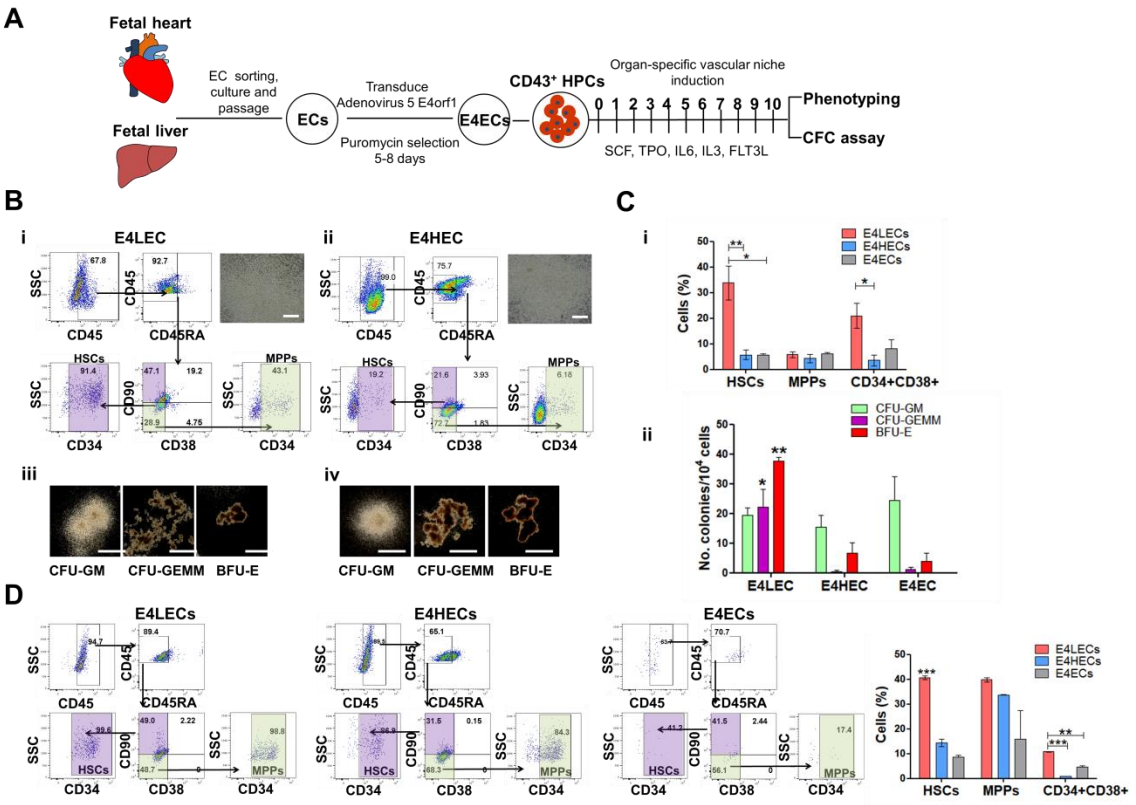

Figure 3.5 Fetal hepatic endothelium promotes development of phenotypic HSCs and multilineage colony forming progenitors A. An experimental schematic showing adenoviral E4ORF1 infection of fetal liver ECs and heart ECs. The engineered endothelial cell lines were cocutlured with liver HPCs for 10 days. B(i)&(ii) Phenotypic HSCs and MPPs and B(iii)&(iv) hematopoietic colonies arise from liver HPCs under liver or heart vascular niche induction (scale bar, 1,000 um). C (i) & (ii) Quantification of lineage output and colonies (n= 2 donors mean ±SEM * p≤0.05, **p≤0.01). D. Representative flow cytometry data showing hESC-derived HECs cocultured with E4LECs give rise to significantly more HSCs and lineage-committed cells compared with other engineered ECs. Quantification of lineage output from hESC-derived HECs is on the right panel. (n= 3 mean ±SEM ***p≤0.01,**p≤0.01)

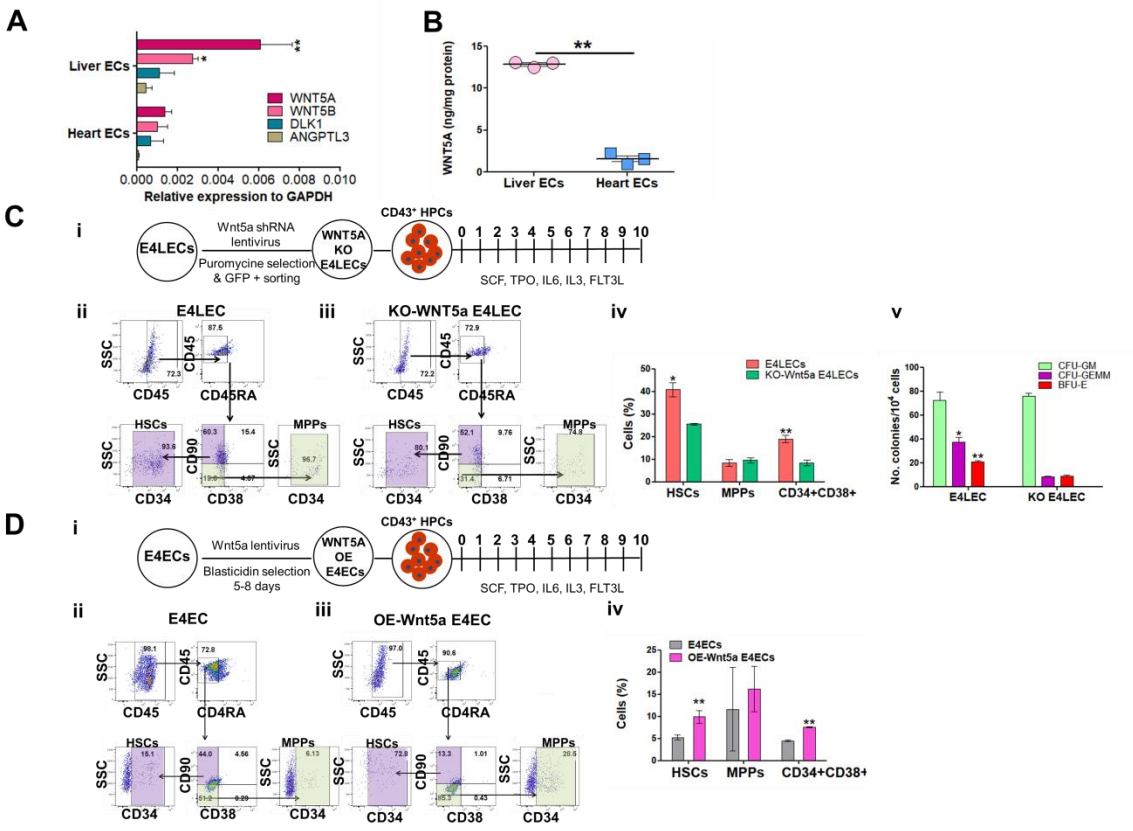

Fig. 3.6 Wnt5a is a major liver-specific vascular niche factors that promotes hematopoiesis (A) qPCR shows that, of the HSC regulatory genes tested, WNT5A and WNT5B are the most differentially expressed by the liver endothelium. (B) ELISA measurement of Wnt5a production from liver ECs and heart ECs for three donor sets (mean ±SEM. **P≤0.005) (Ci) E4LECs transduced with pGIPZ lentiviral shRNA against WNT5A were cocultured with liver HPCs for 10 days. Representative flow cytometry data showing phenotypic HSCs and MPPs arise from liver HPCs coculutred in E4LECs (Cii) and KOE4LECs (Ciii) on day 10. (Civ) Quantification of lineage output and (Cv) colonies (n= 2 donors mean ±SEM * p≤0.05, **p≤0.01).(Di) E4ECs transduced with a lentiviral vector encoding the WNT5A gene were cocutlured with liver HPCs for 10 days. Representative flow cytometry data showing phenotypic HSCs and MPPs arise from liver HPCs coculutred with E4ECs (Dii) and OE E4ECs (Diii) on day 10. (Div) Quantification (n= 3 donors mean ±SEM * p≤0.05, **p≤0.01)

.

Table 1.1 Flow cytometry antibodies

Antigen	Fluorochrome	Source	Catalogue number
CD45	Pacific blue	BioLegend	304022
CD45	APC-Cy™7	BD Biosciences	348795
CD43	APC	BD Biosciences	560198
CD43	Pacific blue	BD Biosciences	744813
CD144	PerCP-Cy™5.5	BD Biosciences	561566
CD73	APC	BioLegend	344005
CD184	PE	Thermo Fisher Scientific	12-9991-81
CD34	FITC	BD Biosciences	555821
CD34	APC	BD Biosciences	555824
CD45RA	PerCP-Cyanine5.5	BioLegend	304121
CD38	FITC	BD Biosciences	560982
CD38	PE	BD Biosciences	555460
CD90	FITC	BD Biosciences	555595
CD90	PE	BD Biosciences	555596
CD90	APC-Cy7	BioLegend	328131
CD235a	PE	Thermo Fisher Scientific	12-9987-80
CD235a	PE/Cy7	BioLegend	349111
CD61	PE	BD Biosciences	555754
CD71	PE	BD Biosciences	555537
CD13	APC	BioLegend	301705

CD10	Pacific blue	BD Biosciences	562902
CD4	Pacific blue	BioLegend	304029
CD8	PE	BD Biosciences	340046
CD5	APC	BioLegend	300611
CD7	PE	BioLegend	343105
Mouse IgG	Pacific blue	BioLegend	400131
Mouse IgG	PE	BD Biosciences	555749
Mouse IgG	APC	BD Pharmingen	555751
Mouse IgG	FITC	BD Biosciences	555748

Chapter 4

Summary and future directions

The above work addressed several of the key challenges associated with tissue engineering and regenerative medicine. In chapter 2 we have examined organ specific endothelial phenotype, both ex vivo and in vitro, from four major human organs - heart, lung, liver and kidneys, from individual fetal tissues at three months gestation. We showed the distinct structural, molecular and functional signatures of these four types of endothelial cells. However, limitations remain with respect to fully understanding intra-organ vascular endothelial cell heterogeneity, and further analysis employing single cell RNA sequencing could identify different endothelial subpopulations. Such information would lead to improved understanding of the origin and differentiation of the endothelium from different vascular beds, and enhance understanding of endothelial crosstalk with individual organs during development. Nevertheless, our findings allowed us to identify for the first time the linkage between human endothelial heterogeneity and organ development and differentiate between the epigenetic and microenvironmental contribution to human endothelial heterogeneity. The availability of methods to isolate and culture organ-specific endothelial cells allows us to engineer organ-specific microvascularized beds in vitro with perfusable luminal geometry and interconnectivity. In the future, engineering organ-specific vasculature co-cultured with organ or tissue resident cells in dense collagen by using our microvessel platform would enable further analysis of cell-cell interactions and vascular remodeling in a 3D platform. This approach may improve the angiogenic potential of the functional vascular network in situ via an active crosstalk with collagen-embedded resident cells. For future regenerative medicine applications, such an approach may facilitate connection to host vascular networks following in vivo transplantation. With further optimization of our platform, organ-specific in situ hierarchical vessel remodeling could be recapitulated, potentially leading to better transportation of oxygen and nutrients to target tissues and improved survival and function of tissue following transplantation. In addition, instructive signals secreted from organ-specific ECs may improve the target parenchymal regeneration and

functionality. Furthermore, our organ-specific ECs hold great promise for improving organ-on-a-chip technologies for drug screening. In recent years, significant improvement has been made in the field of organ-on-a-chip by employing microfluidic technology and 3D cell culture techniques to mimic the complexity of human tissue. However, further development of fully organ-specific human models is needed. This is partially because the active role of organ-specific ECs that support normal and diseased tissue function has been underestimated. Incorporating organotypic ECs into organ-on-a-chip is important to mimic the complex in vivo drug response, thereby obtaining reliable screening readouts.

In spite of extensive efforts over the past decades, the generation of HSCs from hPSCs to permanently reconstitute the blood system of a recipient has not been achieved. This is due in part to limited availability of HSC constructs that exactly recapitulate the complex HSC niche interactions and microenvironmental cues that support blood development. In chapter 3, we developed a novel co-culture system of engineered E4LECs and blood cell components (liver resident HPCs or hESC-derived HPCs). Our system provides signals that mimic those found in vivo within the fetal liver vascular niche, where HSCs undergo maturation, expansion, and multilineage differentiation. In this respect, this system may have significant future implications for the field of regenerative medicine. Using our system as a model, future co-culture constructs could be designed for human transplantation making use of endothelial paracrine signaling to improve donor HSC-derived blood reconstitution in the recipient. In addition, our system could someday lead to the ability to expand hematopoietic cells in vitro in sufficient numbers for transfusion or transplantation purposes.

This dissertation characterizes the structural, molecular and functional heterogeneity found across different organ-specific vascular beds and the active functional role of liver ECs in blood development via endothelial paracrine signaling.

References

1. Herbert, S.P. and D.Y. Stainier, *Molecular control of endothelial cell behaviour during blood vessel morphogenesis.* Nature reviews Molecular cell biology, 2011. **12**(9): p. 551.
2. Udan, R.S., J.C. Culver, and M.E. Dickinson, *Understanding vascular development.* Wiley Interdisciplinary Reviews: Developmental Biology, 2013. **2**(3): p. 327-346.
3. Risau, W., *Mechanisms of angiogenesis.* nature, 1997. **386**(6626): p. 671.
4. Hellström, M., et al., *Dll4 signalling through Notch1 regulates formation of tip cells during angiogenesis.* Nature, 2007. **445**(7129): p. 776.
5. Gerhardt, H., et al., *Neuropilin-1 is required for endothelial tip cell guidance in the developing central nervous system.* Developmental dynamics: an official publication of the American Association of Anatomists, 2004. **231**(3): p. 503-509.
6. Acker, T., H. Beck, and K.H. Plate, *Cell type specific expression of vascular endothelial growth factor and angiopoietin-1 and-2 suggests an important role of astrocytes in cerebellar vascularization.* Mechanisms of development, 2001. **108**(1-2): p. 45-57.
7. Red-Horse, K., et al., *Coronary arteries form by developmental reprogramming of venous cells.* Nature, 2010. **464**(7288): p. 549.
8. Azimi-Nezhad, M., *Vascular endothelial growth factor from embryonic status to cardiovascular pathology.* Reports of biochemistry & molecular biology, 2014. **2**(2): p. 59.
9. Lindahl, P., et al., *Pericyte loss and microaneurysm formation in PDGF-B-deficient mice.* Science, 1997. **277**(5323): p. 242-245.
10. Hirschi, K.K., S.A. Rohovsky, and P.A. D'amore, *PDGF, TGF-β, and heterotypic cell–cell interactions mediate endothelial cell–induced recruitment of 10T1/2 cells and their differentiation to a smooth muscle fate.* The Journal of cell biology, 1998. **141**(3): p. 805-814.
11. Carvalho, R.L., et al., *Defective paracrine signalling by TGFβ in yolk sac vasculature of endoglin mutant mice: a paradigm for hereditary haemorrhagic telangiectasia.* Development, 2004. **131**(24): p. 6237-6247.
12. Vikkula, M., et al., *Vascular dysmorphogenesis caused by an activating mutation in the receptor tyrosine kinase TIE2.* Cell, 1996. **87**(7): p. 1181-1190.
13. Suri, C., et al., *Requisite role of angiopoietin-1, a ligand for the TIE2 receptor, during embryonic angiogenesis.* Cell, 1996. **87**(7): p. 1171-1180.
14. Thurston, G., et al., *Leakage-resistant blood vessels in mice transgenically overexpressing angiopoietin-1.* Science, 1999. **286**(5449): p. 2511-2514.

15. Minami, T. and W.C. Aird, *Endothelial cell gene regulation.* Trends in cardiovascular medicine, 2005. **15**(5): p. 174. e1-174. e24.
16. Tian, X., W.T. Pu, and B. Zhou, *Cellular origin and developmental program of coronary angiogenesis.* Circulation research, 2015. **116**(3): p. 515-530.
17. Augustin, H.G. and G.Y. Koh, *Organotypic vasculature: From descriptive heterogeneity to functional pathophysiology.* Science, 2017. **357**(6353): p. eaal2379.
18. Mikawa, T. and D.A. Fischman, *Retroviral analysis of cardiac morphogenesis: discontinuous formation of coronary vessels.* Proceedings of the National Academy of Sciences, 1992. **89**(20): p. 9504-9508.
19. Luttun, A. and P. Carmeliet, *De novo vasculogenesis in the heart.* Cardiovascular research, 2003. **58**(2): p. 378-389.
20. Perez-Pomares, J., et al., *Experimental studies on the spatiotemporal expression of WT1 and RALDH2 in the embryonic avian heart: a model for the regulation of myocardial and valvuloseptal development by epicardially derived cells (EPDCs).* Developmental biology, 2002. **247**(2): p. 307-326.
21. Bouchey, D., et al., *Distribution of connective tissue proteins during development and neovascularization of the epicardium.* Cardiovascular research, 1996. **31**(supp1): p. E104-E115.
22. Wilm, B., et al., *The serosal mesothelium is a major source of smooth muscle cells of the gut vasculature.* Development, 2005. **132**(23): p. 5317-5328.
23. Wessels, A., et al., *Epicardially derived fibroblasts preferentially contribute to the parietal leaflets of the atrioventricular valves in the murine heart.* Developmental biology, 2012. **366**(2): p. 111-124.
24. Cai, C.-L., et al., *A myocardial lineage derives from Tbx18 epicardial cells.* Nature, 2008. **454**(7200): p. 104.
25. Acharya, A., et al., *Efficient inducible Cre-mediated recombination in Tcf21cell lineages in the heart and kidney.* Genesis, 2011. **49**(11): p. 870-877.
26. Katz, T.C., et al., *Distinct compartments of the proepicardial organ give rise to coronary vascular endothelial cells.* Developmental cell, 2012. **22**(3): p. 639-650.
27. Chen, H.I., et al., *The sinus venosus contributes to coronary vasculature through VEGFC-stimulated angiogenesis.* Development, 2014: p. dev. 113639.
28. Wu, B., et al., *Endocardial cells form the coronary arteries by angiogenesis through myocardial-endocardial VEGF signaling.* Cell, 2012. **151**(5): p. 1083-1096.
29. Hsieh, P.C., et al., *Endothelial-cardiomyocyte interactions in cardiac development and repair.* Annu. Rev. Physiol., 2006. **68**: p. 51-66.
30. Gassmann, M., et al., *Aberrant neural and cardiac development in mice lacking the ErbB4 neuregulin receptor.* Nature, 1995. **378**(6555): p. 390.

31. Lee, K.-F., et al., *Requirement for neuregulin receptor erbB2 in neural and cardiac development.* Nature, 1995. **378**(6555): p. 394.
32. Bjarnegård, M., et al., *Endothelium-specific ablation of PDGFB leads to pericyte loss and glomerular, cardiac and placental abnormalities.* Development, 2004. **131**(8): p. 1847-1857.
33. Warburton, D., et al., *Lung organogenesis*, in *Current topics in developmental biology*. 2010, Elsevier. p. 73-158.
34. Yamamoto, H., et al., *Epithelial–vascular cross talk mediated by VEGF-A and HGF signaling directs primary septae formation during distal lung morphogenesis.* Developmental biology, 2007. **308**(1): p. 44-53.
35. Gerber, H.-P., et al., *VEGF is required for growth and survival in neonatal mice.* Development, 1999. **126**(6): p. 1149-1159.
36. Zeng, X., et al., *VEGF enhances pulmonary vasculogenesis and disrupts lung morphogenesis in vivo.* Developmental dynamics: an official publication of the American Association of Anatomists, 1998. **211**(3): p. 215-227.
37. Aird, W.C., *Phenotypic heterogeneity of the endothelium: I. Structure, function, and mechanisms.* Circulation research, 2007. **100**(2): p. 158-173.
38. Vollmar, B. and M.D. Menger, *The hepatic microcirculation: mechanistic contributions and therapeutic targets in liver injury and repair.* Physiological reviews, 2009. **89**(4): p. 1269-1339.
39. Braet, F. and E. Wisse, *Structural and functional aspects of liver sinusoidal endothelial cell fenestrae: a review.* Comparative hepatology, 2002. **1**(1): p. 1.
40. Rossi, J.M., et al., *Distinct mesodermal signals, including BMPs from the septum transversum mesenchyme, are required in combination for hepatogenesis from the endoderm.* Genes & development, 2001. **15**(15): p. 1998-2009.
41. Matsumoto, K., et al., *Liver organogenesis promoted by endothelial cells prior to vascular function.* Science, 2001. **294**(5542): p. 559-563.
42. Schweitzer, K.M., et al., *Constitutive expression of E-selectin and vascular cell adhesion molecule-1 on endothelial cells of hematopoietic tissues.* The American journal of pathology, 1996. **148**(1): p. 165.
43. Wittig, O., J. Paez-Cortez, and J.E. Cardier, *Liver sinusoidal endothelial cells promote B lymphopoiesis from primitive hematopoietic cells.* Stem cells and development, 2010. **19**(3): p. 341-350.
44. Balazs, A.B., et al., *Endothelial protein C receptor (CD201) explicitly identifies hematopoietic stem cells in murine bone marrow.* Blood, 2006. **107**(6): p. 2317-2321.
45. Iwasaki, H., et al., *Endothelial protein C receptor-expressing hematopoietic stem cells reside in the perisinusoidal niche in fetal liver.* Blood, 2010: p. blood-2009-08-240903.

46. Ohneda, O. and V.L. Bautch, *Murine endothelial cells support fetal liver erythropoiesis and myelopoiesis via distinct interactions.* British journal of haematology, 1997. **98**(4): p. 798-808.
47. Tamai, K., et al., *LDL-receptor-related proteins in Wnt signal transduction.* Nature, 2000. **407**(6803): p. 530.
48. Liu, C., et al., *β-Trcp couples β-catenin phosphorylation-degradation and regulates Xenopus axis formation.* Proceedings of the National Academy of Sciences, 1999. **96**(11): p. 6273-6278.
49. Zeng, X., et al., *Initiation of Wnt signaling: control of Wnt coreceptor Lrp6 phosphorylation/activation via frizzled, dishevelled and axin functions.* Development, 2008. **135**(2): p. 367-375.
50. Behrens, J., et al., *Functional interaction of β-catenin with the transcription factor LEF-1.* Nature, 1996. **382**(6592): p. 638.
51. Slusarski, D.C., V.G. Corces, and R.T. Moon, *Interaction of Wnt and a Frizzled homologue triggers G-protein-linked phosphatidylinositol signalling.* Nature, 1997. **390**(6658): p. 410.
52. Kokolus, K. and M.J. Nemeth, *Non-canonical Wnt signaling pathways in hematopoiesis.* Immunologic research, 2010. **46**(1-3): p. 155-164.
53. Kühl, M., et al., *Ca2+/calmodulin-dependent protein kinase II is stimulated by Wnt and Frizzled homologs and promotes ventral cell fates in Xenopus.* Journal of Biological Chemistry, 2000. **275**(17): p. 12701-12711.
54. Ishitani, T., et al., *The TAK1-NLK mitogen-activated protein kinase cascade functions in the Wnt-5a/Ca2+ pathway to antagonize Wnt/β-catenin signaling.* Molecular and cellular biology, 2003. **23**(1): p. 131-139.
55. Bryja, V., et al., *The extracellular domain of Lrp5/6 inhibits noncanonical Wnt signaling in vivo.* Molecular biology of the cell, 2009. **20**(3): p. 924-936.
56. Ruiz-Herguido, C., et al., *Hematopoietic stem cell development requires transient Wnt/β-catenin activity.* Journal of Experimental Medicine, 2012. **209**(8): p. 1457-1468.
57. Chanda, B., et al., *Retinoic acid signaling is essential for embryonic hematopoietic stem cell development.* Cell, 2013. **155**(1): p. 215-227.
58. Louis, I., et al., *The signaling protein Wnt4 enhances thymopoiesis and expands multipotent hematopoietic progenitors through β-catenin-independent signaling.* Immunity, 2008. **29**(1): p. 57-67.
59. Gao, X., et al., *Angioblast-mesenchyme induction of early kidney development is mediated by Wt1 and Vegfa.* Development, 2005. **132**(24): p. 5437-5449.
60. Eremina, V., et al., *Vascular endothelial growth factor a signaling in the podocyte-endothelial compartment is required for mesangial cell migration and survival.* Journal

of the American Society of Nephrology, 2006. **17**(3): p. 724-735.
61. Coffin, J.D., et al., *Angioblast differentiation and morphogenesis of the vascular endothelium in the mouse embryo.* Developmental Biology, 1991. **148**(1): p. 51-62.
62. Hatzopoulos, A.K., et al., *Isolation and characterization of endothelial progenitor cells from mouse embryos.* Development, 1998. **125**(8): p. 1457-1468.
63. Risau, W., *Mechanisms of angiogenesis.* Nature, 1997. **386**(6626): p. 671-674.
64. Eichmann, A., et al., *Vascular development: from precursor cells to branched arterial and venous networks.* International Journal of Developmental Biology, 2005. **49**(2-3): p. 259-267.
65. Adams, R.H. and K. Alitalo, *Molecular regulation of angiogenesis and lymphangiogenesis.* Nature Reviews Molecular Cell Biology, 2007. **8**(6): p. 464-478.
66. le Noble, F., et al., *Flow regulates arterial-venous differentiation in the chick embryo yolk sac.* Development, 2004. **131**(2): p. 361-375.
67. Carmeliet, P., *Angiogenesis in health and disease.* Nature Medicine, 2003. **9**(6): p. 653-660.
68. Atkins, G.B., M.K. Jain, and A. Hamik, *Endothelial differentiation molecular mechanisms of specification and heterogeneity.* Arteriosclerosis Thrombosis and Vascular Biology, 2011. **31**(7): p. 1476-1484.
69. Red-Horse, K., et al., *Endothelium-microenvironment interactions in the developing embryo and in the adult.* Developmental Cell, 2007. **12**(2): p. 181-194.
70. Goldman, O., et al., *Endoderm Generates Endothelial Cells during Liver Development.* Stem Cell Reports, 2014. **3**(4): p. 556-565.
71. Wang, R., et al., *Glioblastoma stem-like cells give rise to tumour endothelium.* Nature, 2010. **468**(7325): p. 829-U128.
72. Tian, X.Y., W.T. Pu, and B. Zhou, *Cellular origin and developmental program of coronary angiogenesis.* Circulation Research, 2015. **116**(3): p. 515-530.
73. Mugford, J.W., et al., *Osr1 expression demarcates a multi-potent population of intermediate mesoderm that undergoes progressive restriction to an Osr1-dependent nephron progenitor compartment within the mammalian kidney.* Developmental Biology, 2008. **324**(1): p. 88-98.
74. Peng, T., et al., *Coordination of heart and lung co-development by a multipotent cardiopulmonary progenitor.* Nature, 2013. **500**(7464): p. 589-+.
75. Aird, W.C., *Phenotypic heterogeneity of the endothelium I. Structure, function, and mechanisms.* Circulation Research, 2007. **100**(2): p. 158-173.
76. Aird, W.C., *Phenotypic heterogeneity of the endothelium II. Representative vascular beds.* Circulation Research, 2007. **100**(2): p. 174-190.
77. Nolan, D.J., et al., *Molecular Signatures of Tissue-Specific Microvascular Endothelial*

Cell Heterogeneity in Organ Maintenance and Regeneration. Developmental Cell, 2013. **26**(2): p. 204-219.

78. Chi, J.T., et al., *Endothelial cell diversity revealed by global expression profiling.* Proceedings of the National Academy of Sciences of the United States of America, 2003. **100**(19): p. 10623-10628.
79. Aird, W.C., et al., *Vascular bed-specific expression of an endothelial cell gene is programmed by the tissue microenvironment.* Journal of Cell Biology, 1997. **138**(5): p. 1117-1124.
80. Minami, T. and W.C. Aird, *Endothelial cell gene regulation.* Trends in Cardiovascular Medicine, 2005. **15**(5): p. 174-184.
81. Lacorre, D.A., et al., *Plasticity of endothelial cells: rapid dedifferentiation of freshly isolated high endothelial venule endothelial cells outside the lymphoid tissue microenvironment.* Blood, 2004. **103**(11): p. 4164-4172.
82. Burridge, K.A. and M.H. Friedman, *Environment and vascular bed origin influence differences in endothelial transcriptional profiles of coronary and iliac arteries.* American Journal of Physiology-Heart and Circulatory Physiology, 2010. **299**(3): p. H837-H846.
83. Lim, Y.C., et al., *Heterogeneity of endothelial cells from different organ sites in T-cell subset recruitment.* American Journal of Pathology, 2003. **162**(5): p. 1591-1601.
84. Xue, L., et al., *Global expression profiling reveals genetic programs underlying the developmental divergence between mouse and human embryogenesis.* Bmc Genomics, 2013. **14**.
85. Trapnell, C., L. Pachter, and S.L. Salzberg, *TopHat: discovering splice junctions with RNA-Seq.* Bioinformatics, 2009. **25**(9): p. 1105-1111.
86. Anders, S., P.T. Pyl, and W. Huber, *HTSeq-a Python framework to work with high-throughput sequencing data.* Bioinformatics, 2015. **31**(2): p. 166-169.
87. Anders, S. and W. Huber, *Differential expression analysis for sequence count data.* Genome Biology, 2010. **11**(10).
88. Alexa, A., J. Rahnenfuhrer, and T. Lengauer, *Improved scoring of functional groups from gene expression data by decorrelating GO graph structure.* Bioinformatics, 2006. **22**(13): p. 1600-1607.
89. Zheng, Y., et al., *In vitro microvessels for the study of angiogenesis and thrombosis.* Proceedings of the National Academy of Sciences, 2012. **109**(24): p. 9342-9347.
90. Dunn, J.C., M.L. Tompkins Rg Fau - Yarmush, and M.L. Yarmush, *Long-term in vitro function of adult hepatocytes in a collagen sandwich configuration.* (8756-7938 (Print)).
91. Stan, R., *Endothelial stomatal and fenestral diaphragms in normal vessels and angiogenesis.* Journal of cellular and molecular medicine, 2007. **11**(4): p. 621-643.

92. Stan, R.V., et al., *The diaphragms of fenestrated endothelia: gatekeepers of vascular permeability and blood composition.* Developmental cell, 2012. **23**(6): p. 1203-1218.
93. Tkachenko, E., et al., *Caveolae, fenestrae and transendothelial channels retain PV1 on the surface of endothelial cells.* PloS one, 2012. **7**(3): p. e32655.
94. Zheng, Y., et al., *In vitro microvessels for the study of angiogenesis and thrombosis.* Proceedings of the National Academy of Sciences of the United States of America, 2012. **109**(24): p. 9342-9347.
95. Lee, J.W., et al., *Hypoxia-inducible factor (HIF-1)alpha: its protein stability and biological functions.* Experimental and Molecular Medicine, 2004. **36**(1): p. 1-12.
96. Park, C., T.M. Kim, and A.B. Malik, *Transcriptional Regulation of Endothelial Cell and Vascular Development.* Circulation Research, 2013. **112**(10): p. 1380-1400.
97. De Val, S. and B.L. Black, *Transcriptional Control of Endothelial Cell Development.* Developmental Cell, 2009. **16**(2): p. 180-195.
98. Rivera-Feliciano, J., et al., *Development of heart valves requires Gata4 expression in endothelial-derived cells.* Development, 2006. **133**(18): p. 3607-3618.
99. Roche, P., M.P. Czubryt, and J.T. Wigle, *Molecular mechanisms of cardiac development*, in *Cardiac Adaptations*. 2013, Springer. p. 19-39.
100. Fischer, A., et al., *The Notch target genes Hey1 and Hey2 are required for embryonic vascular development.* Genes & Development, 2004. **18**(8): p. 901-911.
101. Rutenberg, J.B., et al., *Developmental patterning of the cardiac atrioventricular canal by Notch and Hairy-related transcription factors.* Development, 2006. **133**(21): p. 4381-4390.
102. Xin, M., et al., *A threshold of GATA4 and GATA6 expression is required for cardiovascular development.* Proceedings of the National Academy of Sciences of the United States of America, 2006. **103**(30): p. 11189-11194.
103. Roche, P., M.P. Czubryt, and J.T. Wigle, *Molecular Mechanisms of Cardiac Development*, in *Cardiac Adaptations: Molecular Mechanisms*, B. Ostadal and N.S. Dhalla, Editors. 2013, Springer New York: New York, NY. p. 19-39.
104. Brand, T., *Heart development: molecular insights into cardiac specification and early morphogenesis.* Developmental Biology, 2003. **258**(1): p. 1-19.
105. Chu, P.H., et al., *Expression patterns of FHL/SLIM family members suggest important functional roles in skeletal muscle and cardiovascular system.* Mechanisms of Development, 2000. **95**(1-2): p. 259-265.
106. Lee, M.P. and K.E. Yutzey, *Twist1 directly regulates genes that promote cell proliferation and migration in developing heart valves.* Plos One, 2011. **6**(12).
107. Chakraborty, S., et al., *Twist1 promotes heart valve cell proliferation and extracellular matrix gene expression during development in vivo and is expressed in human*

diseased aortic valves. Developmental Biology, 2010. **347**(1): p. 167-179.
108. Green, Y.S. and M.L. Vetter, *EBF proteins participate in transcriptional regulation of Xenopus muscle development.* Developmental Biology, 2011. **358**(1): p. 240-250.
109. Rhinn, M. and P. Dolle, *Retinoic acid signalling during development.* Development, 2012. **139**(5): p. 843-858.
110. Bergwerff, M., et al., *Loss of function of the Prx1 and Prx2 homeobox genes alters architecture of the great elastic arteries and ductus arteriosus.* Virchows Archiv-an International Journal of Pathology, 2000. **436**(1): p. 12-19.
111. Chamberlain, A.A., et al., *DNA methylation is developmentally regulated for genes essential for cardiogenesis.* Journal of the American Heart Association, 2014. **3**(3).
112. Fretz, J.A., et al., *Early B-cell factor 1 is an essential transcription factor for postnatal glomerular maturation.* Kidney International, 2014. **85**(5): p. 1091-1102.
113. Schell, C., N. Wanner, and T.B. Huber, *Glomerular development - Shaping the multi-cellular filtration unit.* Seminars in Cell & Developmental Biology, 2014. **36**: p. 39-49.
114. Narlis, M., et al., *Pax2 and Pax8 regulate branching morphogenesis and nephron differentiation in the developing kidney.* Journal of the American Society of Nephrology, 2007. **18**(4): p. 1121-1129.
115. Patterson, L.T. and S.S. Potter, *Atlas of Hox gene expression in the developing kidney.* Developmental Dynamics, 2004. **229**(4): p. 771-779.
116. Lechner, M.S. and G.R. Dressler, *The molecular basis of embryonic kidney development.* Mechanisms of Development, 1997. **62**(2): p. 105-120.
117. Aitola, M., et al., *Forkhead transcription factor FoxF2 is expressed in mesodermal tissues involved in epithelio-mesenchymal interactions.* Developmental Dynamics, 2000. **218**(1): p. 136-149.
118. Arora, R., R.J. Metzger, and V.E. Papaioannou, *Multiple Roles and Interactions of Tbx4 and Tbx5 in Development of the Respiratory System.* Plos Genetics, 2012. **8**(8).
119. Lin, S., et al., *Misexpression of MIA disrupts lung morphogenesis and causes neonatal death.* Developmental Biology, 2008. **316**(2): p. 441-455.
120. Heiss, M., et al., *Endothelial cell spheroids as a versatile tool to study angiogenesis in vitro.* Faseb Journal, 2015. **29**(7): p. 3076-3084.
121. Dieterlen-Lievre, F., A.-M. Duprat, and N. Le Douarin, *Developmental biology: origins and prospects.* Medecine Sciences, 1996. **12**: p. 67-75.
122. Le Douarin, N., F. Dieterlen-Lièvre, and M.-A. Teillet, *Quail-chick transplantations.* Methods Cell Biol, 1996. **51**: p. 23-59.
123. Bazzoni, G. and E. Dejana, *Endothelial cell-to-cell junctions: molecular organization and role in vascular homeostasis.* Physiological reviews, 2004. **84**(3): p. 869-901.
124. Kluger, M.S., et al., *Claudin-5 controls intercellular barriers of human dermal*

microvascular but not human umbilical vein endothelial cells. Arteriosclerosis, thrombosis, and vascular biology, 2013. **33**(3): p. 489-500.

125. Komarova, Y. and A.B. Malik, *Regulation of endothelial permeability via paracellular and transcellular transport pathways.* Annual review of physiology, 2010. **72**: p. 463-493.
126. Mehta, D. and A.B. Malik, *Signaling mechanisms regulating endothelial permeability.* Physiological reviews, 2006. **86**(1): p. 279-367.
127. Hirase, T., et al., *Occludin as a possible determinant of tight junction permeability in endothelial cells.* Journal of cell science, 1997. **110**(14): p. 1603-1613.
128. Schnitzer, J., et al., *Segmental differentiation of permeability, protein glycosylation, and morphology of cultured bovine lung vascular endothelium.* Biochemical and biophysical research communications, 1994. **199**(1): p. 11-19.
129. Zhang, B. and W.T. Pu, *The mysterious origins of coronary vessels.* Cell research, 2013. **23**(9): p. 1063.
130. del Monte, G. and R.P. Harvey, *An endothelial contribution to coronary vessels.* Cell, 2012. **151**(5): p. 932-934.
131. Goldman, O., et al., *Endoderm generates endothelial cells during liver development.* Stem cell reports, 2014. **3**(4): p. 556-565.
132. Mugford, J.W., et al., *Osr1 expression demarcates a multi-potent population of intermediate mesoderm that undergoes progressive restriction to an Osr1-dependent nephron progenitor compartment within the mammalian kidney.* Developmental biology, 2008. **324**(1): p. 88-98.
133. Sims-Lucas, S., et al., *Endothelial progenitors exist within the kidney and lung mesenchyme.* PloS one, 2013. **8**(6): p. e65993.
134. Wang, R., et al., *Glioblastoma stem-like cells give rise to tumour endothelium.* Nature, 2010. **468**(7325): p. 829.
135. Abrahamson, D.R., *Development of kidney glomerular endothelial cells and their role in basement membrane assembly.* Organogenesis, 2009. **5**(1): p. 1-13.
136. Chen, Q., et al., *Endothelial cells are progenitors of cardiac pericytes and vascular smooth muscle cells.* Nature communications, 2016. **7**: p. 12422.
137. Cleaver, O. and D.A. Melton, *Endothelial signaling during development.* Nature medicine, 2003. **9**(6): p. 661.
138. Lammert, E., O. Cleaver, and D. Melton, *Role of endothelial cells in early pancreas and liver development.* Mechanisms of development, 2003. **120**(1): p. 59-64.
139. Schell, C., N. Wanner, and T. Huber. *Glomerular development–shaping the multi-cellular filtration unit*. in *Seminars in cell & developmental biology*. 2014. Elsevier.
140. Tirziu, D. and M. Simons, *Endothelium as master regulator of organ development and*

growth. Vascular pharmacology, 2009. **50**(1-2): p. 1-7.

141. Villasenor, A. and O. Cleaver. *Crosstalk between the developing pancreas and its blood vessels: an evolving dialog*. in *Seminars in cell & developmental biology*. 2012. Elsevier.
142. Eelen, G., et al., *Endothelial Cell Metabolism in Normal and Diseased Vasculature.* Circulation Research, 2015. **116**(7): p. 1231-1244.
143. Marcu, R., et al., *The Mitochondrial Permeability Transition Pore Regulates Endothelial Bioenergetics and Angiogenesis.* Circulation Research, 2015. **116**(8): p. 1336-1345.
144. De Bock, K., M. Georgiadou, and P. Carmeliet, *Role of Endothelial Cell Metabolism in Vessel Sprouting.* Cell Metabolism, 2013. **18**(5): p. 634-647.
145. De Bock, K., et al., *Role of PFKFB3-Driven Glycolysis in Vessel Sprouting.* Cell, 2013. **154**(3): p. 651-663.
146. Teslaa, T. and M.A. Teitell, *Pluripotent stem cell energy metabolism: an update.* Embo Journal, 2015. **34**(2): p. 138-153.
147. Shyh-Chang, N., G.Q. Daley, and L.C. Cantley, *Stem cell metabolism in tissue development and aging*. Development, 2013. **140**(12): p. 2535-2547.
148. Shyh-Chang, N. and G.Q. Daley, *Metabolic Switches Linked to Pluripotency and Embryonic Stem Cell Differentiation.* Cell Metabolism, 2015. **21**(3): p. 349-350.
149. Cumano, A. and I. Godin, *Ontogeny of the hematopoietic system.* Annu. Rev. Immunol., 2007. **25**: p. 745-785.
150. De La Garza, A., A. Sinha, and T.V. Bowman, *Concise review: hematopoietic stem cell origins: lessons from embryogenesis for improving regenerative medicine.* Stem cells translational medicine, 2017. **6**(1): p. 60-67.
151. Palis, J., et al., *Development of erythroid and myeloid progenitors in the yolk sac and embryo proper of the mouse.* Development, 1999. **126**(22): p. 5073-5084.
152. Silver, L. and J. Palis, *Initiation of murine embryonic erythropoiesis: a spatial analysis.* Blood, 1997. **89**(4): p. 1154-1164.
153. Medvinsky, A. and E. Dzierzak, *Definitive hematopoiesis is autonomously initiated by the AGM region.* Cell, 1996. **86**(6): p. 897-906.
154. de Bruijn, M.F., et al., *Definitive hematopoietic stem cells first develop within the major arterial regions of the mouse embryo.* The EMBO journal, 2000. **19**(11): p. 2465-2474.
155. Boisset, J.-C., et al., *In vivo imaging of haematopoietic cells emerging from the mouse aortic endothelium.* Nature, 2010. **464**(7285): p. 116-120.
156. Li, Z., et al., *Mouse embryonic head as a site for hematopoietic stem cell development.* Cell stem cell, 2012. **11**(5): p. 663-675.
157. Yokomizo, T. and E. Dzierzak, *Three-dimensional cartography of hematopoietic clusters in the vasculature of whole mouse embryos.* Development, 2010. **137**(21): p. 3651-3661.

158. Gekas, C., et al., *The placenta is a niche for hematopoietic stem cells.* Developmental cell, 2005. **8**(3): p. 365-375.
159. Hirschi, K.K., *Hemogenic endothelium during development and beyond.* Blood, 2012. **119**(21): p. 4823-4827.
160. McGrath, K.E., et al., *Distinct sources of hematopoietic progenitors emerge before HSCs and provide functional blood cells in the mammalian embryo.* Cell reports, 2015. **11**(12): p. 1892-1904.
161. Sintes, J., et al., *Differential expression of CD150 (SLAM) family receptors by human hematopoietic stem and progenitor cells.* Experimental hematology, 2008. **36**(9): p. 1199-1204.
162. Doulatov, S., et al., *Hematopoiesis: a human perspective.* Cell stem cell, 2012. **10**(2): p. 120-136.
163. Kennedy, M., et al., *T lymphocyte potential marks the emergence of definitive hematopoietic progenitors in human pluripotent stem cell differentiation cultures.* Cell reports, 2012. **2**(6): p. 1722-1735.
164. Slukvin, I.I., *Hematopoietic specification from human pluripotent stem cells: current advances and challenges toward de novo generation of hematopoietic stem cells.* Blood, 2013. **122**(25): p. 4035-4046.
165. Choi, K.-D., et al., *Identification of the hemogenic endothelial progenitor and its direct precursor in human pluripotent stem cell differentiation cultures.* Cell reports, 2012. **2**(3): p. 553-567.
166. Ditadi, A., et al., *Human definitive haemogenic endothelium and arterial vascular endothelium represent distinct lineages.* Nature cell biology, 2015. **17**(5): p. 580-591.
167. Sturgeon, C.M., et al., *Wnt signaling controls the specification of definitive and primitive hematopoiesis from human pluripotent stem cells.* Nature biotechnology, 2014. **32**(6): p. 554.
168. Rafii, S., et al., *Human ESC-derived hemogenic endothelial cells undergo distinct waves of endothelial to hematopoietic transition.* Blood, 2013. **121**(5): p. 770-780.
169. Slukvin, I.I., *Deciphering the hierarchy of angiohematopoietic progenitors from human pluripotent stem cells.* Cell cycle, 2013. **12**(5): p. 720-727.
170. Kiel, M.J., et al., *SLAM family receptors distinguish hematopoietic stem and progenitor cells and reveal endothelial niches for stem cells.* cell, 2005. **121**(7): p. 1109-1121.
171. Nombela-Arrieta, C., et al., *Quantitative imaging of haematopoietic stem and progenitor cell localization and hypoxic status in the bone marrow microenvironment.* Nature cell biology, 2013. **15**(5): p. 533.
172. Hooper, A.T., et al., *Engraftment and reconstitution of hematopoiesis is dependent on VEGFR2-mediated regeneration of sinusoidal endothelial cells.* Cell stem cell, 2009.

4(3): p. 263-274.

173. Ding, L., et al., *Endothelial and perivascular cells maintain haematopoietic stem cells.* Nature, 2012. **481**(7382): p. 457.
174. Palpant, N.J., et al., *Inhibition of β-catenin signaling respecifies anterior-like endothelium into beating human cardiomyocytes.* Development, 2015. **142**(18): p. 3198-3209.
175. Palpant, N.J., et al., *Generating high-purity cardiac and endothelial derivatives from patterned mesoderm using human pluripotent stem cells.* Nature protocols, 2017. **12**(1): p. 15-31.
176. Marcu, R., et al., *Human Organ-specific Endothelial Cell Heterogeneity.* iScience, 2018.
177. Ivanovs, A., et al., *Highly potent human hematopoietic stem cells first emerge in the intraembryonic aorta-gonad-mesonephros region.* Journal of Experimental Medicine, 2011. **208**(12): p. 2417-2427.
178. Robin, C., et al., *Human placenta is a potent hematopoietic niche containing hematopoietic stem and progenitor cells throughout development.* Cell stem cell, 2009. **5**(4): p. 385-395.
179. Sturgeon, C.M., et al., *Wnt signaling controls the specification of definitive and primitive hematopoiesis from human pluripotent stem cells.* Nature biotechnology, 2014. **32**(6): p. 554-561.
180. Chen, M.J., et al., *Erythroid/myeloid progenitors and hematopoietic stem cells originate from distinct populations of endothelial cells.* Cell stem cell, 2011. **9**(6): p. 541-552.
181. Bertrand, J.Y., et al., *Characterization of purified intraembryonic hematopoietic stem cells as a tool to define their site of origin.* Proceedings of the National Academy of Sciences of the United States of America, 2005. **102**(1): p. 134-139.
182. Kasaai, B., et al., *Erythro-myeloid progenitors can differentiate from endothelial cells and modulate embryonic vascular remodeling.* Scientific Reports, 2017. **7**.
183. Palpant, N.J., et al., *Inhibition of β-catenin signaling respecifies anterior-like endothelium into beating human cardiomyocytes.* Development, 2015: p. dev. 117010.
184. Attar, A., *Changes in the cell surface markers during normal hematopoiesis: a guide to cell isolation.* Global J Hematol Blood Transfu, 2014. **1**: p. 20-8.
185. La Motte-Mohs, R.N., E. Herer, and J.C. Zúñiga-Pflücker, *Induction of T-cell development from human cord blood hematopoietic stem cells by Delta-like 1 in vitro.* Blood, 2005. **105**(4): p. 1431-1439.
186. Arai, F., et al., *Tie2/angiopoietin-1 signaling regulates hematopoietic stem cell quiescence in the bone marrow niche.* Cell, 2004. **118**(2): p. 149-161.
187. Jaleco, A.C., et al., *Differential effects of Notch ligands Delta-1 and Jagged-1 in human*

lymphoid differentiation. Journal of Experimental Medicine, 2001. **194**(7): p. 991-1002.

188. Zhang, C.C., et al., *Angiopoietin-like 5 and IGFBP2 stimulate ex vivo expansion of human cord blood hematopoietic stem cells as assayed by NOD/SCID transplantation.* Blood, 2008. **111**(7): p. 3415-3423.
189. Kobayashi, H., et al., *Angiocrine factors from Akt-activated endothelial cells balance self-renewal and differentiation of haematopoietic stem cells.* Nature cell biology, 2010. **12**(11): p. 1046.
190. Schreck, C., et al., *Niche WNT5A regulates the actin cytoskeleton during regeneration of hematopoietic stem cells.* Journal of Experimental Medicine, 2016: p. jem. 20151414.
191. Povinelli, B.J. and M.J. Nemeth, *Wnt5a regulates hematopoietic stem cell proliferation and repopulation through the Ryk receptor.* Stem cells, 2014. **32**(1): p. 105-115.
192. Buckley, S.M., et al., *Maintenance of HSC by Wnt5a secreting AGM-derived stromal cell line.* Experimental hematology, 2011. **39**(1): p. 114-123. e5.
193. Nemeth, M.J., et al., *Wnt5a inhibits canonical Wnt signaling in hematopoietic stem cells and enhances repopulation.* Proceedings of the National Academy of Sciences, 2007. **104**(39): p. 15436-15441.
194. Murdoch, B., et al., *Wnt-5A augments repopulating capacity and primitive hematopoietic development of human blood stem cells in vivo.* Proceedings of the National Academy of Sciences, 2003. **100**(6): p. 3422-3427.
195. Perdiguero, E.G., et al., *Tissue-resident macrophages originate from yolk-sac-derived erythro-myeloid progenitors.* Nature, 2015. **518**(7540): p. 547.
196. Perdiguero, E.G., et al., *Tissue-resident macrophages originate from yolk-sac-derived erythro-myeloid progenitors.* Nature, 2015. **518**(7540): p. 547-551.
197. Kingsley, P.D., et al., *"Maturational" globin switching in primary primitive erythroid cells.* Blood, 2006. **107**(4): p. 1665-1672.
198. Ditadi, A., C.M. Sturgeon, and G. Keller, *A view of human haematopoietic development from the Petri dish.* Nature Reviews Molecular Cell Biology, 2017. **18**(1): p. 56-67.
199. Rowe, R.G., et al., *Engineering hematopoietic stem cells: lessons from development.* Cell Stem Cell, 2016. **18**(6): p. 707-720.
200. Stamatoyannopoulos, G., *Control of globin gene expression during development and erythroid differentiation.* Experimental hematology, 2005. **33**(3): p. 259-271.
201. Ditadi, A., et al., *Human definitive haemogenic endothelium and arterial vascular endothelium represent distinct lineages.* Nature cell biology, 2015. **17**(5): p. 580.
202. Austin, T.W., et al., *A role for the Wnt gene family in hematopoiesis: expansion of multilineage progenitor cells.* Blood, 1997. **89**(10): p. 3624-3635.
203. Reya, T., et al., *Wnt signaling regulates B lymphocyte proliferation through a LEF-1 dependent mechanism.* Immunity, 2000. **13**(1): p. 15-24.

204. Van Den Berg, D.J., et al., *Role of members of the Wnt gene family in human hematopoiesis.* Blood, 1998. **92**(9): p. 3189-3202.

Appendix A

Supplement to Chapter 2

List of supplementary Figures

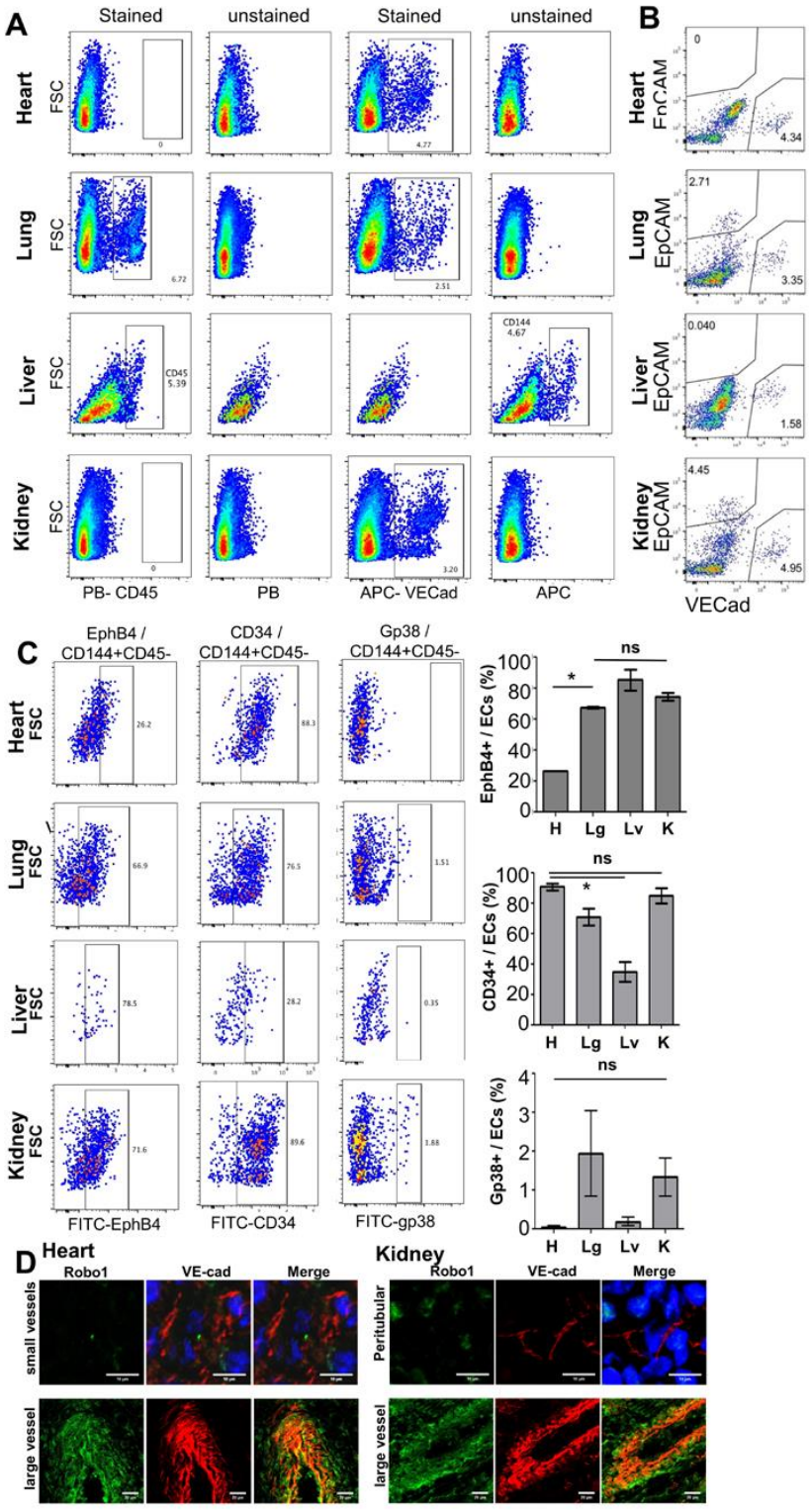

Supplementary Figure 1. Characterization of cell population in human fetal tissue
A-B Representative flow cytometry profiles of fresh total cell tissue suspension from fetal human heart, lung, liver and kidney stained with antibodies (A) against CD45 and

CD144 (VECad), in comparison with unstained controls, and (B) VECad amd EpCam. **C.** Flow cytometry analysis of EC population in fresh fetal tissue for EphB4+, CD34+, and Gp38+ with quantification for three donor sets. **D**. Representative immunofluorescence images of small vessels and large vessels in frozen heart and kidney tissue sections stained with antibodies against Robo1 and VECad.

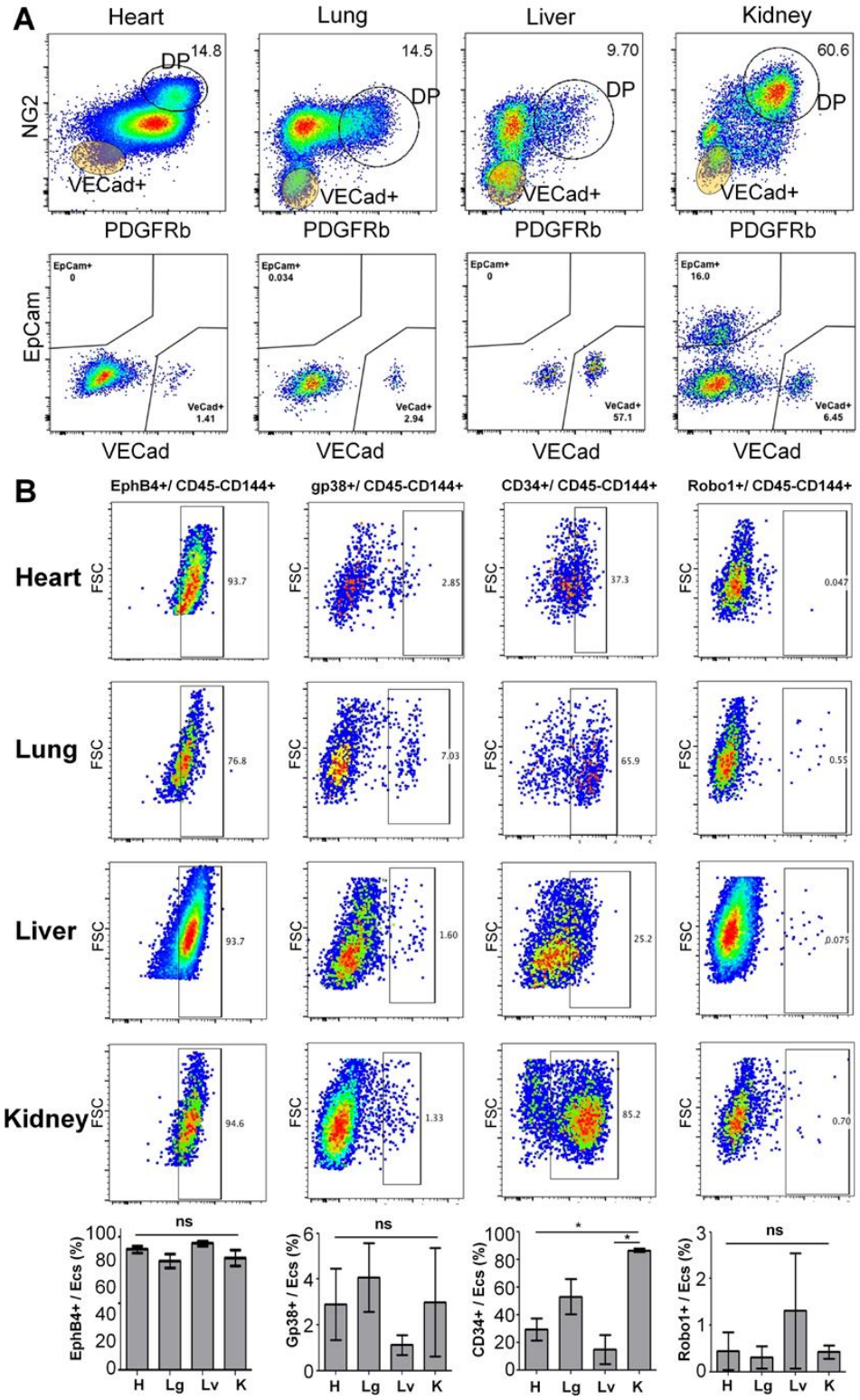

Supplementary Figure 2. Analysis of enriched cell suspension A. Representative flow cytometry and sorting profiles of enriched cell suspension from fetal human heart, lung, liver and kidney, stained with antibodies against NG2 and PDGFRb, with VECad+

population from Fig.2A marked as orange circles. B. Flow cytometry analysis of cultured human heart, lung, liver, and kidney EC populations for EphB4+, Gp38+, CD34+ and Robo1+.

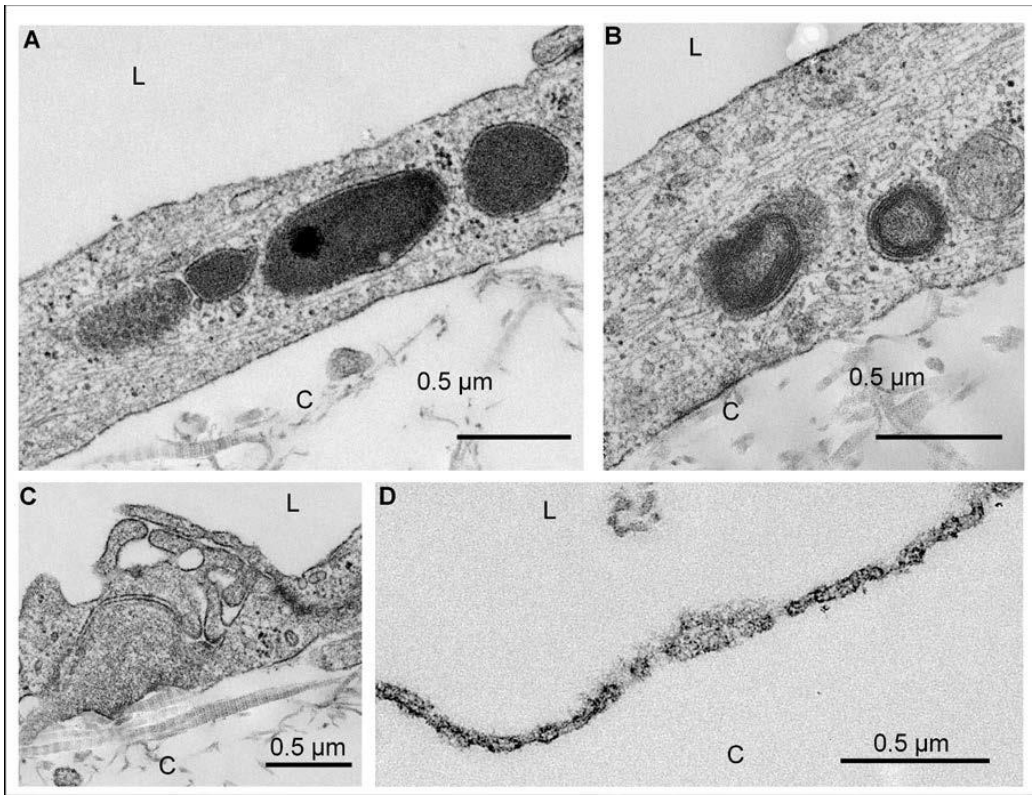

Supplementary Figure 3. Ultrastructural images of human fetal liver ECs A-B. Ultrastructural images of multivascular bodies, lysosomes, and other intracellular features in liver ECs. C-D. Sinusoidal and fenestrated features on liver EC membranes.

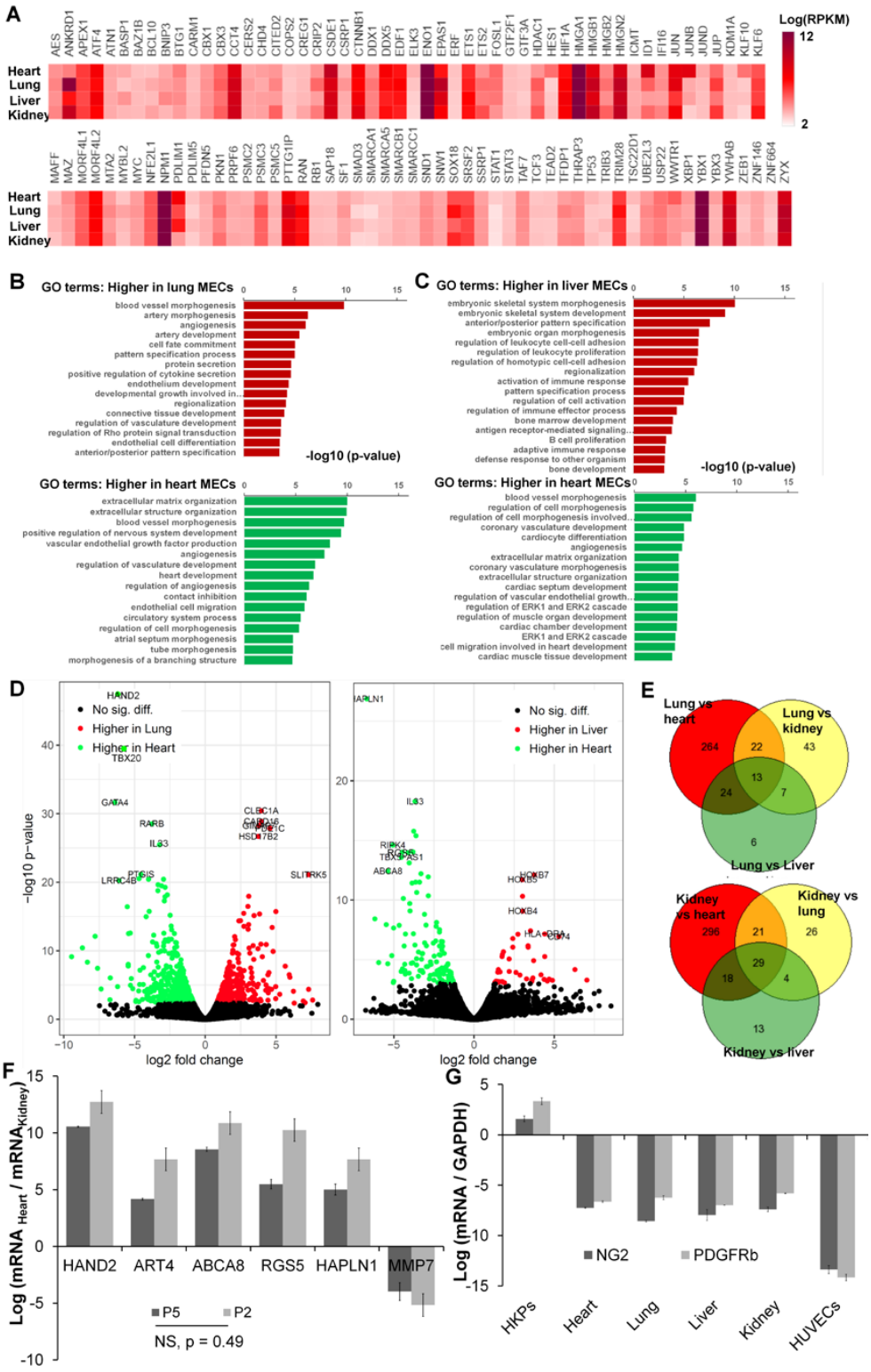

Supplementary Figure 4. Global RNA sequencing analysis for four types of human fetal ECs and gene validation A. Top expressed transcripts (107 TFs) for organspecific ECs. Colormap: log(RPKM). **B-C**. Gene Ontology terminology analysis for lung vs.

heart (B) and liver vs. heart (C) differentially expressed EC genes. **D**. Volcano plots of -log10 p-value vs. log2 fold change for lung vs. heart (left), and liver vs. heart (right) differentially expressed EC genes. **E**. Venn diagram showing organ-specific, differentially expressed genes for the lung and kidney ECs. **F.** Log fold changes of selected gene expression comparing heart vs. kidney ECs at passage 2 and 5, showing no significant difference. **G.** mRNA expression of NG2 and PDGFRb comparing four isolated and cultured fetal ECs with HUVECs and human kidney pericytes (HKPs), the isolated NG2+PDGFRb+ population shown in Supplementary Fig. 2.

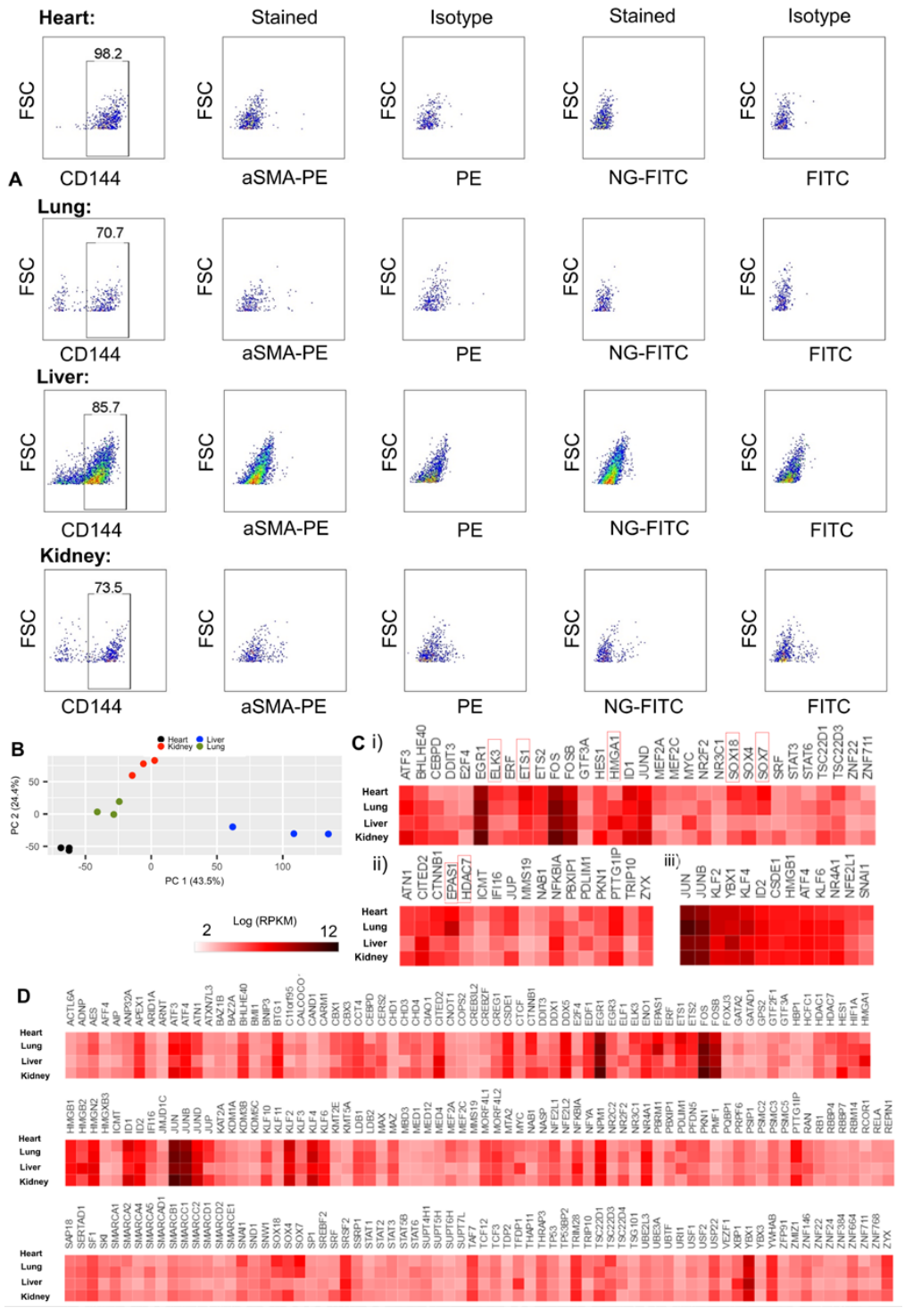

Supplementary Figure 5. Characterization of freshly isolated ECs A. Representative flow cytometry analysis of freshly isolated ECs via MACS column purification from fetal human heart, lung, liver and kidney stained with antibodies against CD144 (VECad), α-SMA and NG2, in comparison with isotype controls. **B**. 2D principal component

analysisof RNA sequencing data shows organ-specific clusters. **C**. Heat map of differentially expressed transcription factors (TFs) (i) and co-factors (ii), and other top expressed TFs (iii) in top 20% expressed transcripts in freshly isolated ECs. C. Heat map of the top 20% expressed TFs and co-factors in freshly isolated heart, lung, liver and kidney ECs. Colormap: log(RPKM).

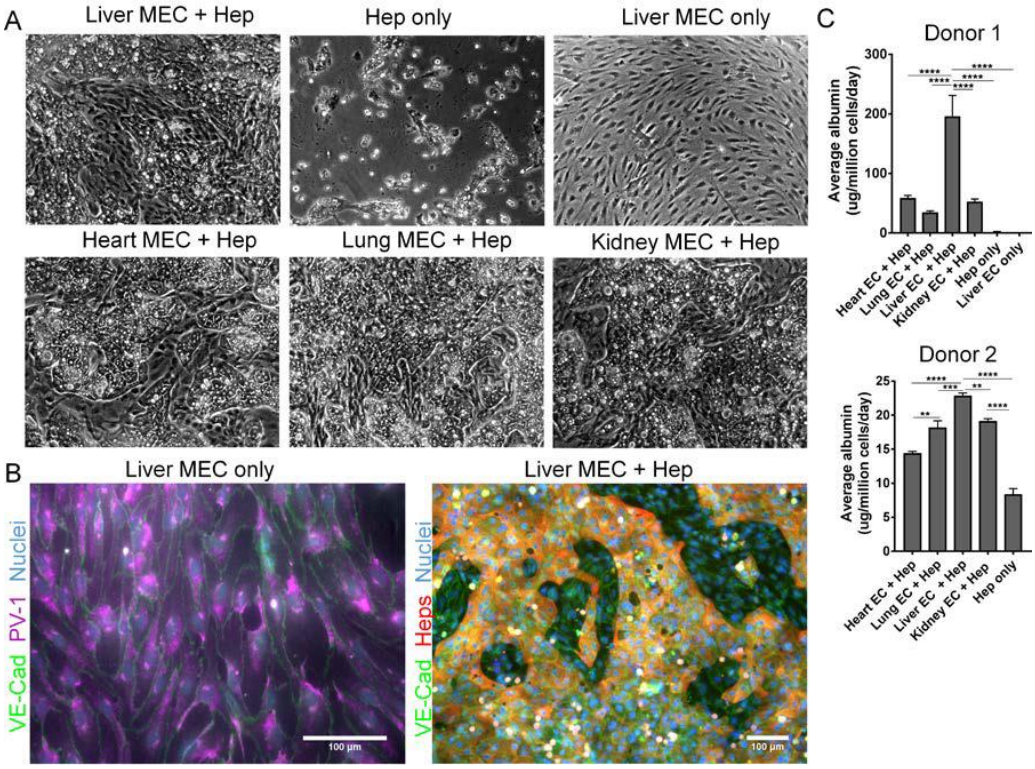

Supplementary Figure 6. Human fetal liver ECs superiorly support hepatocytes function. A. Bright field images of 2-D culture after 7 days for EC co-cultured with hepatocytes, hepatocytes alone, or liver ECs alone. B. Immunofluorence image of liver ECs alone and them co-cultured with hepatocytes after 7 days. Hepatocytes were stained with anti-cytokeratin. C. ELISA measurement of albumin production from rat hepatocytes when cultured alone and co-cultured with heart, lung, liver and kidney ECs after 7 days for two donor sets with four replicates in each donor.
Data information: data is presented as mean ± SEM. *p≤0.05, ** p≤0.01, ***p≤0.001,****p≤0.0001.

Appendix B

Supplement to Chapter 3

List of supplementary Figures

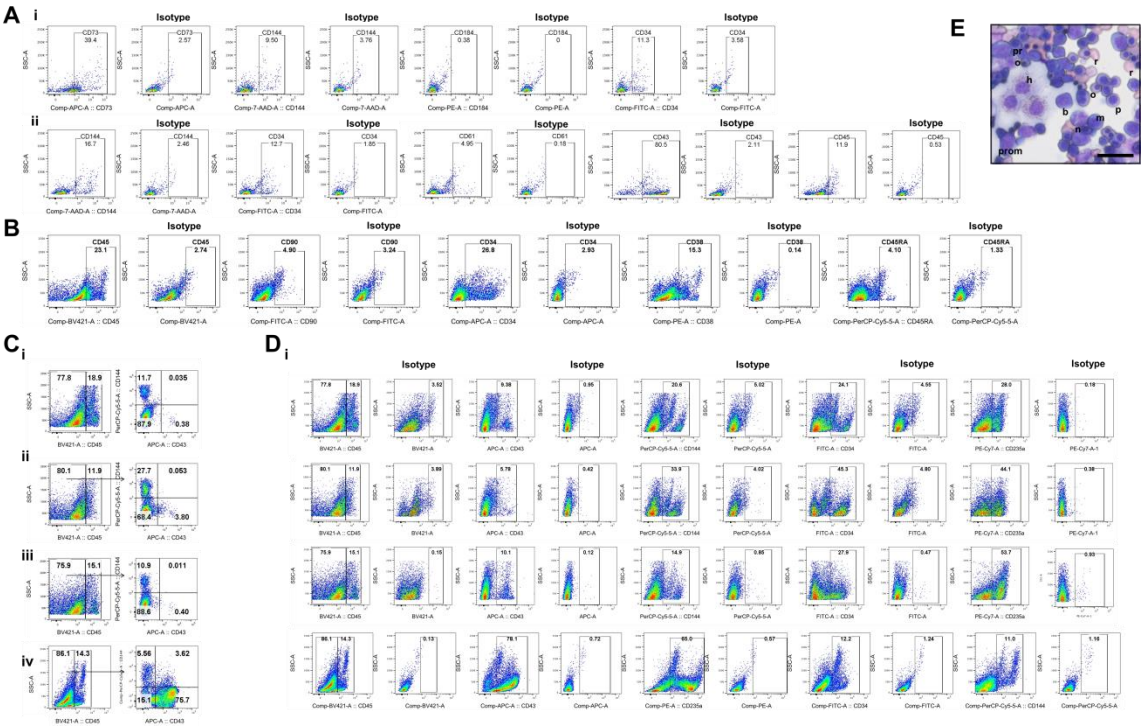

Supplementary Figure 1. Analysis of hematopoietic stem/progenitor cells in the fetal liver. The representative plots of the freshly-digested liver stained with (A) different combinatorial marker defining definitive HECs and (B) HSCs and MPPs markers.(C) Earlier hematopoietic populations that have not yet acquire CD45 expression in fetal human kidney(i), heart(ii) , lung(iii) and liver(iv) (D) Representative flow cytometry profiles of fresh total cell tissue suspension from fetal human kidney(i), heart(ii) , lung(iii) and liver(iv) stained with markers for multilineage HPCs and AHPs. (E) Representative cytospin of Giemsa stained unsorted liver cells. scale bar, 30 um. pro, pronormoblast, b, basophilic normoblast, p, polychromatic normoblast, o, orthochromatic normblast, h, hepatocyte, r, reticulocyte, pr, promonocyte, n, neutrophilic band, m, myeloblast, prom, promyeloblast

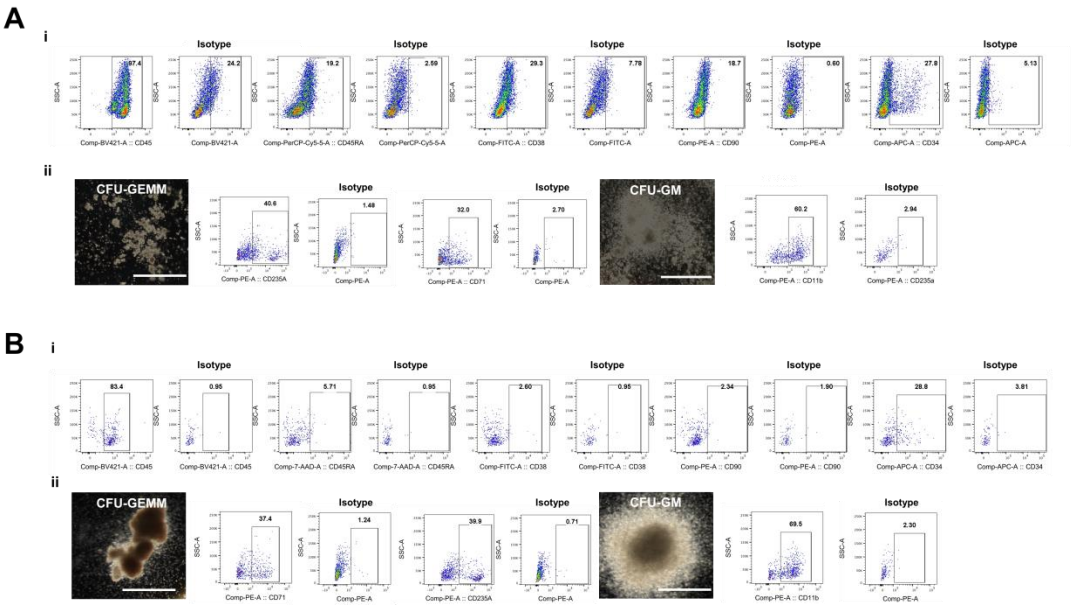

Supplementary Figure 2. Analysis of multilineage HPCs and AHP Gating scheme for HSCs and MPPs generated from multlineage HPCs(Ai) and AHPs(Bi). Representative flow cytometry of hematopoieitic colonies arise from multilineage HPCs (Bii) and AHPs (Cii) stained with erythroid and myeloid markers. (scale bar, 1,000 um).

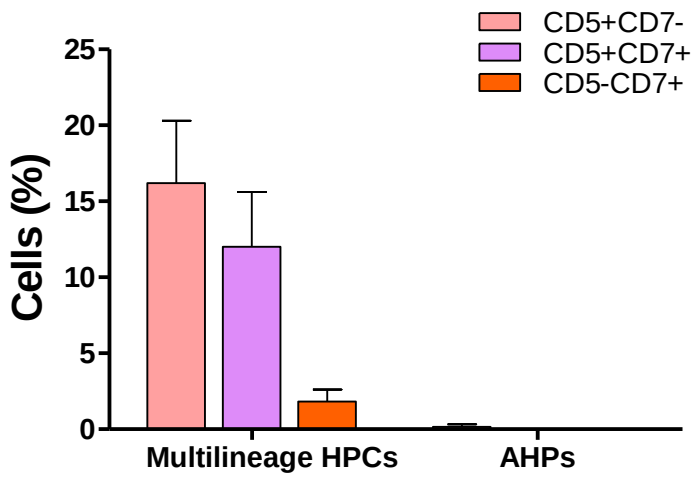

Supplementary Figure 3. Quantification of T cells T cells generated from multilineage HPCs and AHPs after secondary OP9-dll4 co-culture were quantified. (n= 3 donors mean ±SEM)

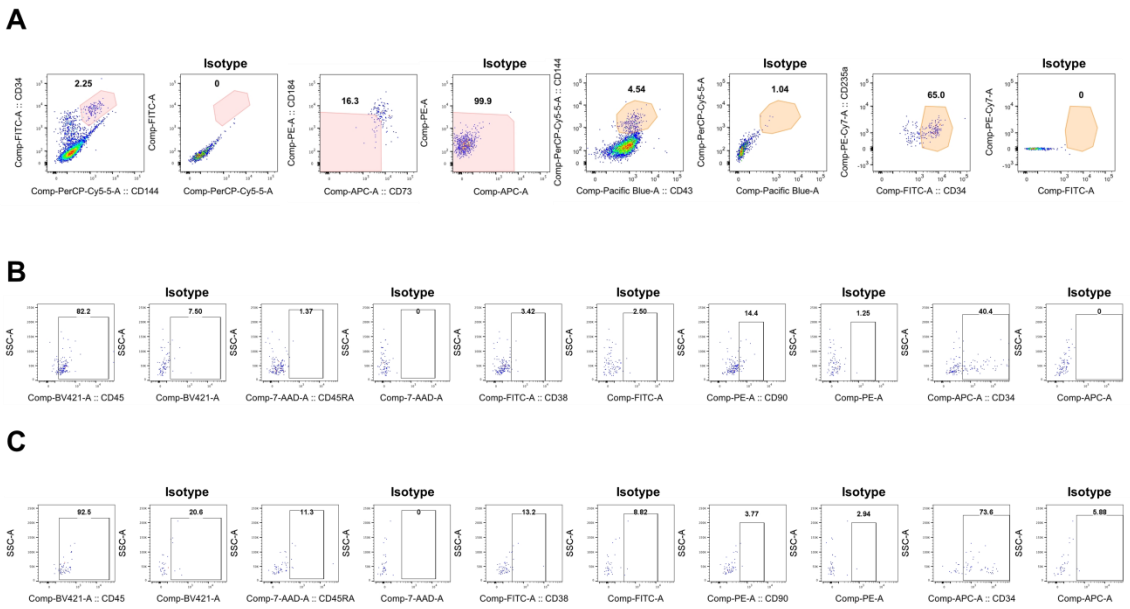

Supplementary Figure 4. hESC-HECs and AHPs characterization Detailed FACS scheme of (A) hESC-derived HECs and AHPs. Gating scheme for HSCs and MPPs generated from (B) hESC-derived HECs and (C) AHPs

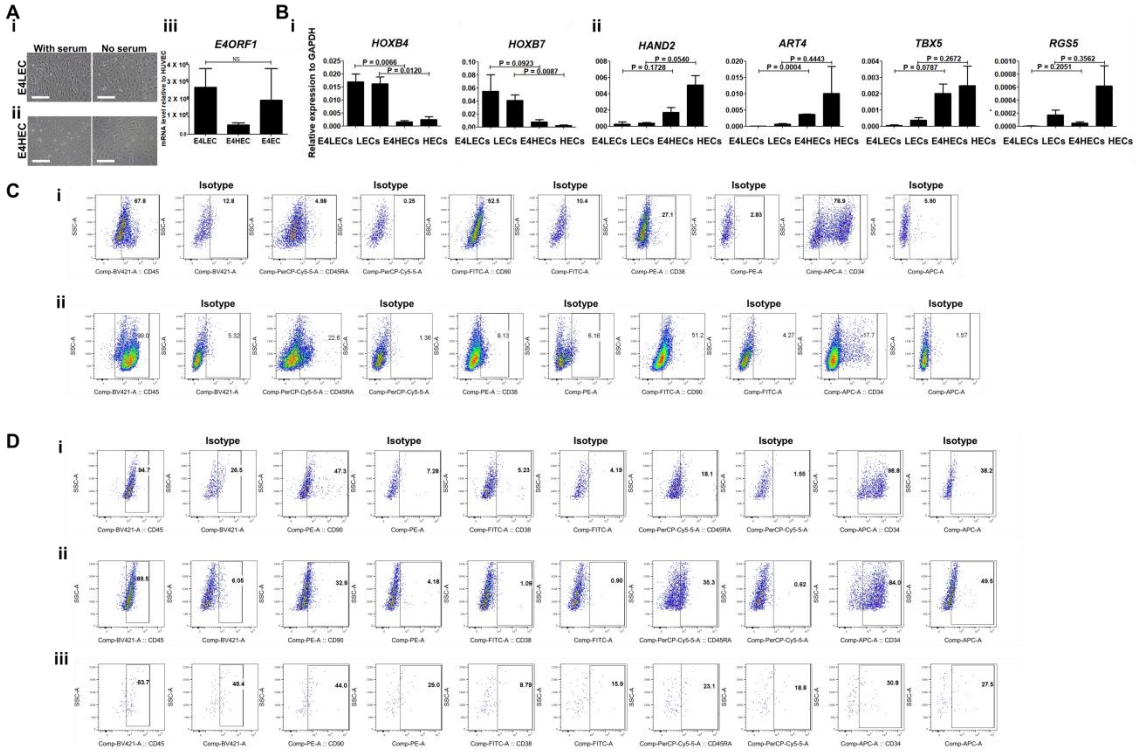

Supplementary Figure 5. Gene expression of E4LECs and E4HECs and gating scheme for the hematopoietic stem/progenitor cells (A) Brightfield image of E4ORF1-transduced liver ECs (i) and heart ECs (ii) cultured with and without serum media. Scale bar = 200 um (right panel) (B) (i)Liver endo-specific and (ii)heart specific genes were quantified. (C) Gating scheme for HSCs, MPP, and lineage committed CD34+CD38+ cells from liver CD43+ HPC cocultured with (i) E4LECs and (ii) E4HECs. (D) Gating scheme for HSCs, MPP, and lineage committed CD34+CD38+ cells from hESC-derived HECs co-cultured with (i) E4LECs (ii) E4HECs and (iii) E4ECs

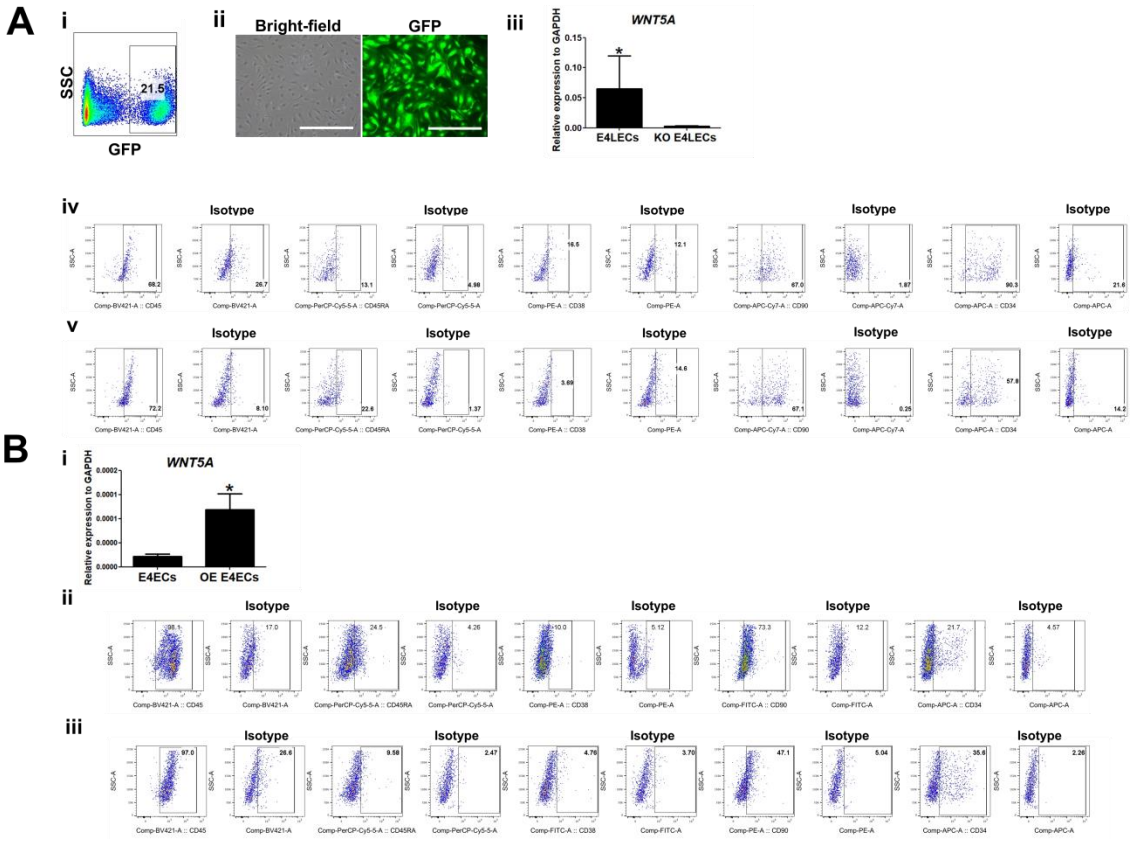

Supplementary Figure 6. Gene expression of Wnt5a KO E4LECs and OE E4ECs and gating scheme for the hematopoietic stem/progenitor cells (A) E4LECs were transduced with lentiviral vectors containing Wnt5a (Wnt5a-IRES-GFP) under the control of CMV promoter (i) GFP positive cells were FACS sorted. (ii) Representative images of FACS sorted GFP+ E4LECs. Scale bar 0.5 mm. iii)Knockdown is confirmed using qRT–PCR (n= 2 donors mean ±SEM * p≤0.05) Gating scheme for HSCs, MPP, and lineage committed CD34+CD38+ cells from liver CD43+ HPC co-cultured with (iv) E4LECs and (v) KO E4LECs. (vi) Bar graph shows the fold decrease of the numbers of colony forming progenitors, particularly CFU-GEMM and BFU-E cultured with KO E4LECs compared with E4LEC. (1 biological replicate and three technical replicate mean ±SEM * p≤0.05,** p≤0.01) (B) (i)qRT-PCR confirms that Wnt5a is overexpressed in E4ECs.(n=2 mean ±SEM * p≤0.05) (ii) Gating scheme for HSCs, MPP, and lineage committed CD34+CD38+ cells from liver CD43+ HPC co-cultured with (ii) E4ECs and (iii) OE E4ECs.

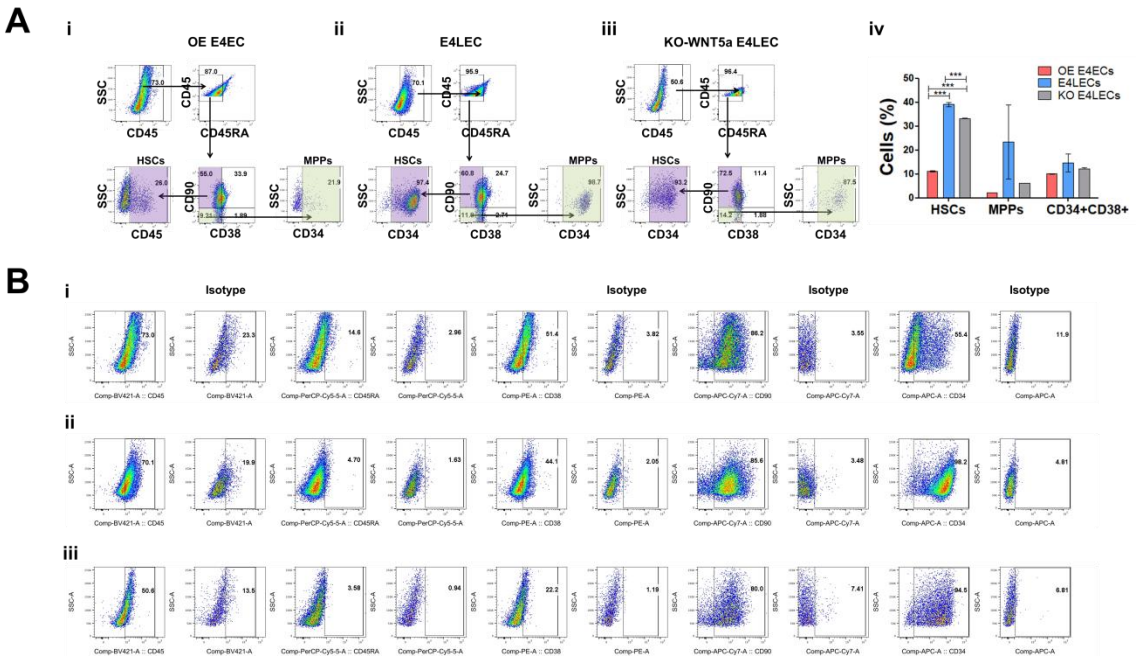

Supplementary Figure 7. Comparison of in vitro generation of multilineage hematopoietic progenitors from hESC-HECs co-cultured with OE E4EC, E4LEC, and KO-E4LECs (A) Representative FACS plot showing phenotypic HSCs and MPPs arise from hESC derived HECs cocultured with (i) OE E4ECs, (ii) E4LECs, and (iii) KO E4LECs. (iv) Quantification of lineage output (n= 2 mean ±SEM, **p≤0.01) B. Gating scheme for HSCs, MPP, and lineage committed CD34+CD38+ cells arise from hESC derived HECs cocultured with (i) OE E4ECs, (ii) E4LECs, and (iii) KO E4LECs